
ISAPP 2019 @ the Pierre Auger Observatory
International School on AstroParticle Physics
Cosmic ray Vision from the Southern Sky
March 1-9
Malargüe, MZ, Argentina
35.4845° S, 69.5797° W
COVERED TOPICS:
UHE Cosmic rays
Cosmic rays sources and propagation
Multi-messenger astronomy
Gravitational waves
High-energy neutrinos
Gamma Rays
INTERNATIONAL ADVISORY COMMITEE:
Antonio Bueno
Francis Halzen
Karl-Heinz Kampert
Rene A. Ong
Alan A. Watson
And the ISAPP Steering Committee
https://www.isapp-schools.org/steering-committee
INFO AND REGISTRATION:
isapp.auger.2019@gmail.com
https://indico.nucleares.unam.mx/e/isapp2019
LOCAL ORGANIZING COMMITTEE:
Lorenzo Perrone - chair
Ingo Allekotte
Gualberto Avila
Antonella Castellina
Ralph Engel
Jörg Hörandel
Lukas Nellen
Mario Pimenta
Miguel A. Sánchez-Conde
Viviana Scherini
Tiina Suomijärvi
Enrique Zas
SECRETARIAT:
Carla Gentile, Lucia Sideli - INFN Lecce
Rosa Pacheco - Observatorio Pierre Auger
Photo: Steven Saffi University of Adelaide

Gamma Rays

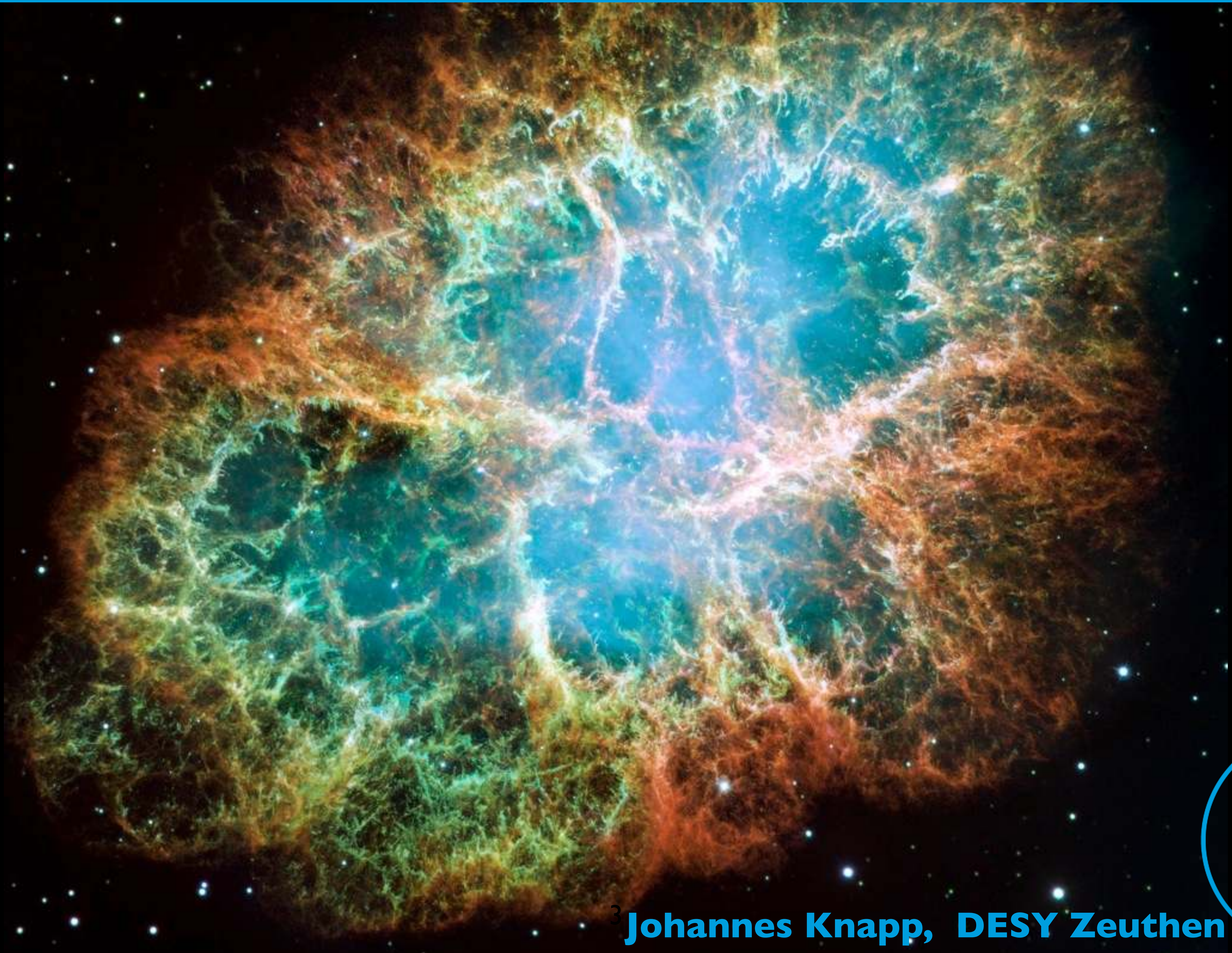

Johannes Knapp, DESY Zeuthen

Gamma Rays

Part I: Intro & Techniques

Astro-Particles

energetic (elementary) **particles**
from space (Sun, Milky Way, distant galaxies)
bombard Earth continuously.

Energies from MeV .... >10^{20} eV

1 eV = 1.6 x10^{-19} J

most relativistic particles in the Universe

Astrophysics with photons and particles.

Particle physics with probes of astrophysical origin.

What are these cosmic particles?

must be stable (to survive travel to us)

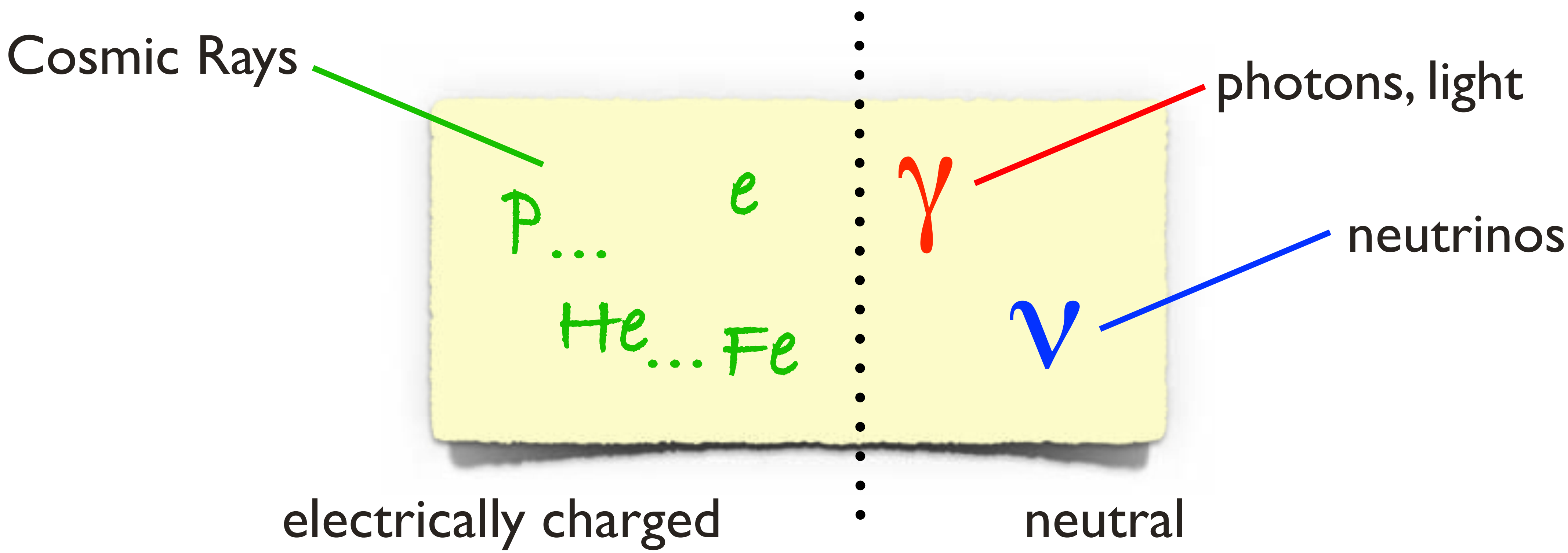

+ can be accelerated in electric fields
– are deflected in magnetic fields

+ move in straight lines
– secondary particles

(good for astronomy)

other astro particles: **dark matter**

... not in this talk.

Energy scale:

the range of astroparticle physics

radio IR visible light UV X rays γ rays

||

meV ... eV ... keV ... MeV ... GeV ... TeV ... PeV ... EeV ... ZeV

10^{-3} ... 1 ... 10^{3} ... 10^{6} ... 10^{9} ... 10^{12} ... 10^{15} ... 10^{18} ... 10^{21} eV

non-thermal processes

Photons: astronomy

charged: p, He, ... Fe, ... completely ionised nuclei

electrons

Neutrinos:

Cosmic rays, gamma rays and neutrinos come likely from the same sources

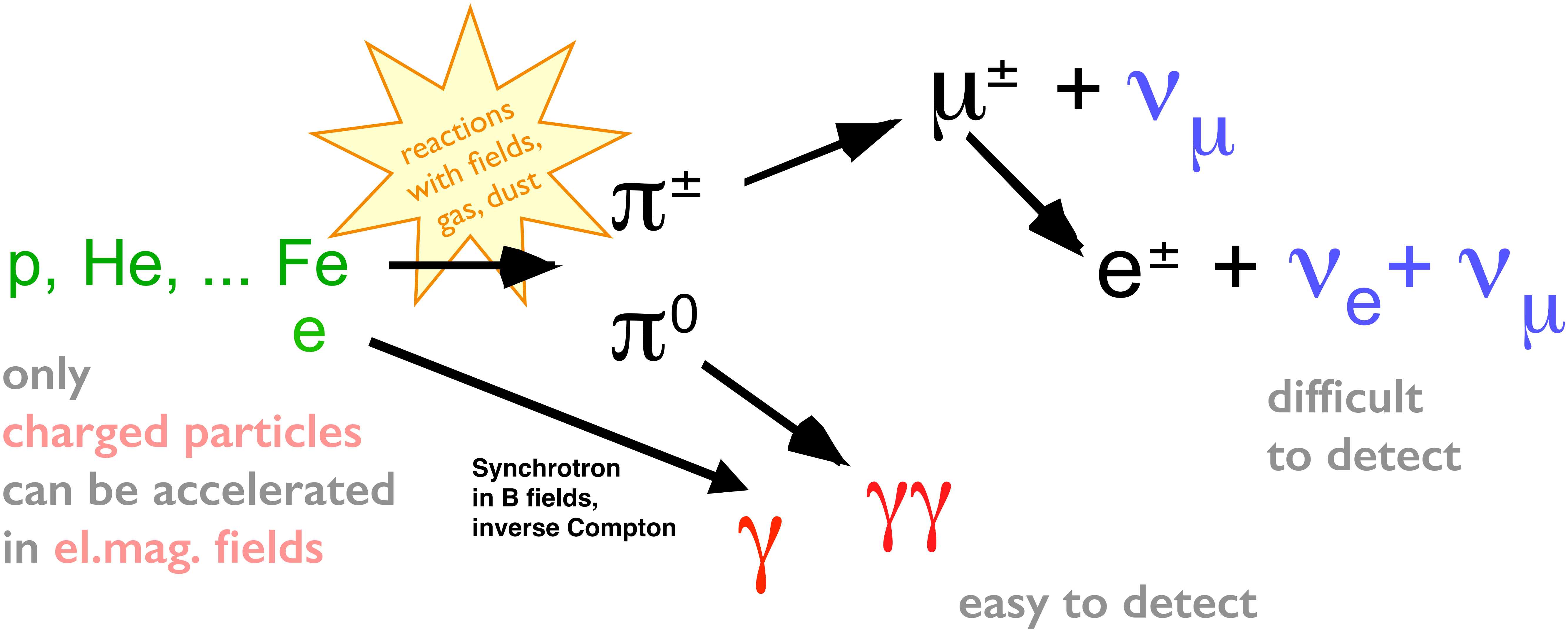

"multi-messenger astrophysics"

but gamma rays are currently the most "productive" messengers.

γ, ν

point back to sources
(good for astronomy)
but serious backgrounds

Cosmic accelerators

The highest-energy particles come from the most violent environments (physics in extreme conditions)

The highest-energy CRs, γ and ν come likely from the same sources.

The energy frontier

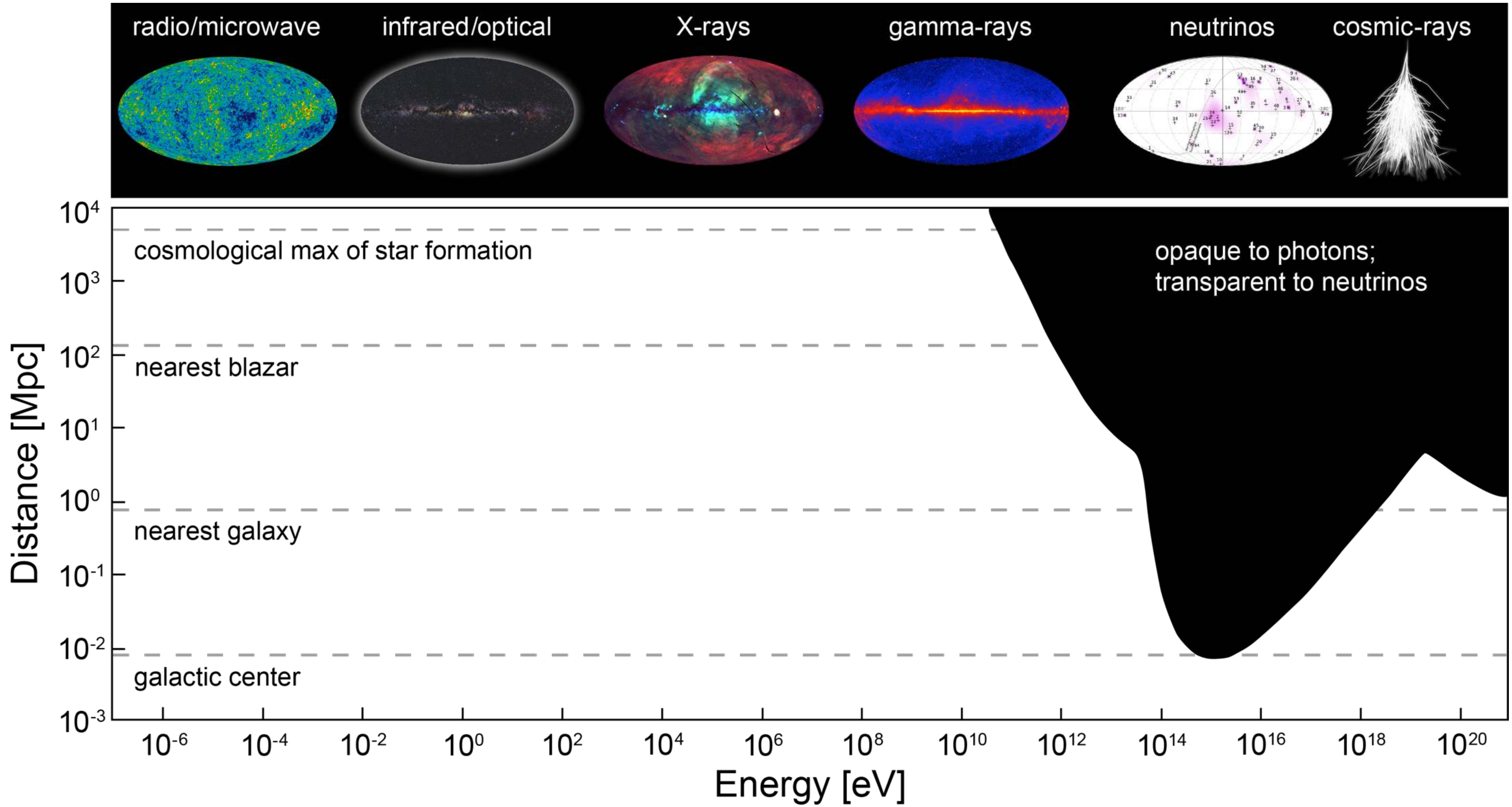

The Universe is opaque to photons for ¼ of the spectrum

Cosmic particle spectra

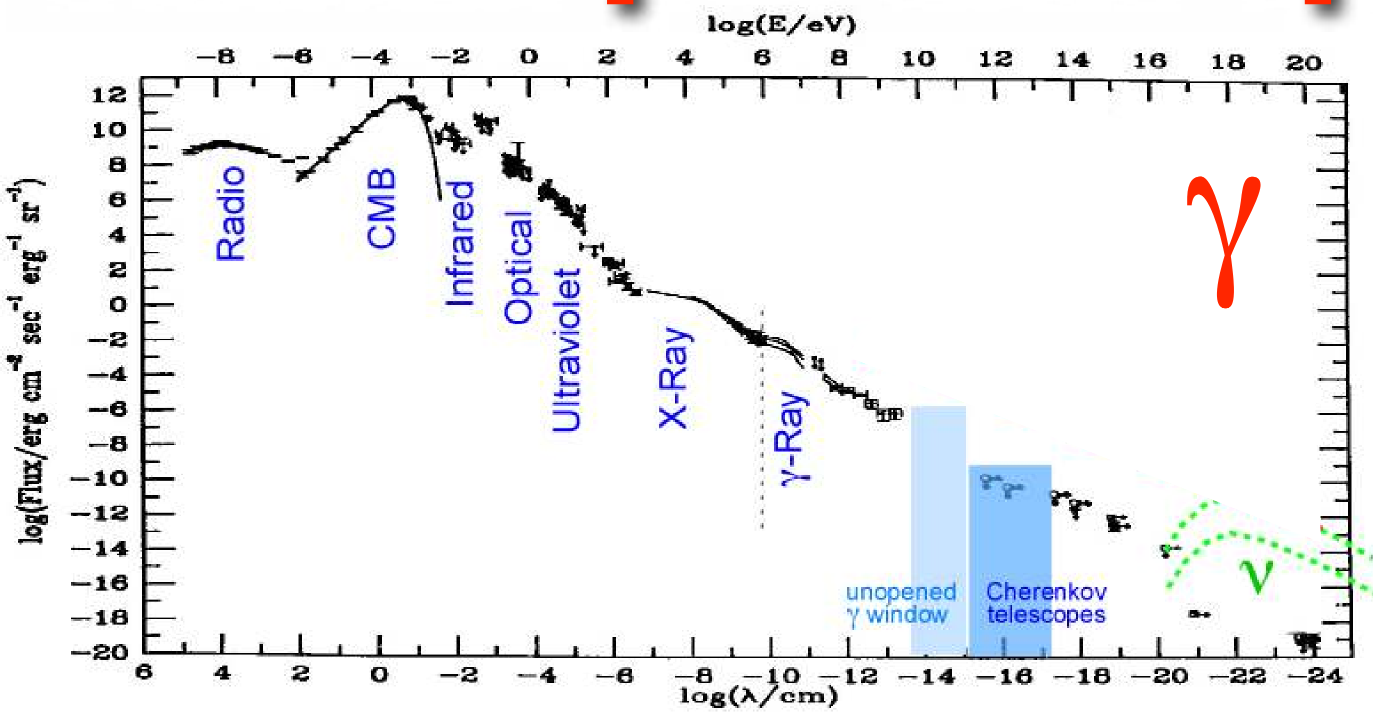

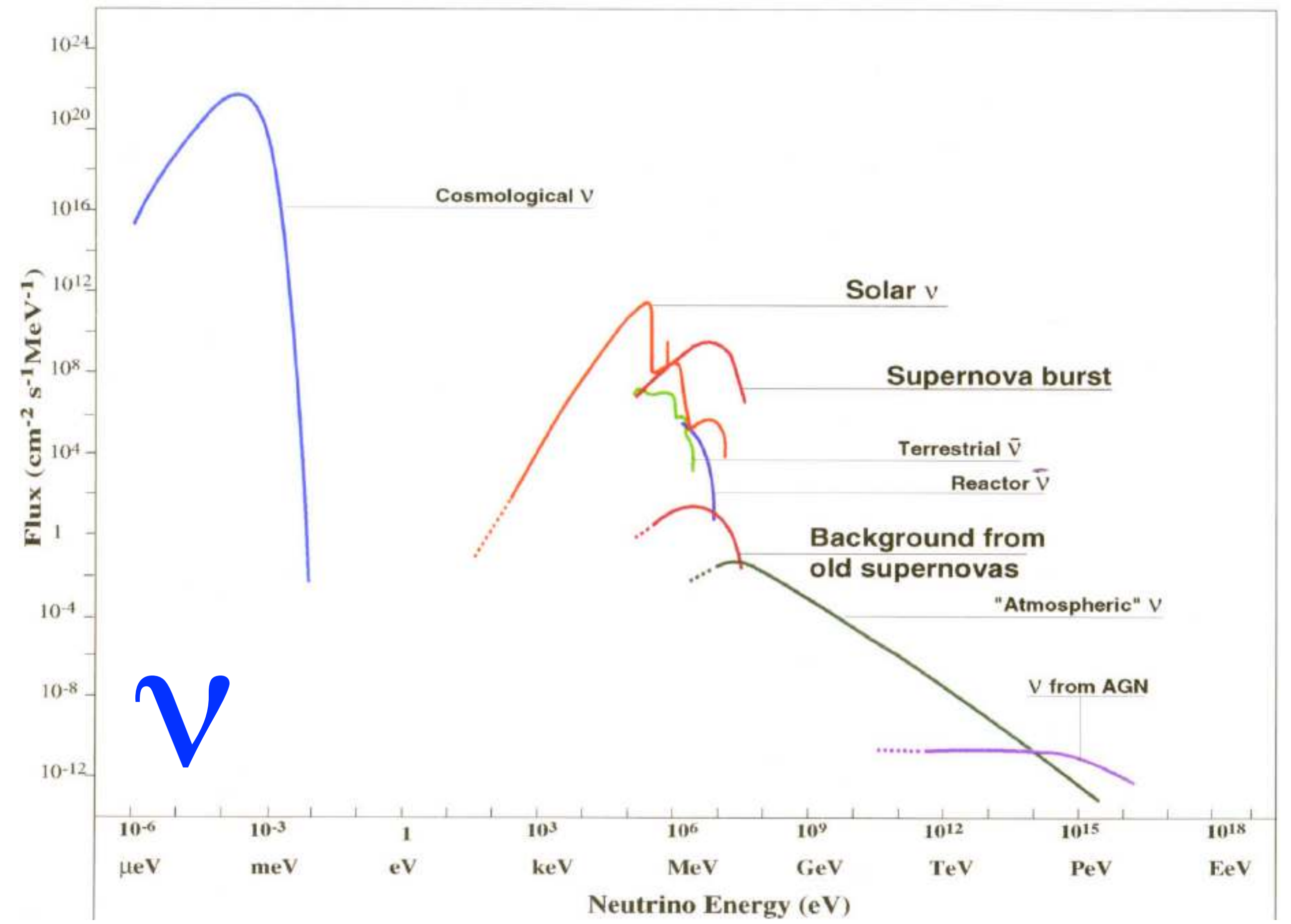

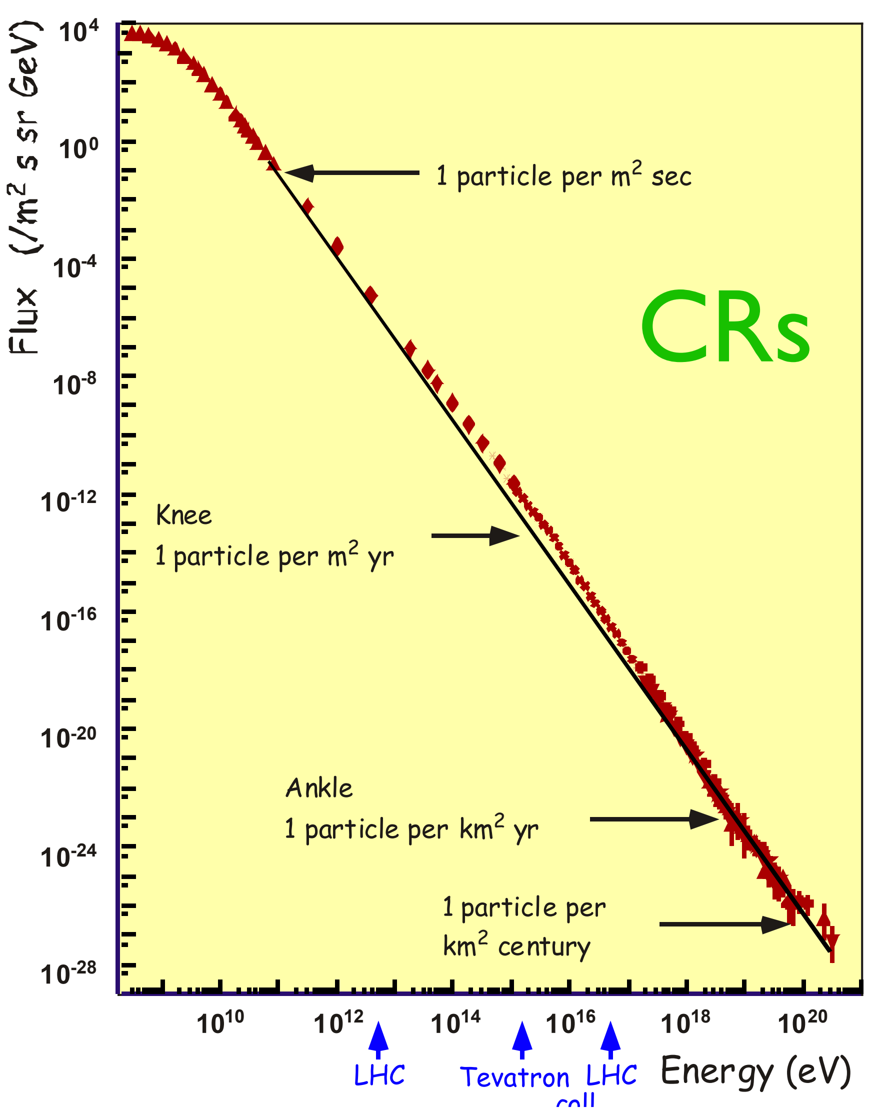

steeply falling spectra,
low fluxes at high energies

require huge detectors

in general: for all particle types

the higher the energy,
the lower the flux

the lower the flux,
the larger the required detectors

$$N_{evts} = \text{flux} \times \text{area} \times \text{time}$$

> 100

small,
given by nature

$\approx 1\ m^2$
for satellite expts.

≈ 3 yrs

Detector size limits the smallest measurable fluxes.

Large, natural volumes become part of our detectors:

atmosphere,
ice shields,
oceans,
...

instrument (sparsely) to record secondaries produced by particle interactions

understand / monitor the "target"

primary particle: E, type, θ, φ

indirect measurement: extensive showers

(in air, ice, water, …)

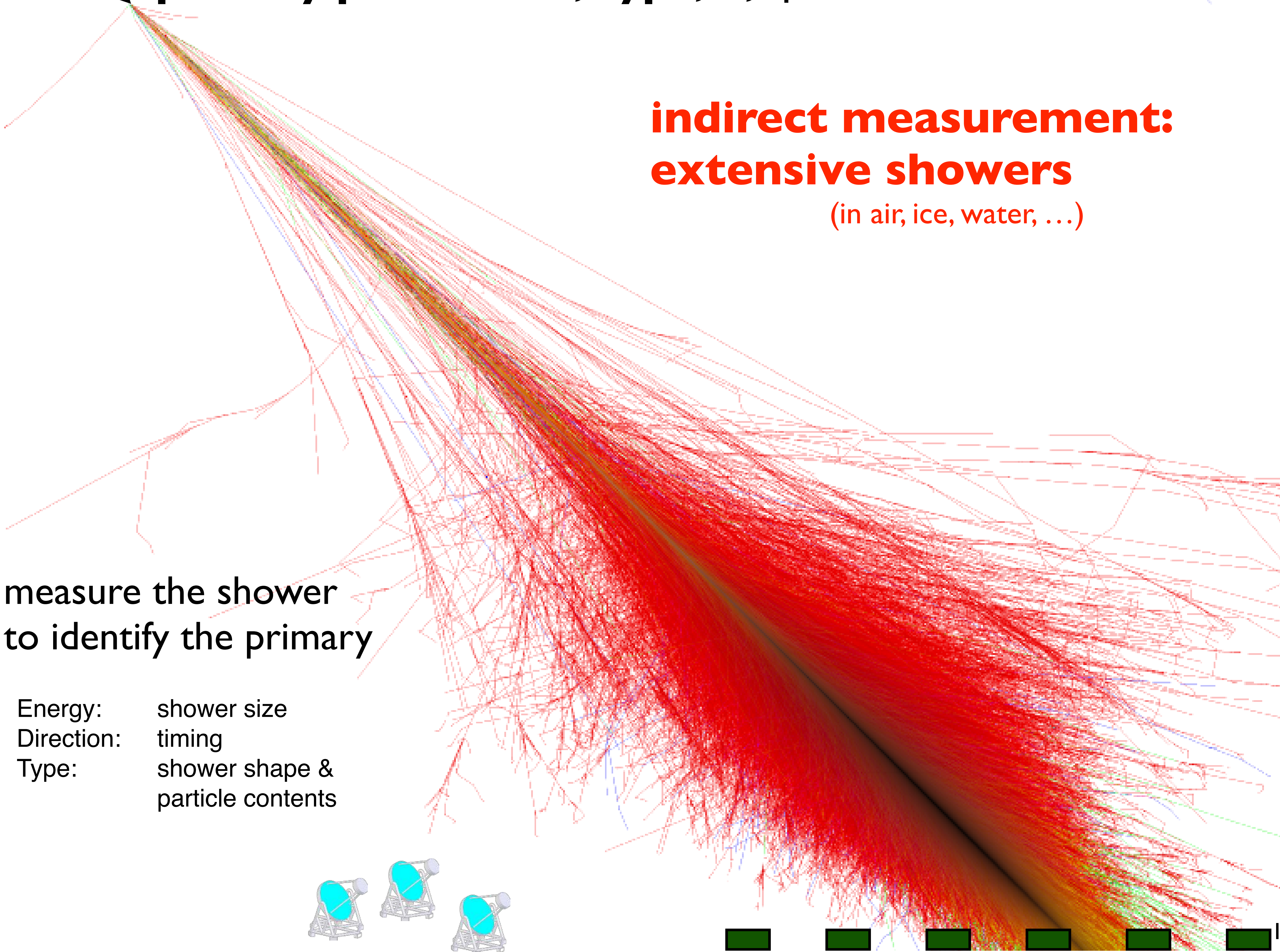

measure the shower
to identify the primary

Energy:	shower size
Direction:	timing
Type:	shower shape & particle contents

CRs: each CR makes an air shower, easy to detect

(difficult to identify the primary)

γ : each γ makes an air shower, easy to detect

(but 100 -10000 x more CRs, separate them from γ)

ν: only very few ν interact in/near detector,

high-energy e, μ, τ make showers in ice

(but many atmospheric neutrinos from CR interactions)

serious backgrounds

Backgrounds

cosmic
gamma rays
(pointing back at source)

cosmic
nuclei
(diffuse)

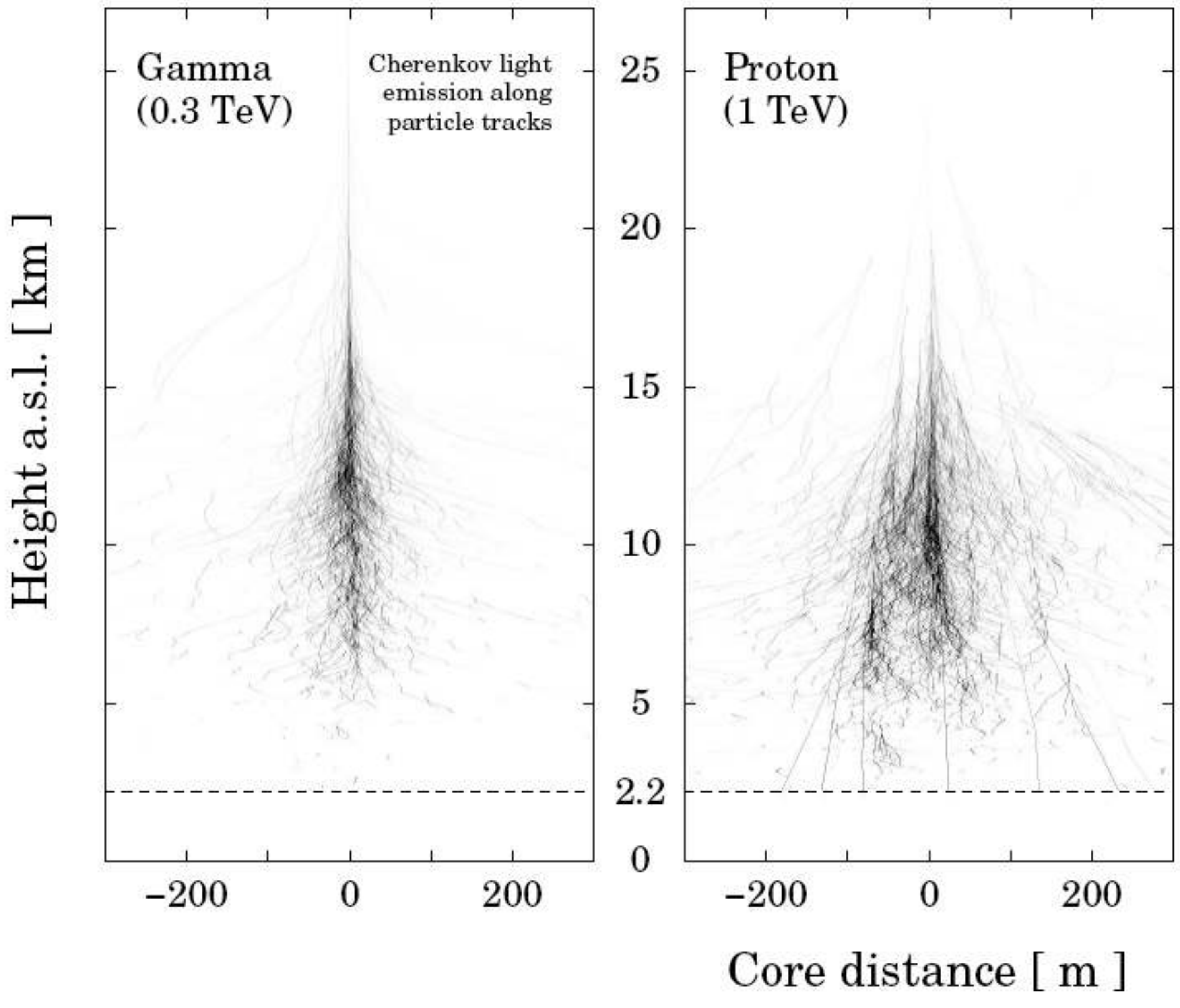

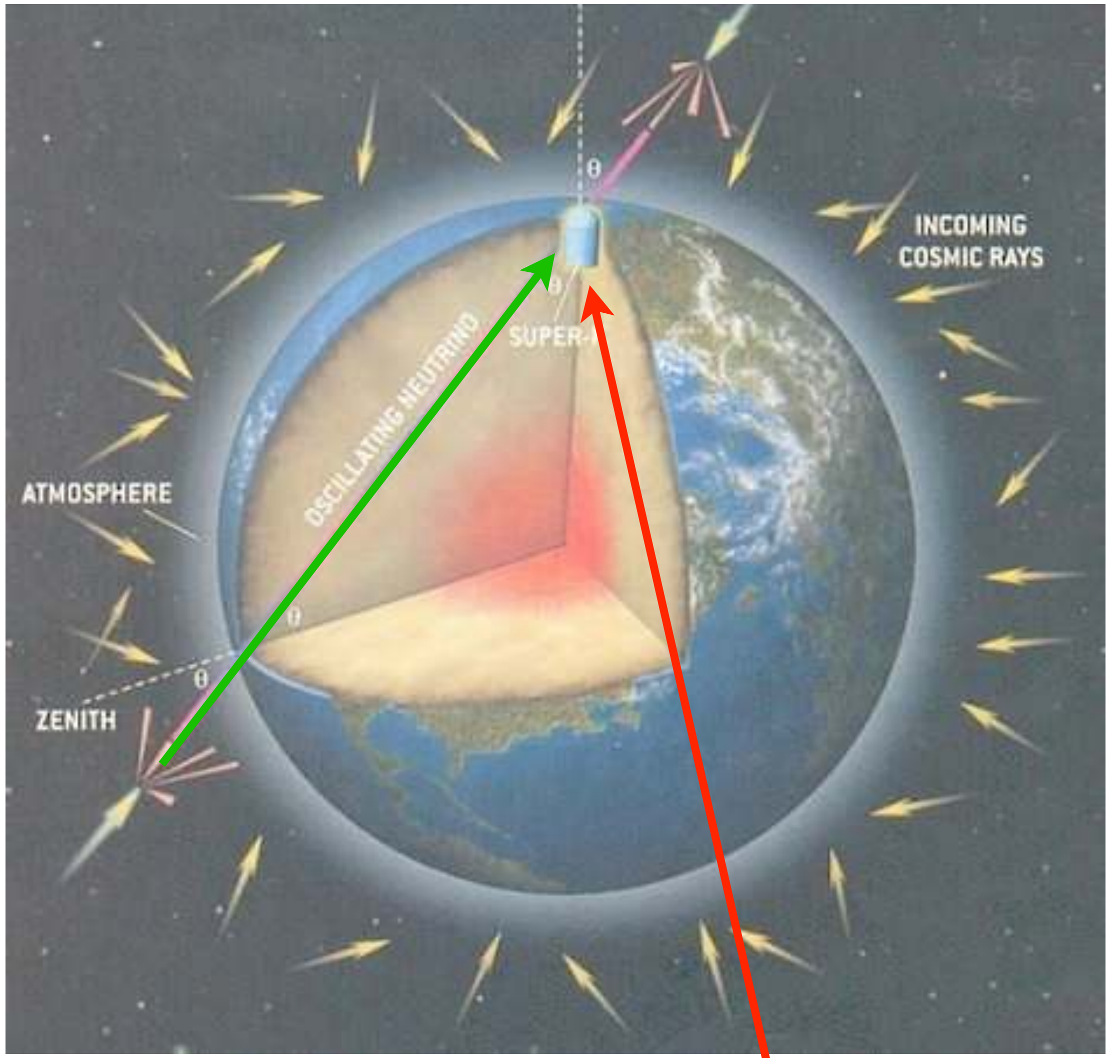

atmospheric ν

astrophysical ν

(dominant at high energies)

10000x more abundant

Interactions of radiation with matter

Charged and neutral particles:
How to detect them?

Interactions of Radiation with Matter

Detection of an object relies always on its "interaction" with a detector !

e.g.

vision:	photon absorbed in the eye
hearing:	sound wave absorbed in ear
liquid level:	liquid changes capacitance
....	

Particles: let them ionise atoms & record ionisation charge

(mostly electromagnetic interaction, atomic physics)

- charged particles ($e^{\pm}$, $\mu^{\pm}$, p, $\pi^{\pm}$, He^{++}, ...):

  ionisation, bremsstrahlung, multiple scattering

  Cherenkov & transition radiation

- photons:

  photo effect, Compton effect, pair production

- neutrons:

  collision and recoil, n-capture

This is the basis of all particle detection.

Ionisation

charged particle (m, Z·e, v) "hits" electron in an atomic shell
with its electrical field

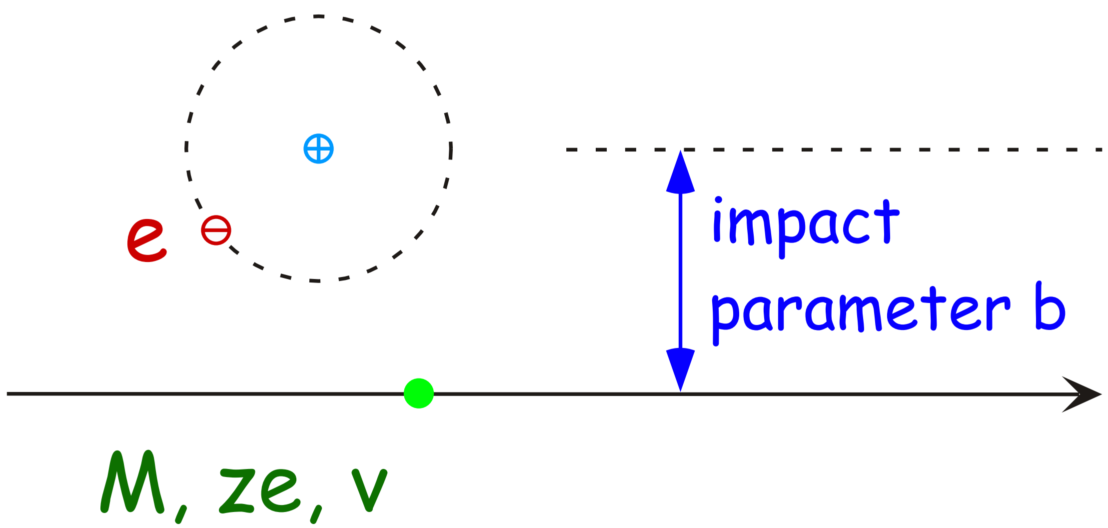

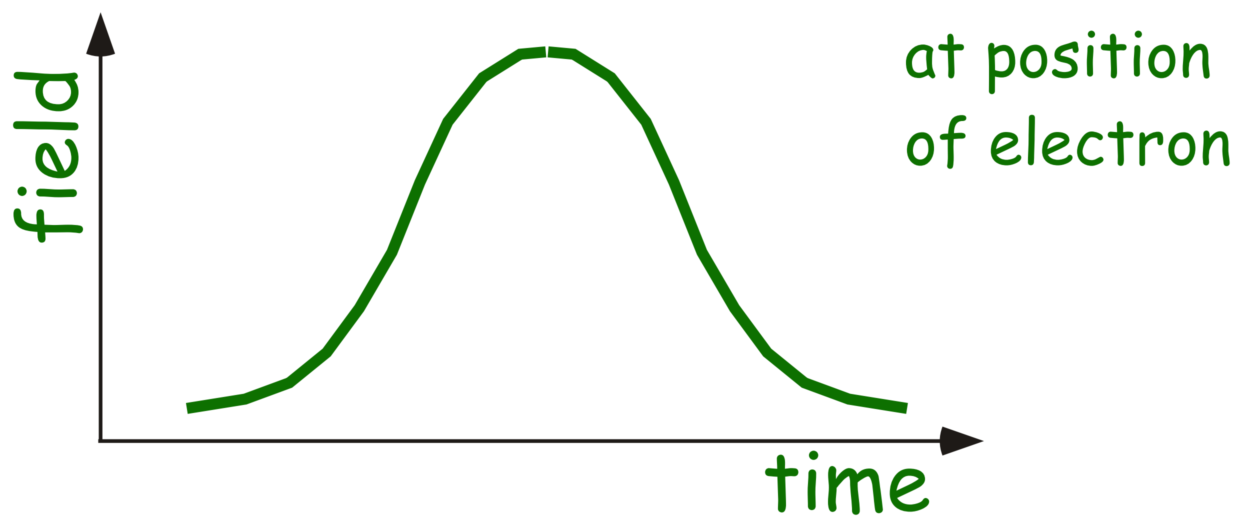

Electron feels kick and gains energy, which comes from the passing particle.

maximum velocity: $v_e \leq v$ for $M \gg m_e$

transfer of E_{kin} to one electron $= \dfrac{z^2 e^4}{8\, m_e\, \pi^2\, \varepsilon_0^2\, b^2\, v^2}$

If energy transfer > binding energy, then the electron is released from the atom and a free electron-ion pair is produced.

Ionisation processes happen very often and the average over many gives the total energy loss of the projectile.

Ionisation (cont'd)

Bethe-Bloch formula:

$$-\frac{dE}{dx} = K z^2 \frac{Z}{A} \frac{1}{\beta^2} \left[\frac{1}{2} \ln \frac{2 m_e c^2 \beta^2 \gamma^2 T_{max}}{I^2} - \beta^2 - \frac{\delta}{2} \right]$$

average energy loss (in units of MeV/(g cm^{-2})) of a charged particle (z, β, γ)

in a medium (Z, A, I, δ)

- x is pathlength in g/cm^2, i.e. independent of density

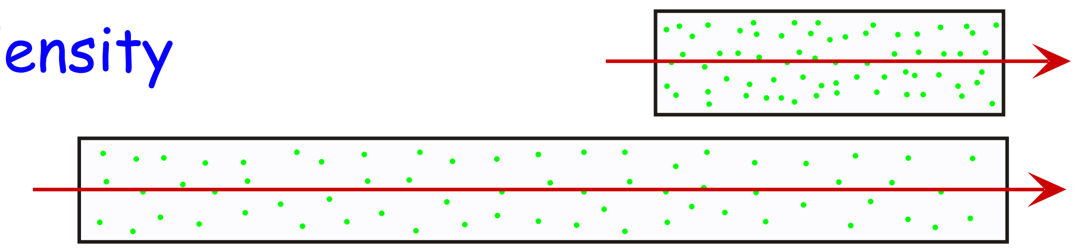

- small dependence on projectile mass M through T_{max}

  ($T_{max} = \dfrac{2 m_e c^2 \beta^2 \gamma^2}{1 + 2 \gamma m_e/M + (m_e/M)^2}$ = max. kin. energy transfer)

- in most materials (except H) particles have very similar energy losses

  (due to $Z/A \approx 0.5$, for H : $Z/A \approx 1$)

- dependence on density (via density correction δ)
- dependent on z^2 and β^{-2} only
- broad minimum at $p/M = \beta\gamma = 3 \ldots 3.5$ for $z = 7 \ldots 100$

  (particles close to minimum: minimum ionising particles, MIPs)

- below minimum: $-dE/dx \sim \beta^{-2}$ (~ $1/E_{kin}$)
- above minimum: $-dE/dx \sim \ln \gamma^2$ slow, logarithmic rise

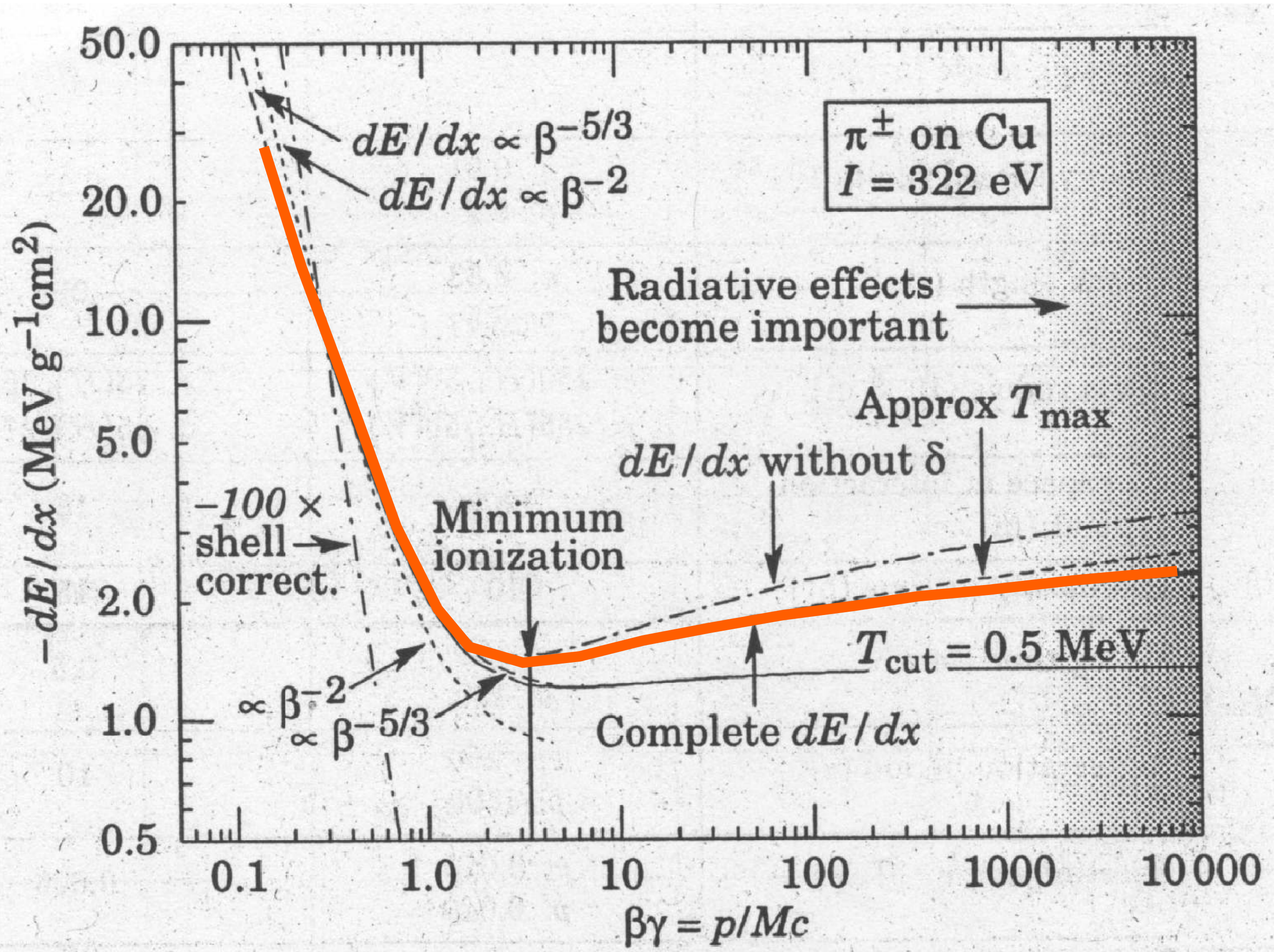

Figure 23.1: Energy loss rate in copper. The function without the density-effect correction, δ, is also shown, as is the loss rate excluding energy transfers with $T > 0.5$ MeV. The shell correction is indicated. The conventional β^{-2} low-energy approximation is compared with $\beta^{-5/3}$.

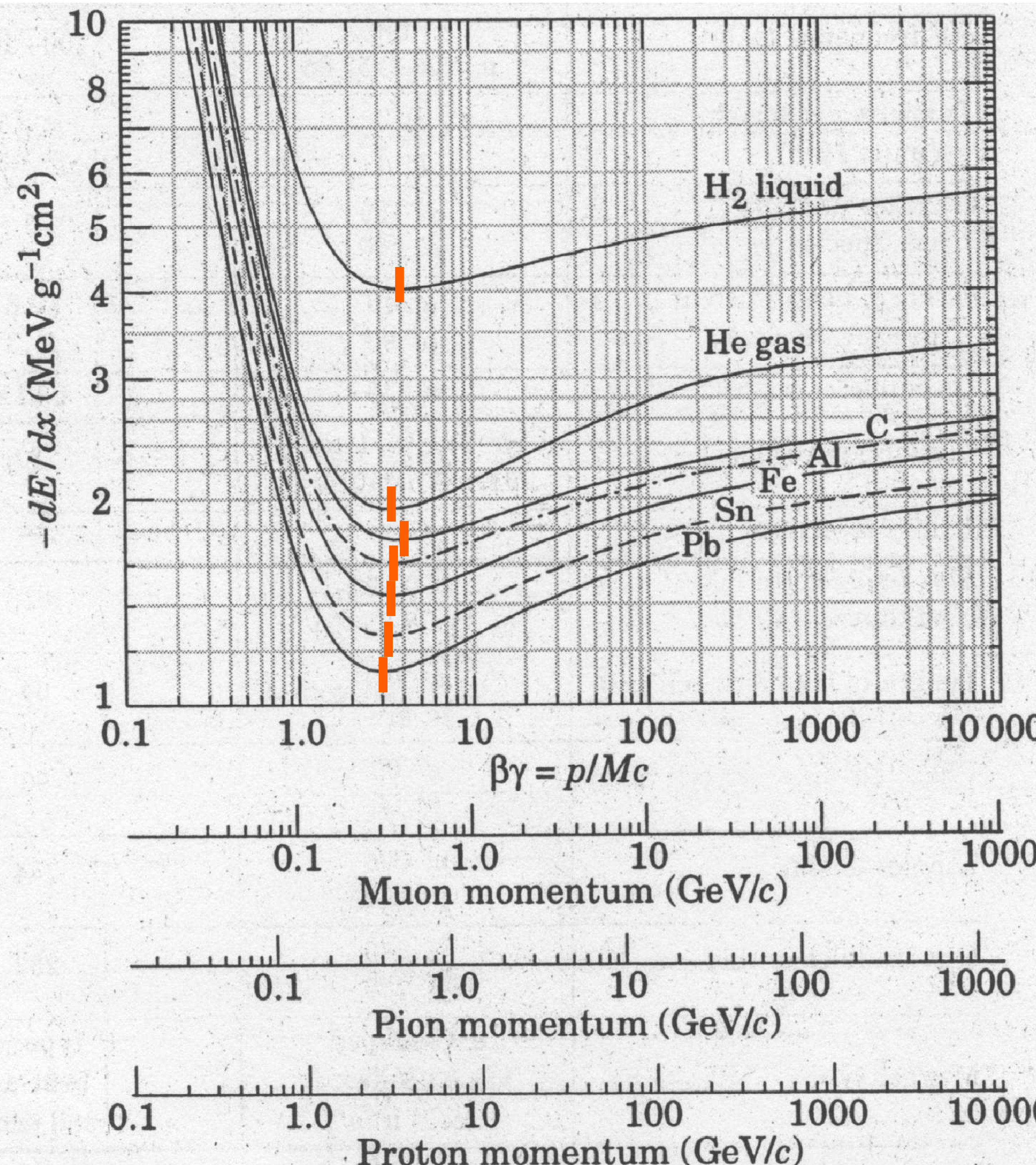

Figure 23.2: Energy loss rate in liquid (bubble chamber) hydrogen, gaseous helium, carbon, aluminum, tin, and lead.

The Bethe - Bloch Formula

for energy loss of charged particles in matter

logarithmic rise: electric field relativistically compressed, reaches further out to ionise more atoms

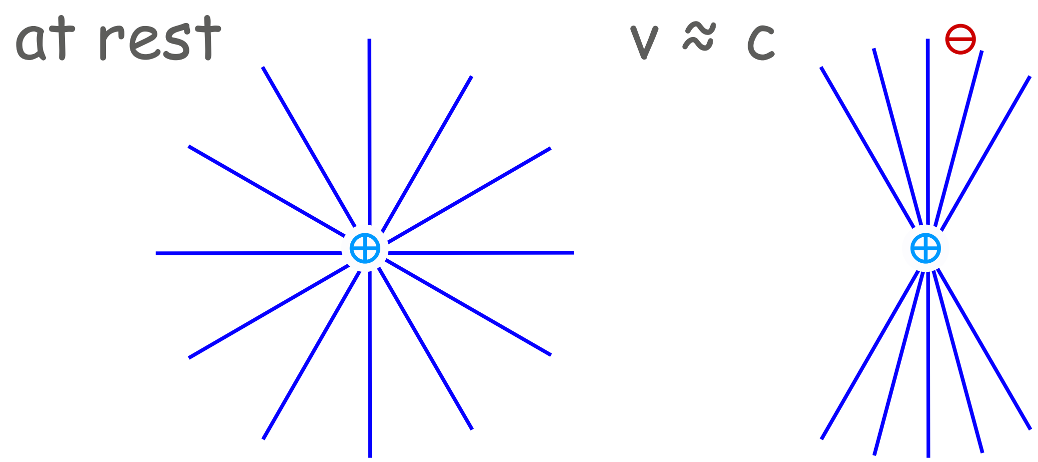

saturation: atoms shield field in larger distances (density effect)

universal curve: $\dfrac{-dE/dx}{z^2} = f(v)$ for (almost) all particles/materials

fluctuations: ionisation is statistical process; $N_{collisions}$ and dE/dx vary

deflection: depends on projectile mass: less for heavy particles (like p)
more for light ones (like e)

Applications: if E_{kin} known, $dE/dx \sim z^2$ is sensible measure for z

$(dE/dx)_{min} \approx 2\ z^2\ \mathrm{MeV/(gcm^{-2})}$ also good z measurement

if particle stopped, energy measurement

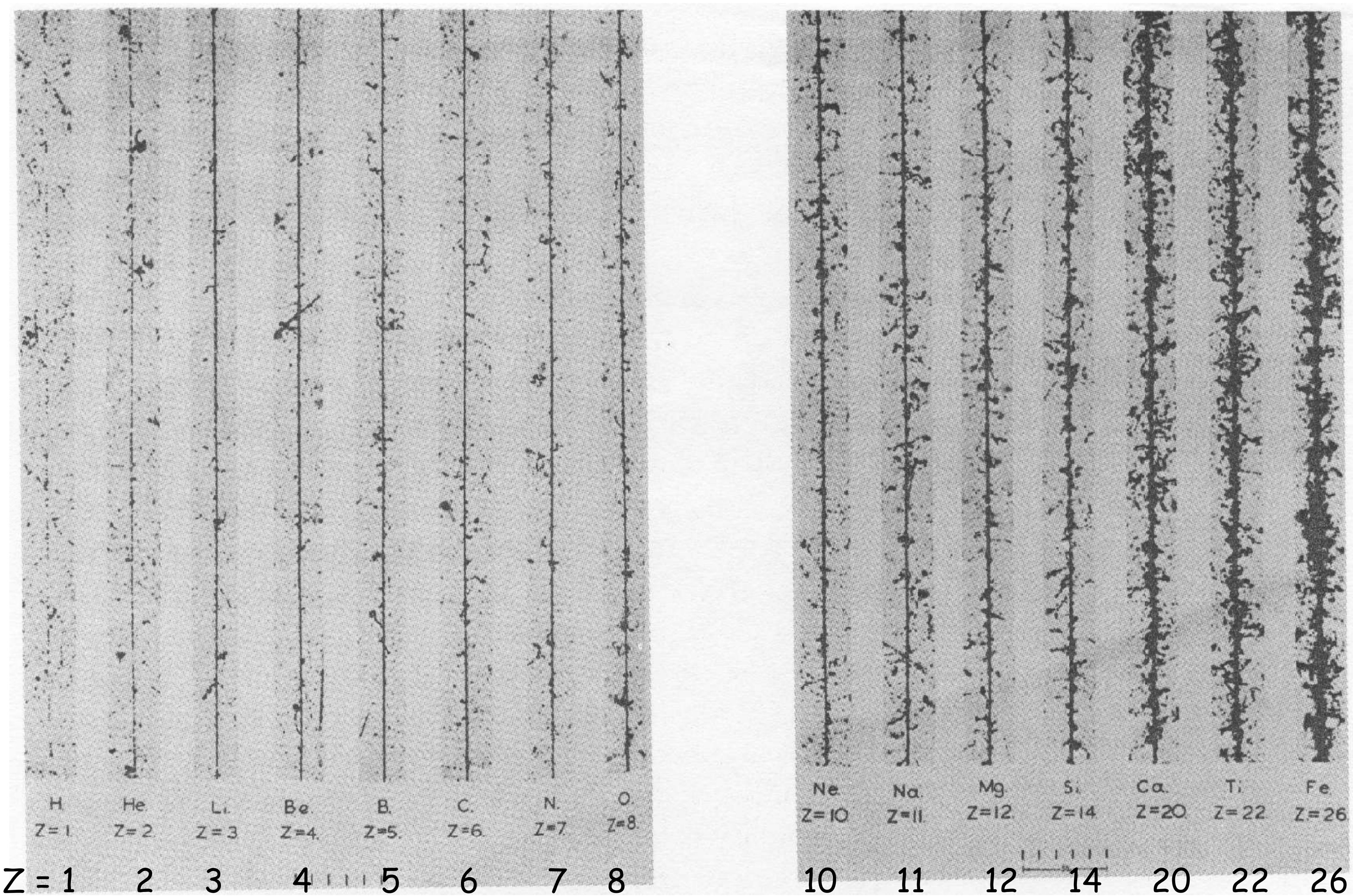

Figure 5.4
Tracks of fast primary cosmic rays, showing the dependence of their ionization on their charge. The number of grains and slow secondary electrons (δ-rays) increases with Z^2. (Photograph courtesy of Peter Fowler.)

Ionisation tracks seen in photographic emulsions as function of Z of the particle.

dE/dx for different nuclei

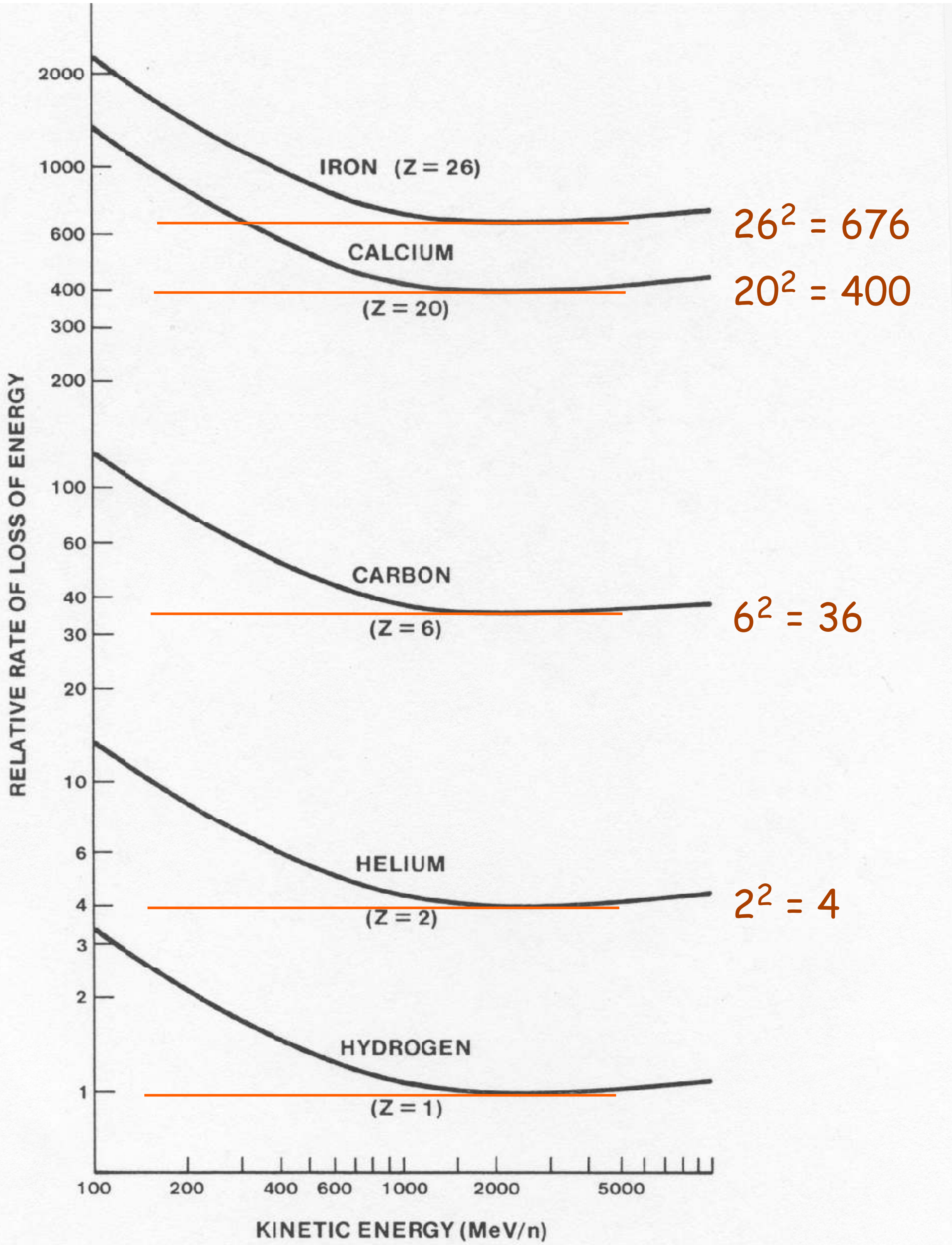

Figure 5.3 *Rates of energy loss shown for several particles with different charge (Z). The curves show the Z^2 dependence in their vertical spacing. From 100 to around 800 MeV/n, the energy loss rate decreases with the square of the particle's speed; after a broad minimum, the loss rate increases only slowly.*

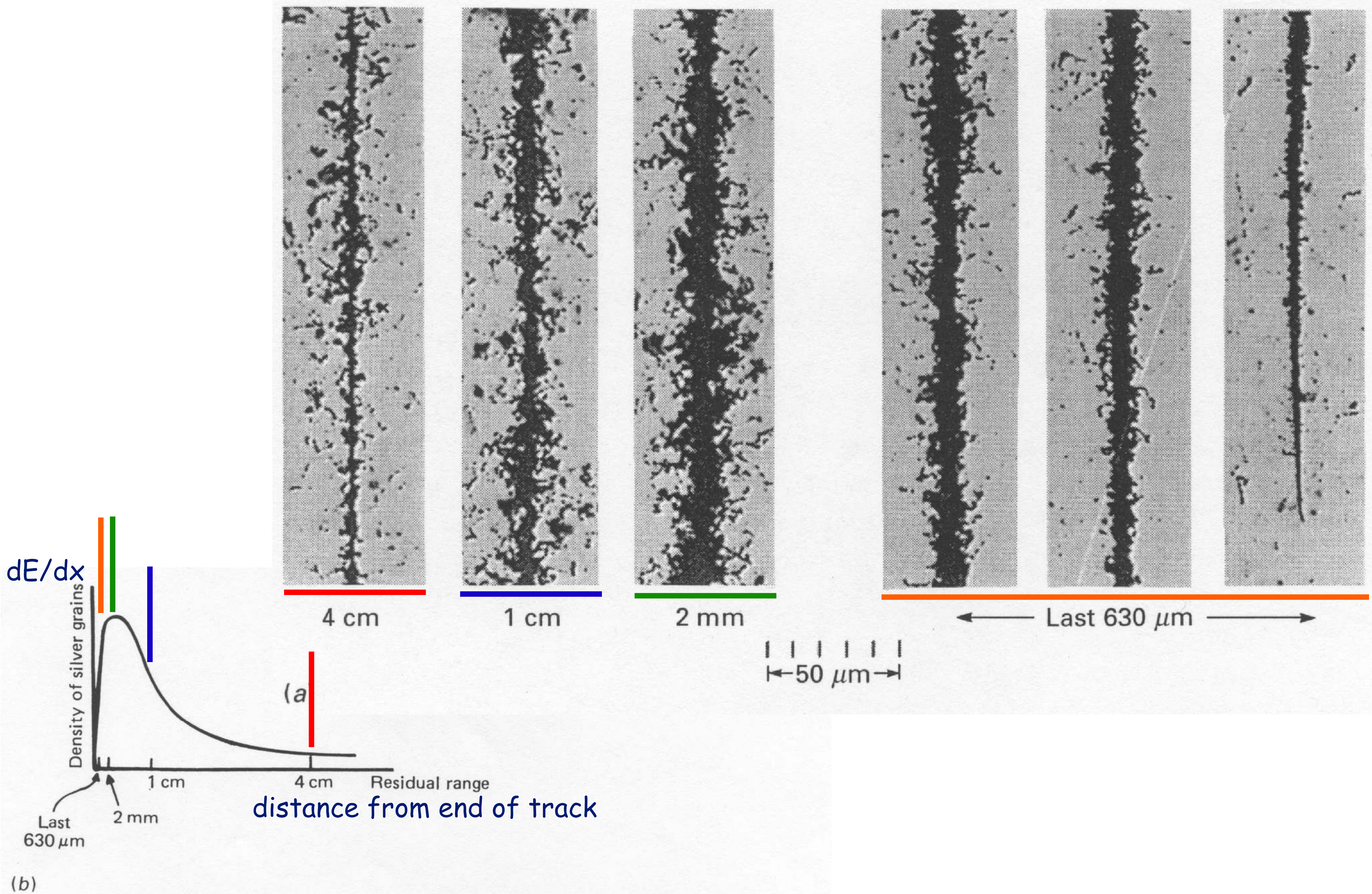

Figure 6.2. (*a*) Nuclear emulsion photographs of the track of a cosmic ray iron nucleus at various stages in its deceleration from relativistic velocities to rest. The distances are the residual ranges at which the track is observed; these positions are shown schematically in (*b*). (Photograph from M. M. Shapiro and R. Silberberg (1970). *Ann. Rev. Nucl. Sci.*, **20**, 328.)

Bremsstrahlung :

another energy loss mechanism for charged particles

Radiation is always emitted when charges are accelerated (or decelerated)

(imagine as transition between unbound states)

in magnetic fields: **synchrotron radiation**

in static electrical fields: **bremsstrahlung**

(e.g. field of a nucleus) (= braking radiation)

$$-\frac{dE}{dx} \sim \frac{Z(Z+1.3)\ E}{16\,\pi^3\,\varepsilon_0^3\,m^2\,c^4\hbar}\left[\ln\frac{183}{Z^{1/3}}+\frac{1}{8}\right]$$

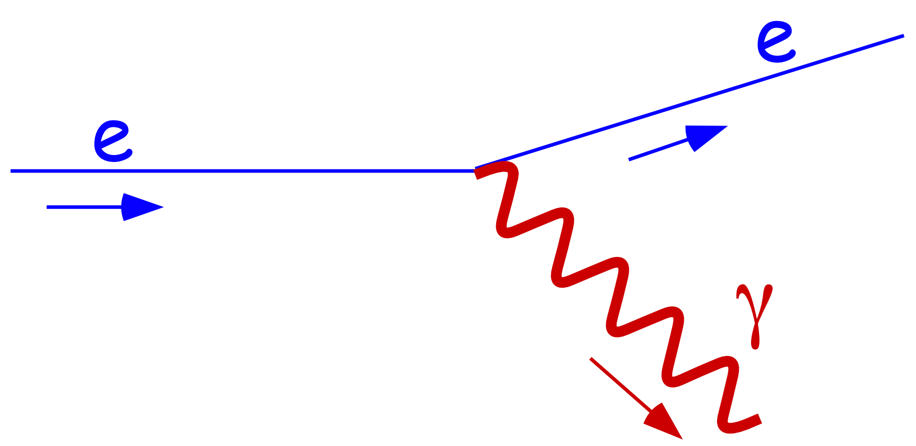

Bethe-Heitler

Z: charge of medium
E: energy of projectile
m: mass of projectile

(assume charge of projectile to be = 1 e)

$-dE/dx \sim Z^2\,E\,/\,m^2$ at energies < 100 GeV only important for electrons

$m_e/m_\mu = 1/200$ $(dE/dx)_e\,/\,(dE/dx)_\mu = 1/40000$

$-dE/dx \sim E$ i.e. exponential form of energy loss

$(\,E = E_0\exp(-x/X_0)\,;\ -dE/dx = E_0\,/X_0\,)$

radiation length X_0: path length on which the electron is slowed down to 1/e of its initial energy by bremsstrahlung

X_0 is characteristic length for a radiation process

(on 1 X_0, typically one bremsstrahlungs photon is emitted)

$$X_0 = \frac{716\ \mathrm{g/cm^2}\ A}{Z(Z+1.3)\,(\ln 183/Z^{1/3} + 1/8)}$$

from Bethe-Heitler formula

$$X_0 = \frac{716.4\ \mathrm{g/cm^2}\ A}{Z(Z+1.0)\,(\ln 287/Z^{1/2})}$$

from fit to experiment

(precise within 5% for H
and 2.5% for all other elements)

for small electron energies: loss by ionisation is dominant,
for large energies: loss by bremsstrahlung is dominant

critical energy E_{crit}: both loss rates are equal
(for electrons)

dividing line between ionisation and radiation regime
depends on form of ionisation and radiation loss

$E_{crit} \approx 610\ \mathrm{MeV}/(Z+1.24)$ in solids and liquids (± 2.2%)
$E_{crit} \approx 710\ \mathrm{MeV}/(Z+0.92)$ in gases (± 4%)
from experiments

E_{crit} for muons: analogue definition (but much higher energies)

$E_{crit} \approx 6224\ \mathrm{GeV}/(Z+2.05)^{0.876}$ in solids and liquids (± 4%)
$E_{crit} \approx 7788\ \mathrm{GeV}/(Z+2.01)^{0.888}$ in gases (± 1.4%)
10^4x higher than for e^-

Critical Energy as Function of Z of the Material

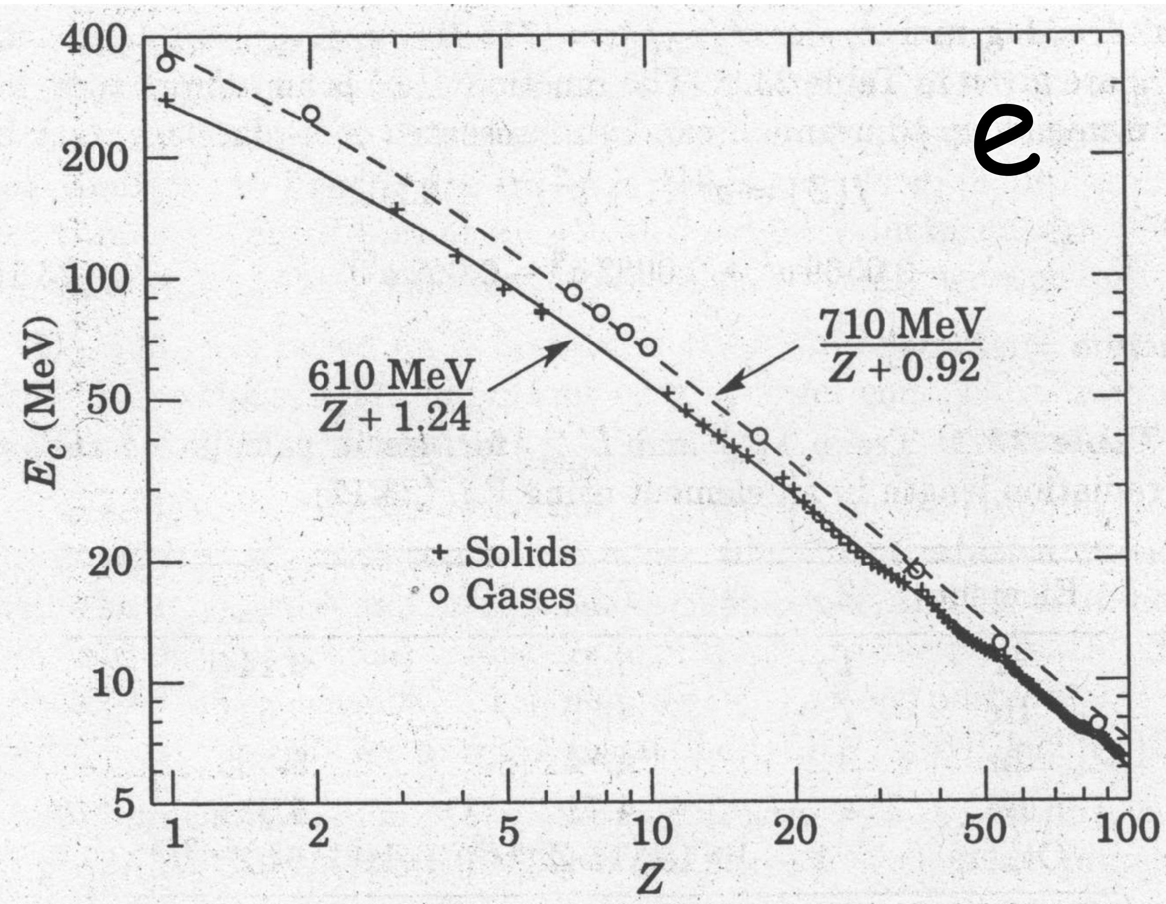

Figure 23.7: Electron critical energy for the chemical elements, using Rossi's definition [1]. The fits shown are for solids and liquids (solid line) and gases (dashed line). The rms deviation is 2.2% for the solids and 4.0% for the gases. (Computed with code supplied by A. Fassó.)

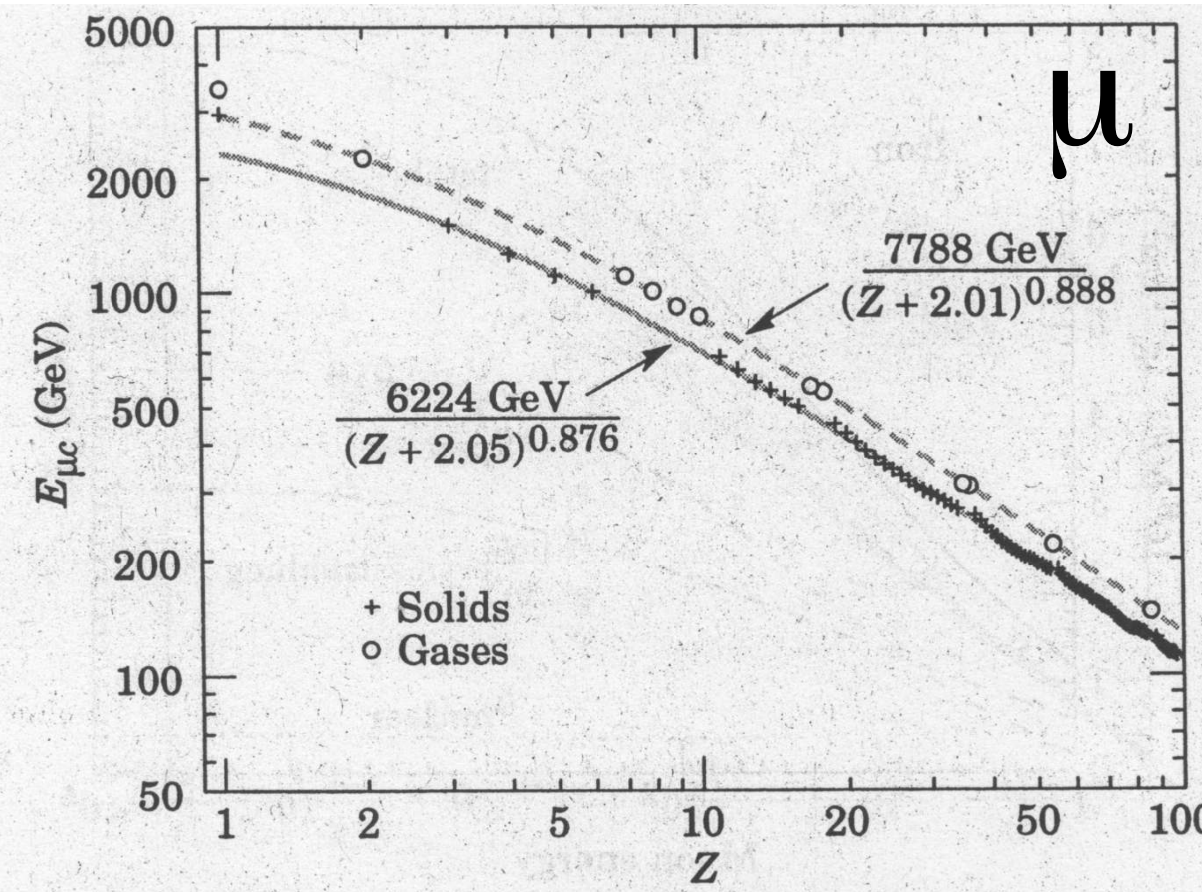

Figure 23.12: Muon critical energy for the chemical elements, defined as the energy at which radiative and ionization energy loss rates are equal. The equality comes at a higher energy for gases than for solids or liquids with the same atomic number because of a smaller density effect reduction of the ionization losses. The fits shown in the figure exclude hydrogen. Alkali metals fall 3–4% above the fitted function for alkali metals, while most other solids are within 2% of the function. Among the gases the worst fit is for neon (1.4% high). (Courtesy of N.V. Mokhov and S.I. Striganov.)

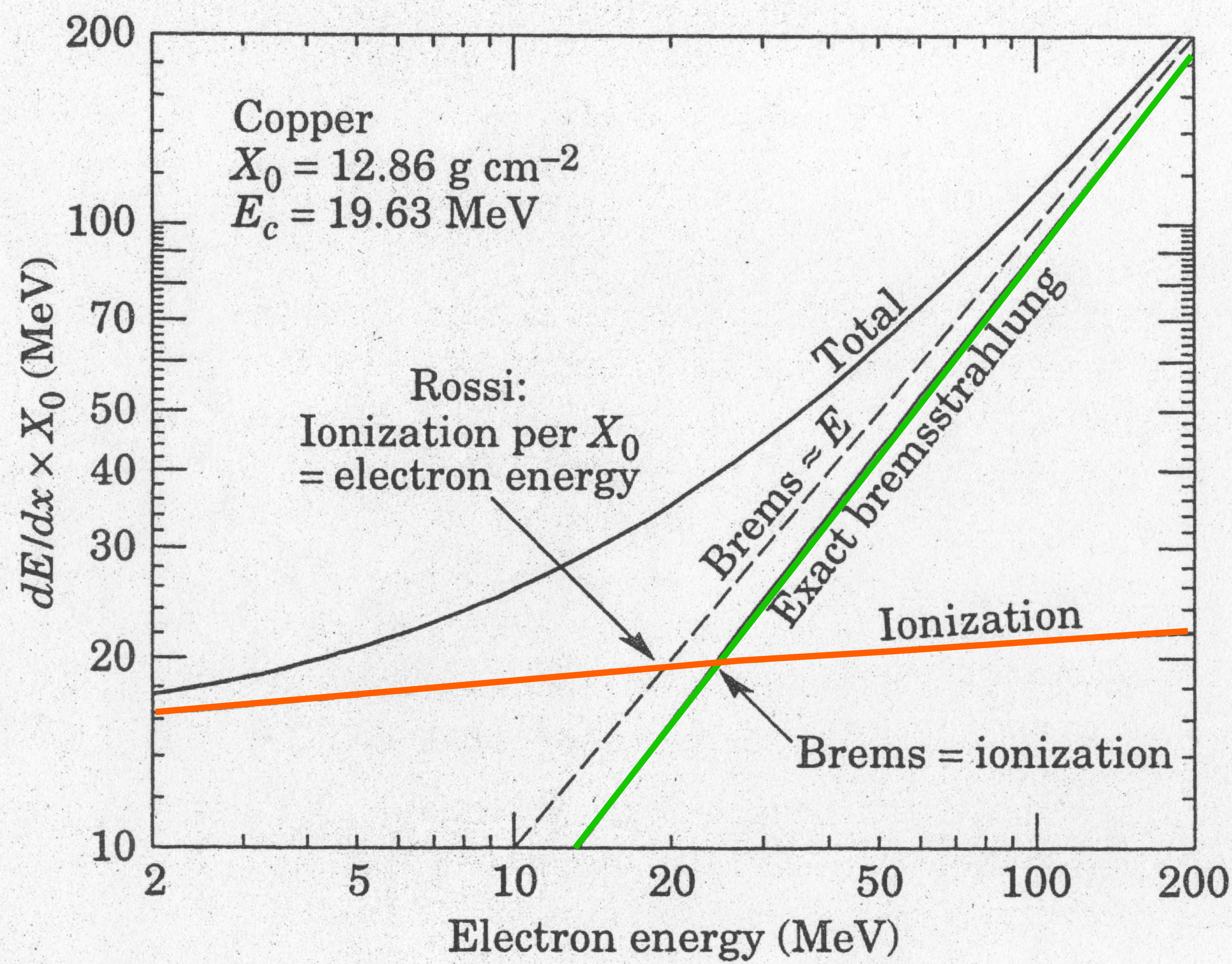

Figure 23.6: Two definitions of the critical energy E_c.

Some Values:

Elem.	Z	X_0 (g/cm^2)	X_0 (cm)	$E_{crit,e}$ (MeV)	$E_{crit,\mu}$ (GeV)	dE/dx (MeV/gcm^{-1})
H	1	61.28	865 *	370	2927	4.10
He	2	94.32	755 *	243	2269	1.94
C	6	42.70	18.8	84	1001	1.75
N	7	37.99	47.0*	90	1106	1.83
O	8	34.24	30.0*	80	1007	1.80
Fe	26	13.84	1.76	22	335	1.45
Pb	82	6.37	0.56	7.3	128	1.12
U	92	6.00	0.32	6.5	116	1.08

*gases: for density at standard conditions

Energy of radiated photons:

$$dN/E_\gamma \sim \frac{Z^2\, a^3\, h^2\, c^2}{m_e^{\,2}\, c^4\, E_\gamma} \sim 1/E_\gamma$$

i.e. $dN/E_\gamma \cdot E_\gamma = \text{const.}$

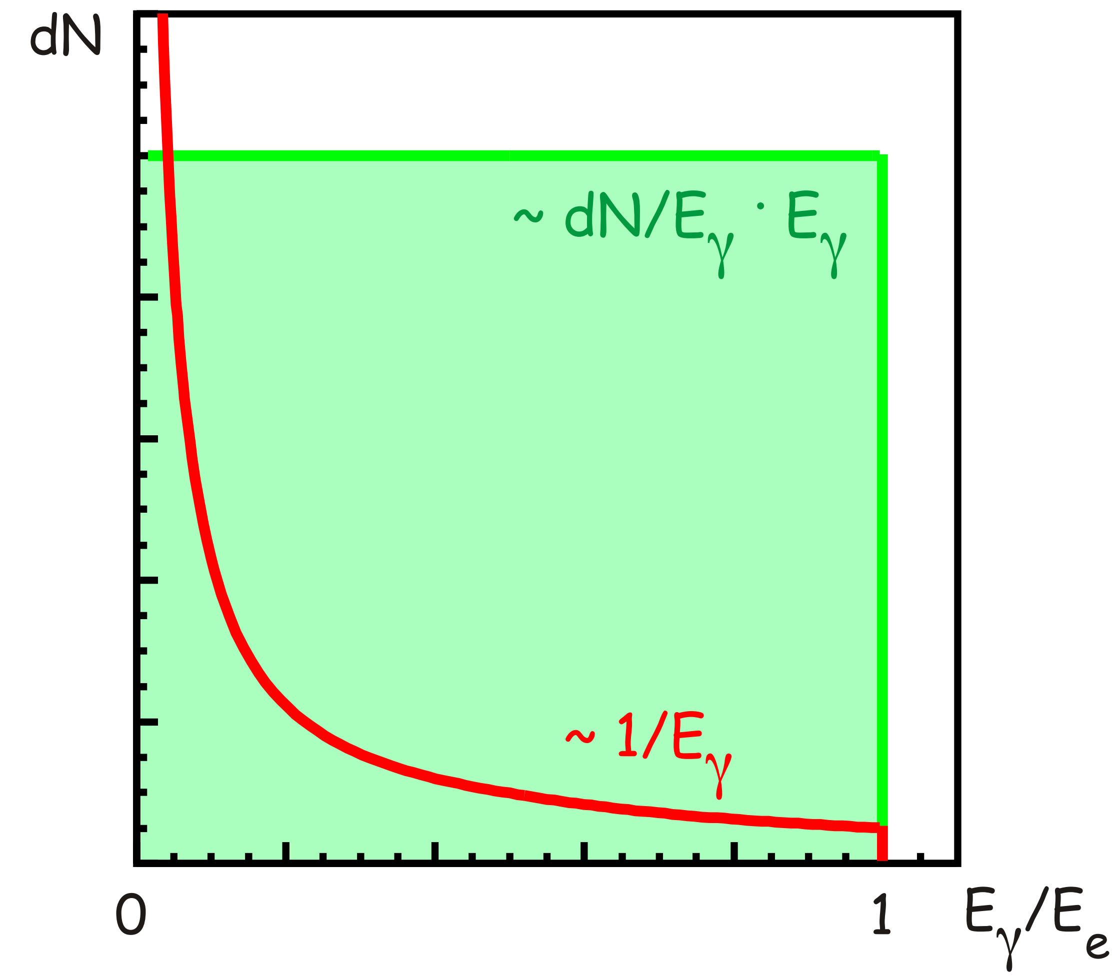

- Each energy interval receives on average same amount of energy.
- Radiation of photons with up to full electron energy E_e possible.

➔ catastrophic process !!!

(for ionisation: many, but always small losses,
i.e. continuous process)

total energy loss: sum of ionisation and radiation

$$-dE/dx = a \ln(E) + b\,E$$

6. ATOMIC AND NUCLEAR PROPERTIES OF MATERIALS

Table 6.1. Table revised June 1994. Gases are evaluated at 20°C, 1 atm, (in parentheses) or at STP [square brackets].

Material	Z	A	Nuclear[a] total cross section σ_T [barn]	Nuclear[b] inelastic cross section σ_I [barn]	Nuclear[c] collision length λ_T [g/cm^2]	Nuclear[c] interaction length λ_I [g/cm^2]	$dE/dx\vert_{\min}$[d] $\left[\frac{\text{MeV}}{\text{g/cm}^2}\right]$ () is for gas	Radiation length[e] X_0 [g/cm^2]	Radiation length[e] X_0 [cm] () is for gas	Density[f] [g/cm^3] () is for gas [g/ℓ]	Refractive index n[f] () is $(n-1)\times10^6$ for gas
H_2 gas	1	1.01	0.0387	0.033	43.3	50.8	(4.103)	61.28	865	(0.0838)[0.090]	[140]
H_2 (B.C., 26K)	1	1.01	0.0387	0.033	43.3	50.8	4.045	61.28	865	0.0708	1.112
D_2	1	2.01	0.073	0.061	45.7	54.7	(2.052)	122.6	757	0.162[0.177]	1.128
He	2	4.00	0.133	0.102	49.9	65.1	(1.937)	94.32	755	0.125[0.178]	1.024[35]
Li	3	6.94	0.211	0.157	54.6	73.4	1.639	82.76	155	0.534	—
Be	4	9.01	0.268	0.199	55.8	75.2	1.594	65.19	35.3	1.848	—
C	6	12.01	0.331	0.231	60.2	86.3	1.745	42.70	18.8	2.265[g]	—
N_2	7	14.01	0.379	0.265	61.4	87.8	(1.825)	37.99	47.0	0.808[1.25]	1.205[300]
O_2	8	16.00	0.420	0.292	63.2	91.0	(1.801)	34.24	30.0	1.14[1.43]	1.22[266]
Ne	10	20.18	0.507	0.347	66.1	96.6	(1.724)	28.94	24.0	1.207[0.900]	1.092[67]
Al	13	26.98	0.634	0.421	70.6	106.4	1.615	24.01	8.9	2.70	—
Si	14	28.09	0.660	0.440	70.6	106.0	1.664	21.82	9.36	2.33	—
Ar	18	39.95	0.868	0.566	76.4	117.2	(1.519)	19.55	14.0	1.40[1.782]	1.233[283]
Ti	22	47.88	0.995	0.637	79.9	124.9	1.476	16.17	3.56	4.54	—
Fe	26	55.85	1.120	0.703	82.8	131.9	1.451	13.84	1.76	7.87	—
Cu	29	63.55	1.232	0.782	85.6	134.9	1.403	12.86	1.43	8.96	—
Ge	32	72.59	1.365	0.858	88.3	140.5	1.371	12.25	2.30	5.323	—
Sn	50	118.69	1.967	1.21	100.2	163	1.264	8.82	1.21	7.31	—
Xe	54	131.29	2.120	1.29	102.8	169	(1.255)	8.48	2.77	3.057[5.858]	[705]
W	74	183.85	2.767	1.65	110.3	185	1.145	6.76	0.35	19.3	—
Pt	78	195.08	2.861	1.708	113.3	189.7	1.129	6.54	0.305	21.45	—
Pb	82	207.19	2.960	1.77	116.2	194	1.123	6.37	0.56	11.35	—
U	92	238.03	3.378	1.98	117.0	199	1.082	6.00	≈0.32	≈18.95	—
Air, (20°C, 1 atm.), [STP]					62.0	90.0	(1.815)	36.66	[30420]	(1.205)[1.29]	(273)[293]
H_2O					60.1	84.9	1.991	36.08	36.1	1.00	1.33
CO_2					62.4	90.5	(1.819)	36.2	[18310]	[1.977]	[410]
Shielding concrete[h]					67.4	99.9	1.711	26.7	10.7	2.5	—
Borosilicate glass (Pyrex)[ℓ]					66.2	97.6	1.695	28.3	12.7	2.23	1.474
SiO_2 (fused quartz)[m]					67.0	99.2	1.697	27.05	11.7	2.32[m]	1.458
Methane (CH_4)					54.7	74.0	(2.417)	46.5	[64850]	0.423[0.717]	[444]
Ethane (C_2H_6)					55.73	75.71	(2.304)	45.66	[34035]	0.509(1.356)[n]	(1.038)[n]
Propane (C_3H_8)					—	—	(2.262)	—	—	(1.879)	
Isobutane ($(CH_3)_2CHCH_3$)					56.3	77.4	(2.239)	45.2	[16930]	[2.67]	[1900]
Octane, liquid ($CH_3(CH_2)_6CH_3$)					—	—	2.123	—	—	0.703	
Paraffin wax ($CH_3(CH_2)_nCH_3$, $\langle n\rangle \approx 25$)					—	—	2.087	—	—	0.93	
Nylon, type 6					—	—	1.974	—	—	1.14	
Polycarbonate (Lexan)					—	—	1.886	—	—	1.200	
Polyethylene terephthlate (Mylar) ($C_5H_4O_2$)					60.2	85.7	1.848	39.95	28.7	1.39	—
Polyethylene (monomer $CH_2=CH_2$)					56.9	78.8	2.076	44.8	≈47.9	0.92–0.95	—
Polyimide film (Kapton)					—	—	1.820	—	—	1.420	
Polymethylmethacralate (Lucite, Plexiglas) (monomer ($CH_2=C(CH_3)CO_2CH_3$))					59.2	83.6	1.929	40.55	≈34.4	1.16–1.20	≈1.49
Polystyrene, scintillator (monomer $C_6H_5CH=CH_2$)					58.4	82.0	1.936	43.8	42.4	1.032	1.581
Polytetrafluoroethylene (Teflon) (monomer $CF_2=CF_2$)					—	—	1.671	—	—	2.20	
Polyvinyltolulene, scintillator (monomer 2-$CH_3C_6H_4CH=CH_2$)					—	—	1.956	—	—	1.032	
Barium fluoride (BaF_2)					92.1	146	1.303	9.91	2.05	4.89	1.56
Bismuth germanate (BGO) ($Bi_4Ge_3O_{12}$)					97.4	156	1.251	7.98	1.12	7.1	2.15
Cesium iodide (CsI)					—	—	1.243	—	—	4.51	
Lithium fluoride (LiF)					62.00	88.24	1.614	39.25	14.91	2.632	1.392
Sodium fluoride (NaF)					66.78	97.57	1.69	29.87	11.68	2.558	1.336
Sodium iodide (NaI)					94.8	152	1.305	9.49	2.59	3.67	1.775
Silica Aerogel[o]					65.5	95.7	1.83	29.85	≈150	0.1–0.3	1.0+0.25ρ
NEMA G10 plate[p]					62.6	90.2	1.87	33.0	19.4	1.7	—

dE/dx X_0 ρ

Multiple scattering:

particles are interacting many times when passing through matter.

each interaction is connected with a small deflection

(the lighter the particle the larger the scattering: largest effect for electrons)

Result: approx. Gaussian distribution of scattering angles

$$\frac{dN}{d\theta_{space}} = \frac{1}{2\,\pi\,\theta_0^2}\,\exp - \frac{\theta_{space}^2}{2\,\theta_0^2}$$

$$\frac{dN}{d\theta_{plane}} = \frac{1}{\sqrt{2\,\pi}\,\theta_0}\,\exp - \frac{\theta_{plane}^2}{2\,\theta_0^2}$$

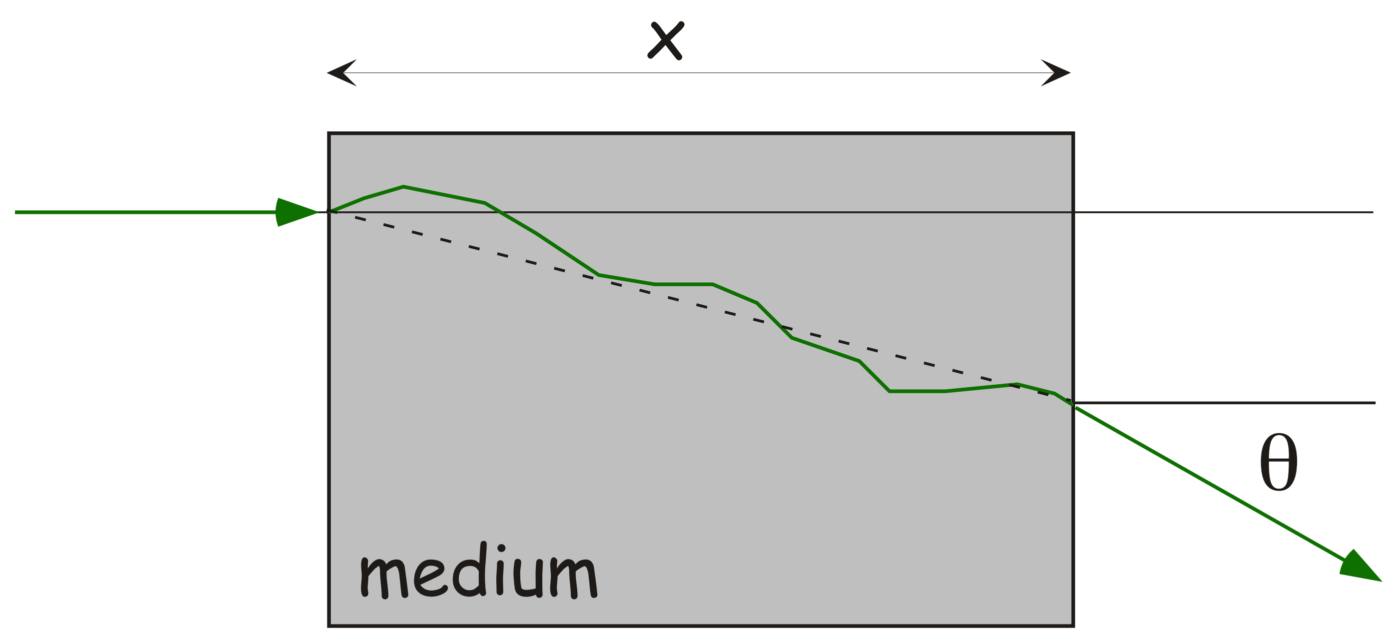

θ_0 : width of distribution

$$\theta_0 = \frac{13.6\text{ MeV}}{\beta\, c\, p}\; z\,\sqrt{x/X_0}\,(1+0.038\,\ln(x/X_0))$$

in rad

x/X_0	thickness of scattering material in units of X_0
$\theta_0 \sim 1/p$	small deflections for large momenta

distinguish space and plane: $\theta_{space}^2 \approx \theta_{plane,y}^2 + \theta_{plane,z}^2$

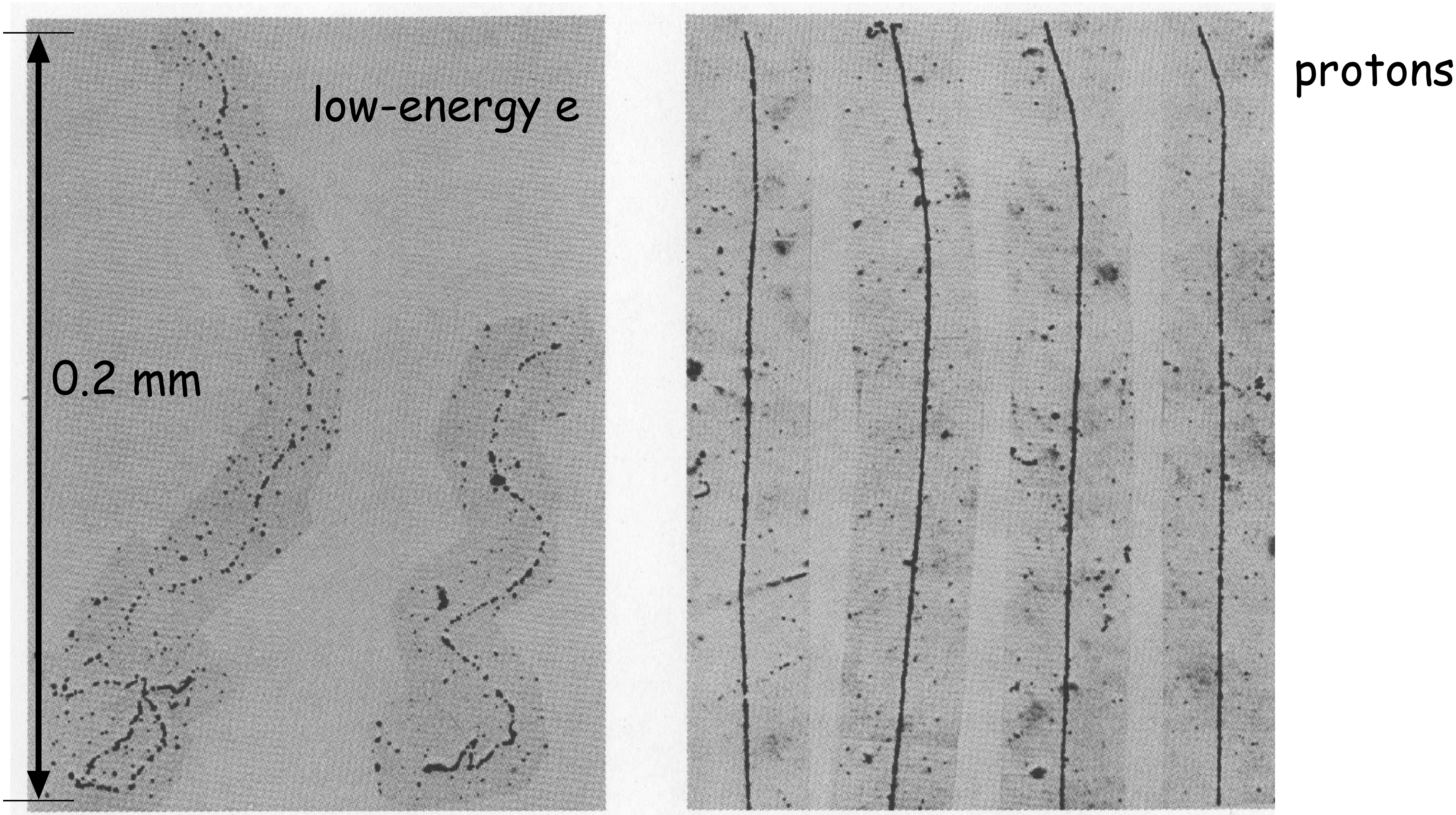

Figure 2.4 *(left) Tracks of slow electrons showing the large amounts of multiple scattering that result from the electrons' small mass. Note also the increase in ionization as the electrons slow down. The tracks shown are about 0.2 mm long. (right) Proton tracks (about 0.2 mm long) generally show a much higher degree of ionization and are much straighter, even to the very end where they stop (at top of photo). (Photograph courtesy of Peter Fowler, University of Bristol.)*

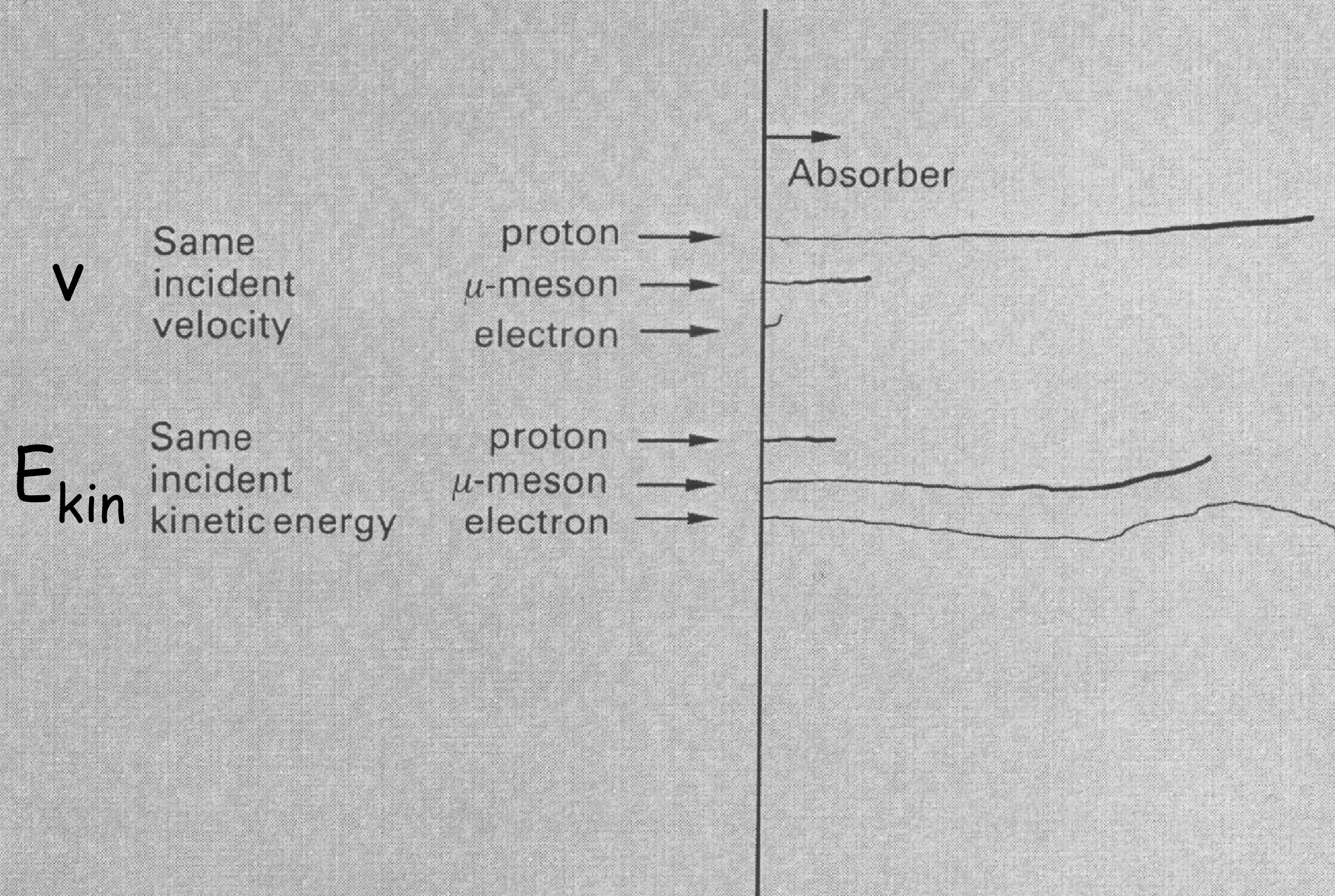

Fig. 11.5 Sketches showing typical paths for protons, μ-mesons and electrons coming to rest in an absorber (kinetic energies of a few megaelectronvolts). The electrons are lightest and suffer the greatest multiple scattering. As described in the text, for the same incident velocity the stopping power is initially the same and the most energetic particles, the protons, have the greatest range. For the same incident kinetic energy the stopping power is least for the electrons and therefore their path length is greatest. These remarks apply only at energies low enough that there are no energy-loss mechanisms other than loss by ionization. The length of the last electron path is under-represented.

Cherenkov Radiation:

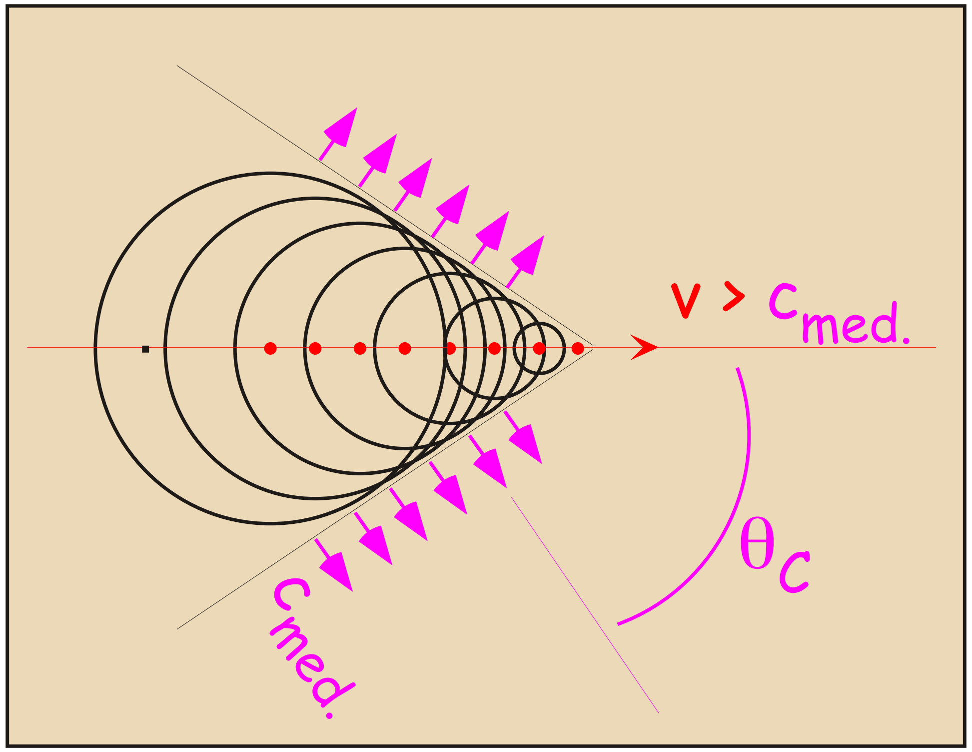

in medium : refractive index $n = c_{vac.} / c_{med.}$

If a **charged** particle moves faster than $c_{med.}$,

then it emits "Cherenkov light".

$v > c_{med.}$ (or $\beta = v/c_{vac.} > c_{med.}/c_{vac.} = 1/n$

or $n\beta > 1$)

(similar to bang of supersonic airplane)

emission angle: $\cos\theta_C = c_{med.}/v = 1/n\beta \leq 1$

for $v = c_{med.} + \varepsilon : \theta_C \approx 0$

for $v = c_{vac.}$: $\theta_C = \cos^{-1}(1/n)$

number of photons: $$\frac{d^2N_c}{ds\, d\lambda} = 2\pi\alpha \sin^2\theta_C \frac{z^2}{\lambda^2}$$

energy: blue - ultraviolet, $\approx$ 10 eV,
peak at short wavelengths

energy loss negligible compared to ionisation

blue glow in nucl. reactor

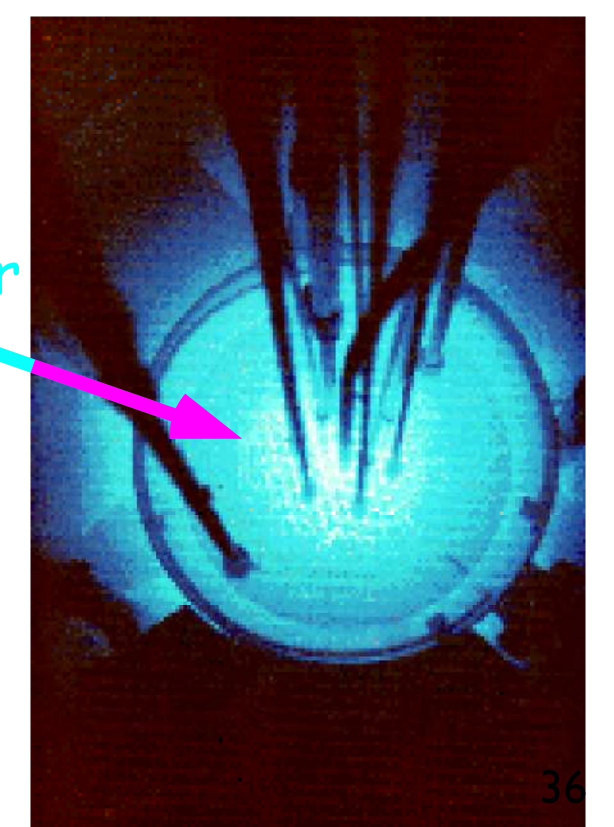

applications: θ_C measures β of particle

N_c measures z^2, if θ_C and λ are known

is important for particle identification

Interactions of Photons (γ) with Matter I:

Photoelectric effect:

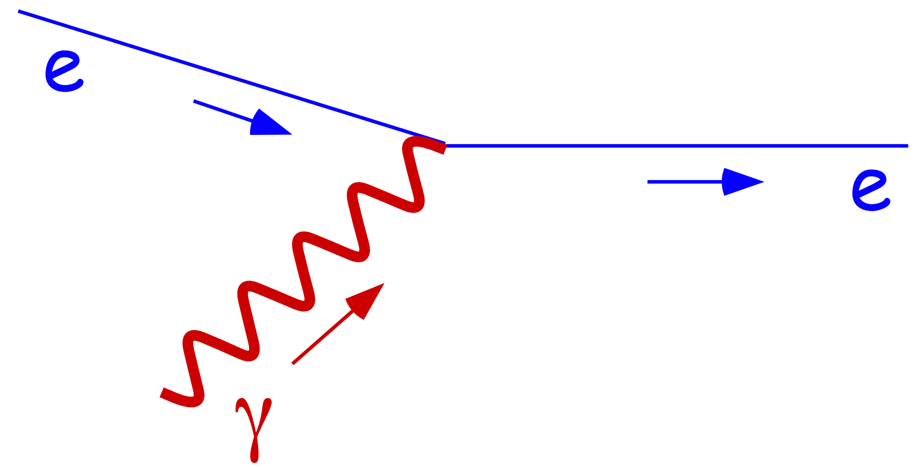

$$E_\gamma = h\nu > E_B$$

binding energy of electron

photon is absorbed, e^- is set free with kin. energy $h\nu - E_B$

for $E_B \ll E\gamma \ll m_e c^2$ photoeffect from k-shell dominant

$$\boxed{\sigma_k = \frac{e^{12}\, m_e^{3/2}}{192\sqrt{2}\pi^5\, \varepsilon_0^{\,6}\, c\, \hbar^4} \; \frac{Z^5}{(h\nu)^{7/2}}}$$

$=7/2$ if $E_\gamma < m_e c^2$

$=1$ if $E_\gamma \gg m_e c^2$

reaction probability ("cross section")

strong rise with Z, decrease with E_γ

electrons from many shells available:

shell structure reflected in reaction probability

The higher the reaction probability,
the smaller the average path length to the next reaction:

$$\lambda \sim 1/\sigma$$

Nobel Prize A. Einstein 1905:
"particle nature of light"

for waves:
energy of released e- should grow with intensity since $I \sim E^2$ and $F \sim e\,E$

observed (big surprise):
electron energy depends only on photon frequency !
This means: light comes in "energy packets" of $E_\gamma = h\nu$ (i.e. like a particle).
"Quanta" give natural explanation of experimental results.

Interactions of Photons with Matter II:

Nobel Prize A.H. Compton 1927: "for his effect, confirming the particle nature of light"

Compton effect:

- photon is scattered at a "quasi free" (i.e. loosely bound) electron
- photon looses, e^- gaines energy
  energy change depends on γ scattering angle:

$$\frac{\Delta\lambda}{\lambda_i} = \frac{\lambda_f - \lambda_i}{\lambda_i} = \frac{h\nu}{m_e c^2}(1 - \cos\theta)$$

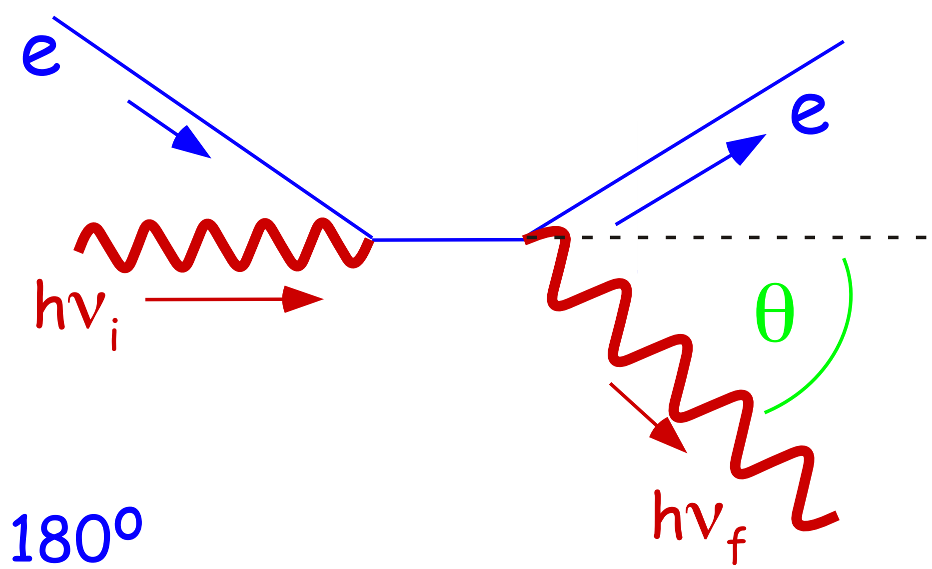

- maximum change (i.e. max. electron energy) : $\theta = 180^o$
-

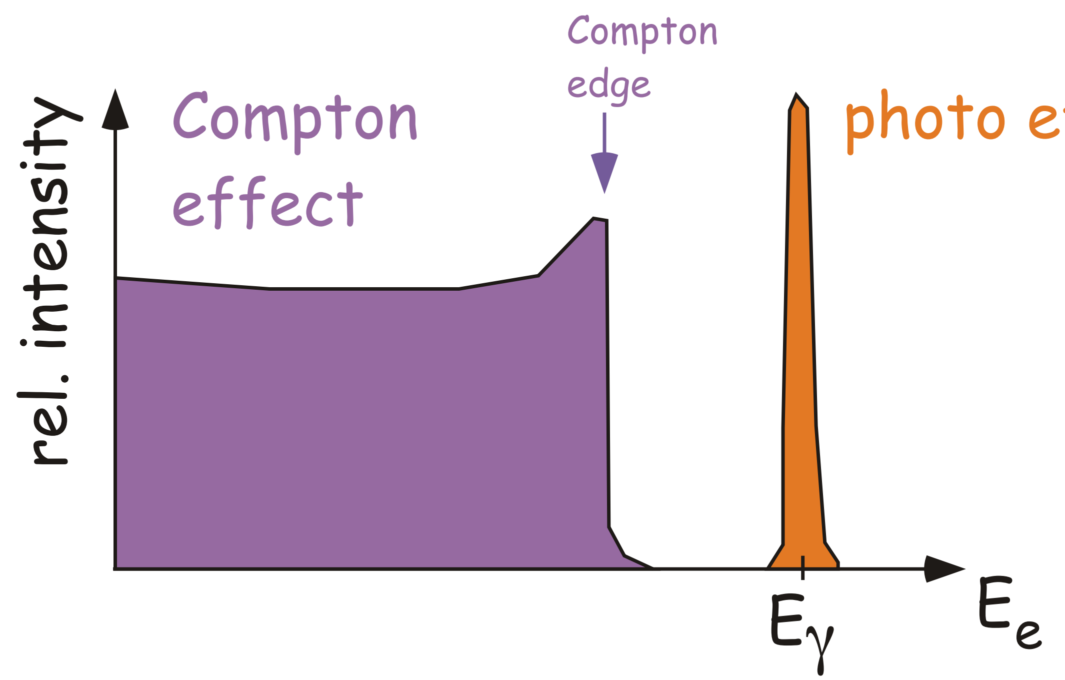

Electron energy E_e is what can be measured !

photo effect: (almost) all energy
Compton effect: only part of energy transferred onto electron

- $\sigma_C \sim \ln(E_\gamma) / E_\gamma$ maximal for $E_\gamma \approx 0.1 - 1$ MeV

Interactions of Photons with Matter III:

e^+e^- pair production:

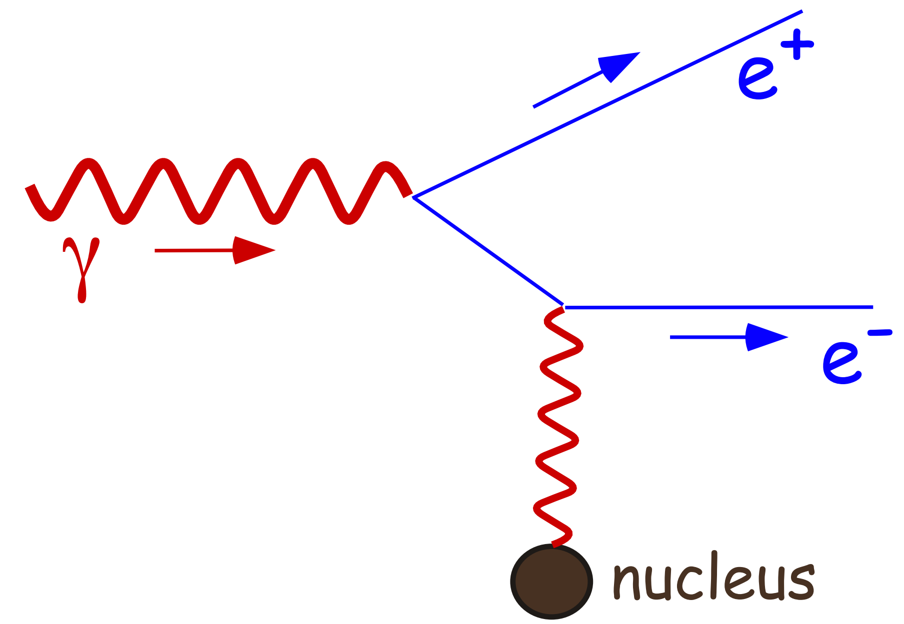

- $\gamma \longrightarrow e^+e^-$ photon is absorbed, e^+e^- pair is produced (only possible if a nucleus takes some momentum)
- $E_\gamma > 2\, m_e c^2 = 1.022$ MeV
- $$\boxed{\sigma_{pair} \sim \frac{28}{9} \frac{Z^2 \alpha^3 (\hbar c)^2}{(m_e c^2)^2} \left[\ln \frac{183}{Z^{1/3}} - \frac{2}{7} \right]}$$ limit for large energies, i.e. $E_\gamma \gg m_e c^2$

  reaction probability ("cross section")
- mean free path $\lambda_{pair} \approx \frac{9}{7}\, \lambda_{brems} \approx \frac{9}{7}\, X_0$ same length scale than bremsstrahlung

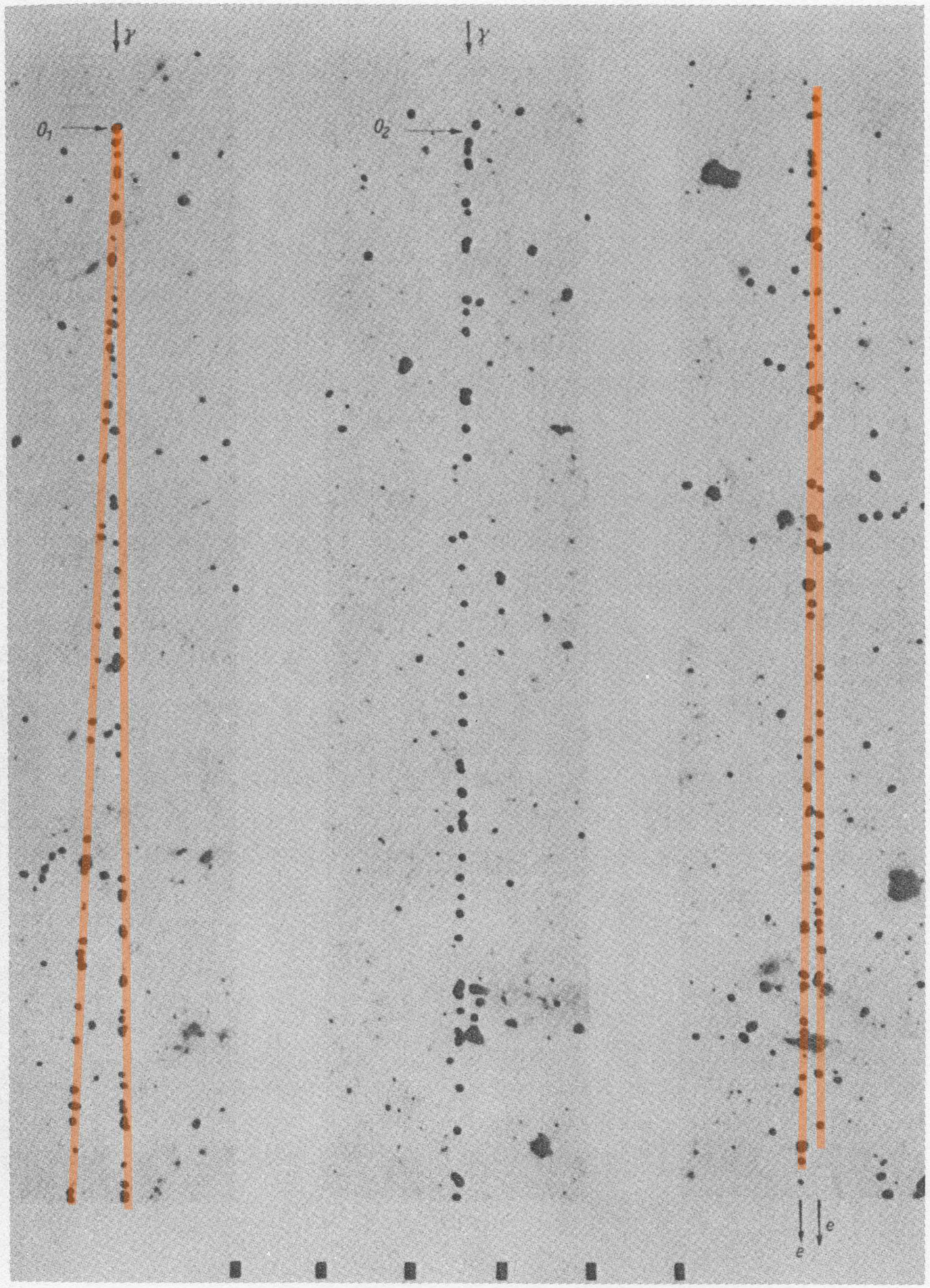

Figure 5.8 *Electron pairs produced by gamma ray photons. At the point where a gamma ray is converted into an electron-positron pair, the two particles are very close together. Their separate tracks can be seen after a short distance. (Photograph courtesy of Peter Fowler.)*

pair production

$\gamma \rightarrow e^{+} + e^{-}$

EGRET: a pair-production γ ray telescope

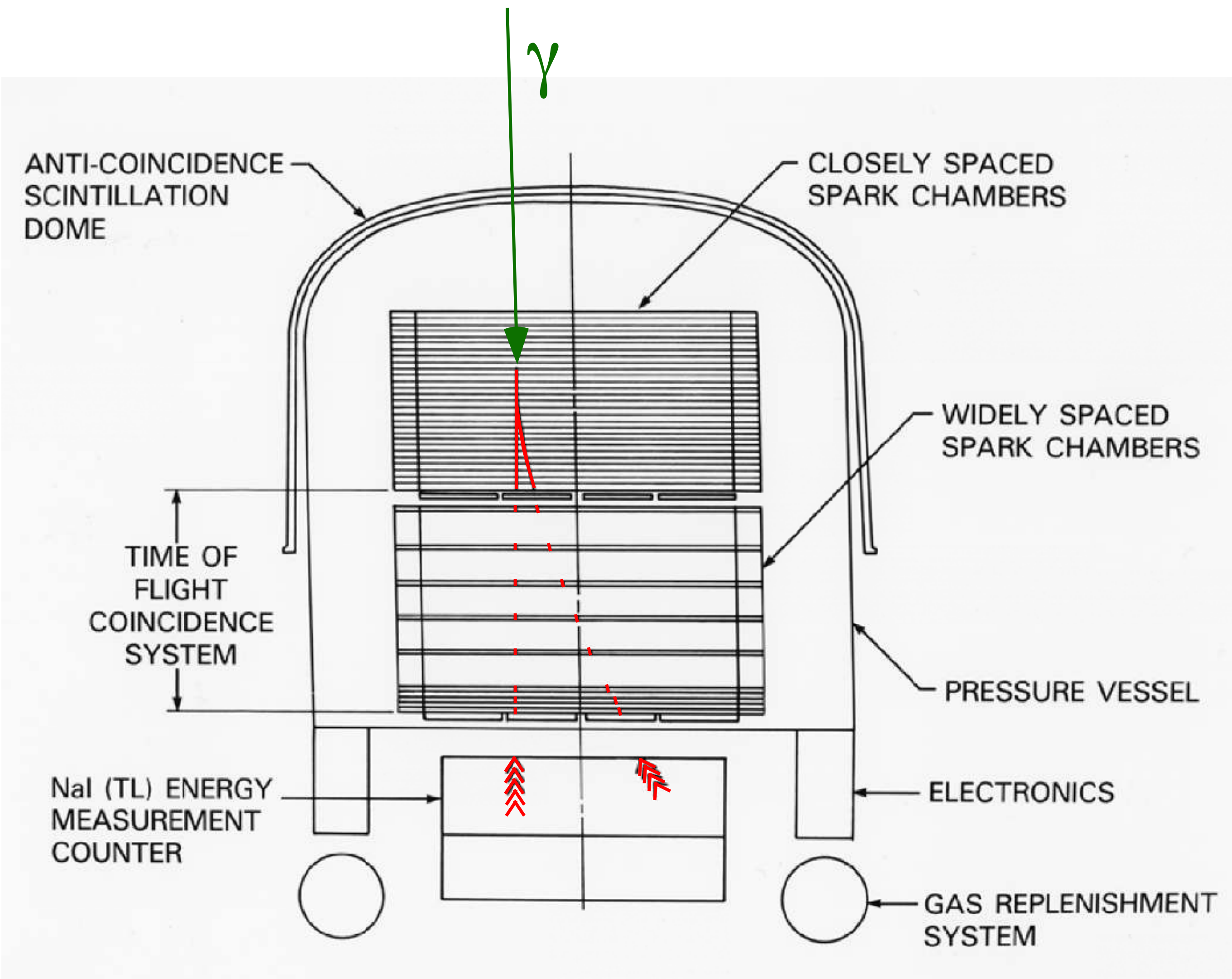

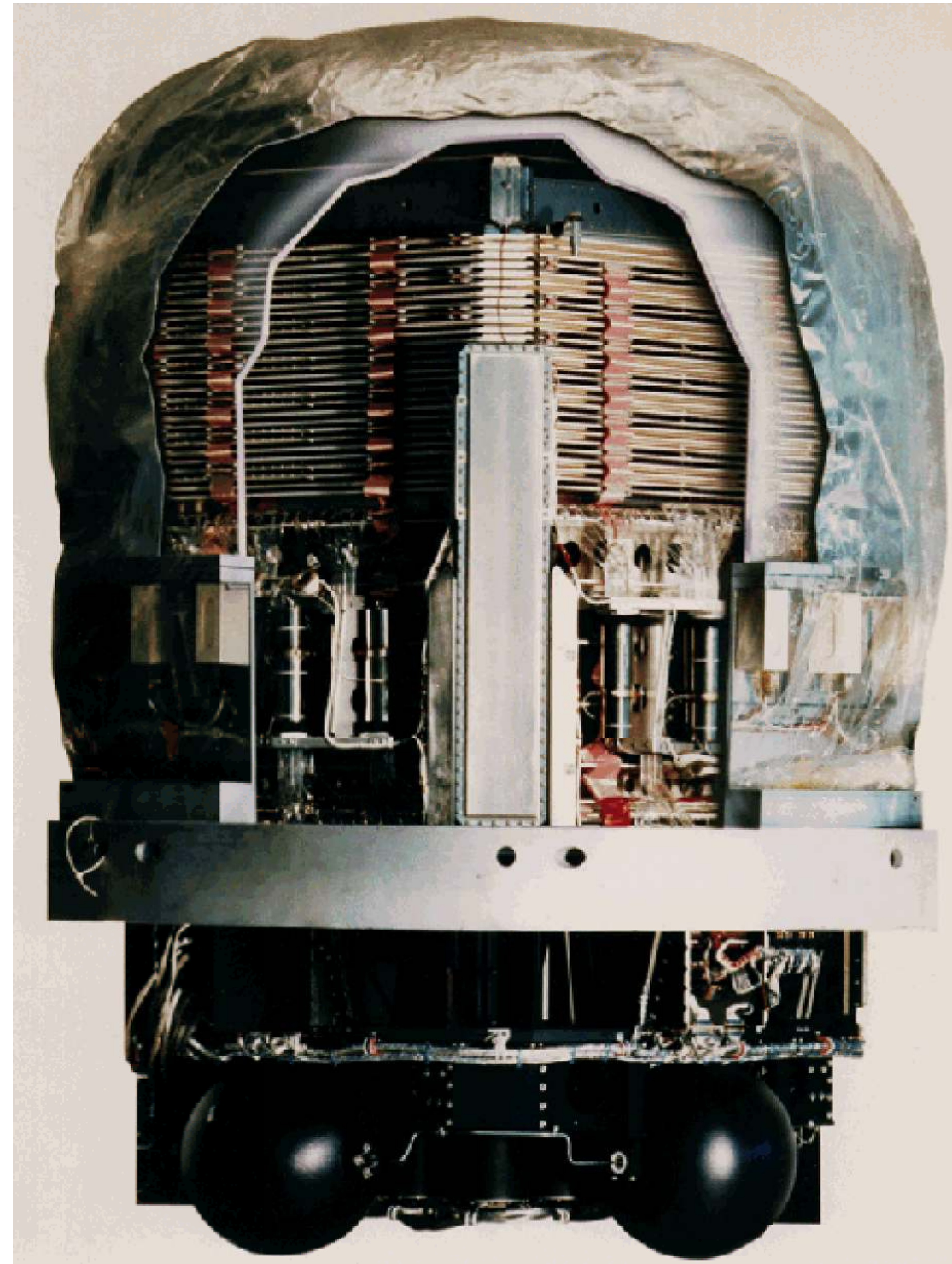

electromagnetic showers:

bremsstrahlung: $e \longrightarrow e + \gamma$

pair production: $\gamma \longrightarrow e^+ + e^-$

cascade of secondaries

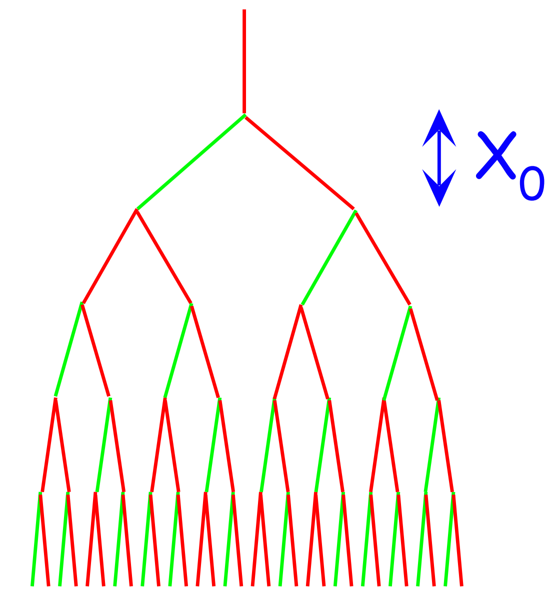

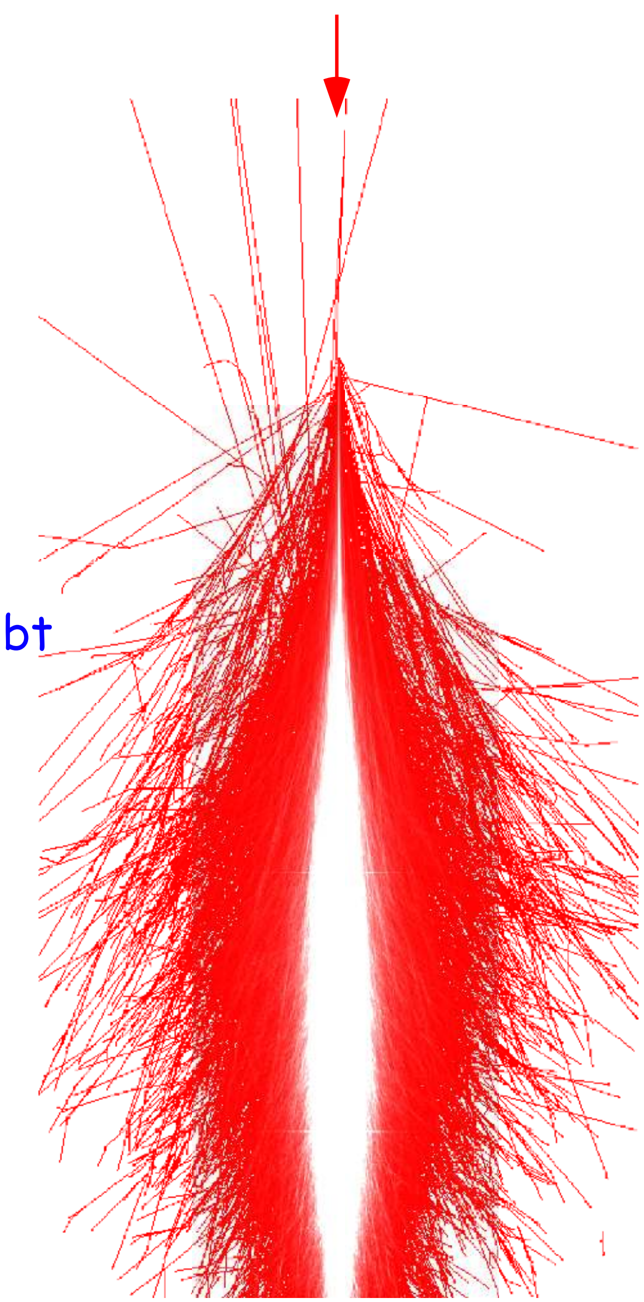

very simple model:

each step doubles particle number until $E < E_{crit}$

then ionisation takes over

$N \sim 2^t \qquad t = x/X_0$

$E \sim E_0/2^t$

$N_{max} \sim E_0/E_{crit}$

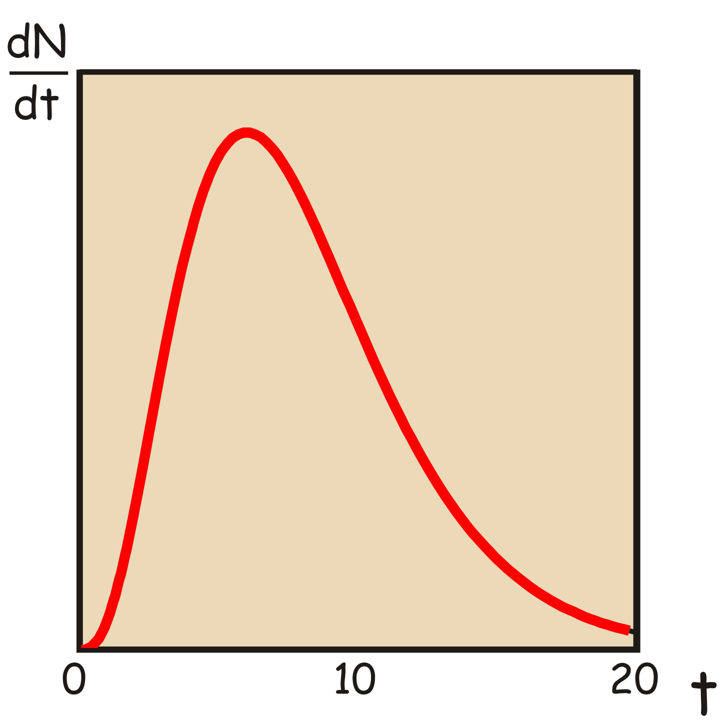

$$\frac{dN}{dt} \sim \frac{dE}{dt} = E_0\, b\, \frac{(bt)^{a-1}\, e^{-bt}}{\Gamma(a)} \sim t^a\, e^{-bt}$$

typical shower curve (a, b, E_0 are parameters)

width of shower:

cylinder with radius

$R_M = X_0$ 21 MeV / E_{crit}

contains 90% of energy

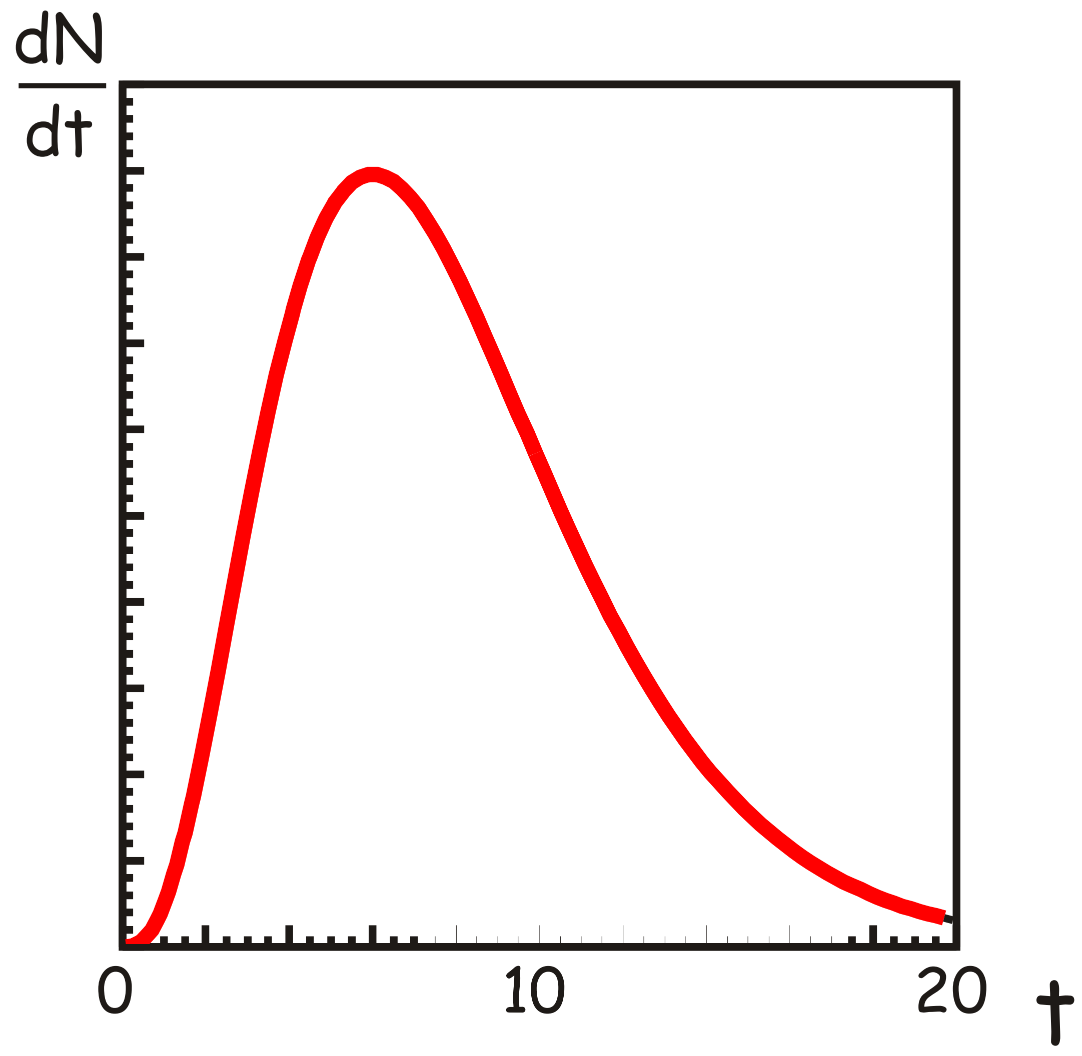

Energy of the primary particle:
from integral over the measured profile

$$E_0 = \text{const.} \times \int \frac{dN}{dt}\, dt$$

from calibration in the lab.

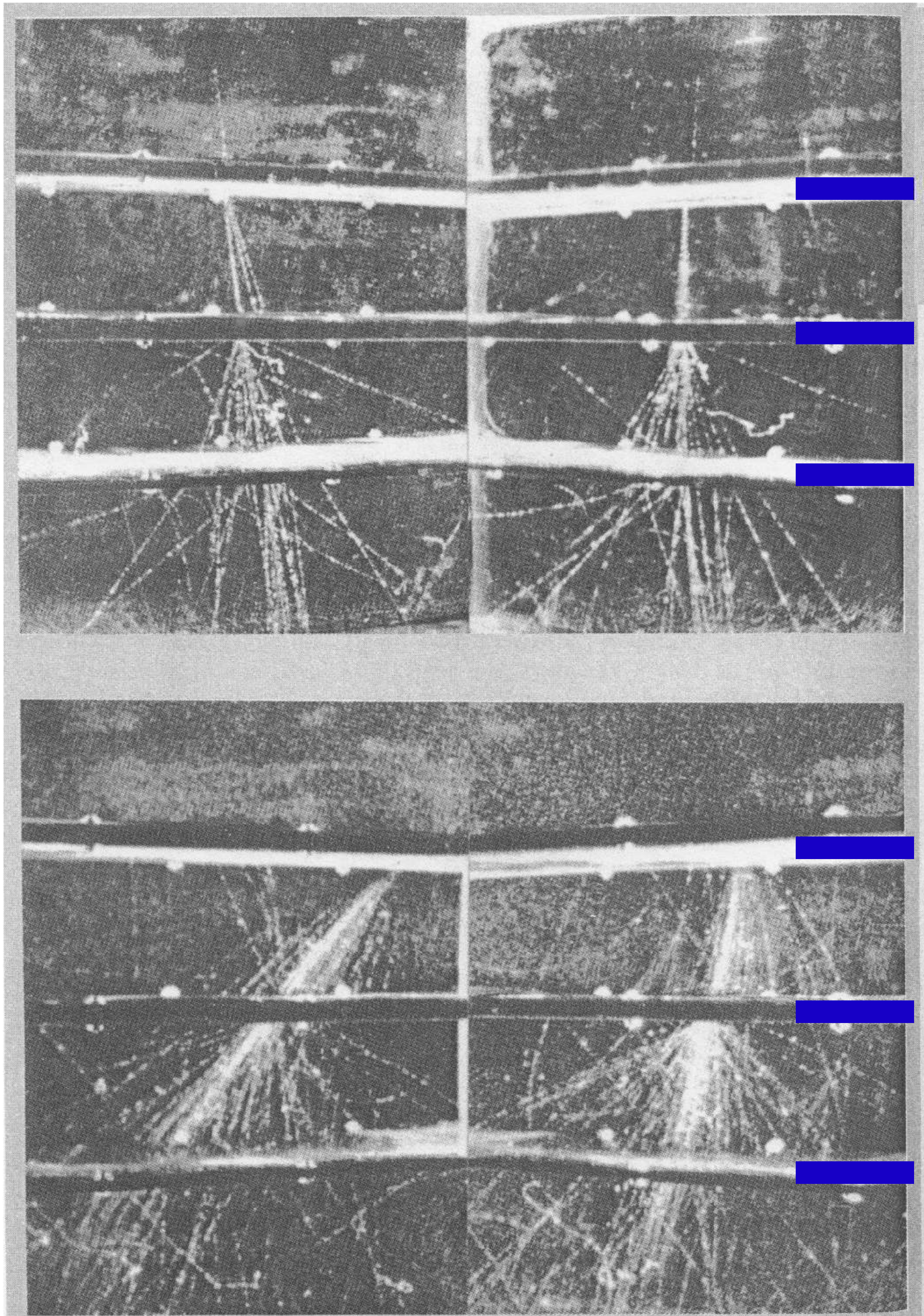

Fig. 11.8 Two cloud-chamber photographs of electromagnetic showers developing in lead plates (thicknesses from top down 1.1, 1.1, and 0.13 radiation lengths) placed within the chamber which was exposed to cosmic radiation at sea level. There are two views in each photo, obtained by aiming the camera so that it sees simultaneously directly and via a mirror into the chamber. The lower photograph shows a shower which was either started by a photon or missed the sensitive region above the top plate. In both, the growth and attenuation of the shower is evident. Note that many of the tracks have systematic curvature or distortion, probably due to some difficulty in maintaining stable and uniform temperature conditions in the chamber. These photographs were obtained by L. Fussel and used in a talk by J. C. Street which was published in 1939.

Absorber plates

$$\sigma_{photo} \sim \frac{1}{E\gamma}$$

$E_\gamma \leq 0.1$ MeV

$$\sigma_{Compton} \sim \frac{\ln E\gamma}{E\gamma}$$

0.1 MeV $\leq E_\gamma \leq$ 10 MeV

$$\sigma_{pair} \approx \frac{Z^2 \alpha^3}{(m_e c^2)^2}$$

$E_\gamma \geq$ 10 MeV

Contributions to Photon Cross Section in Carbon and Lead

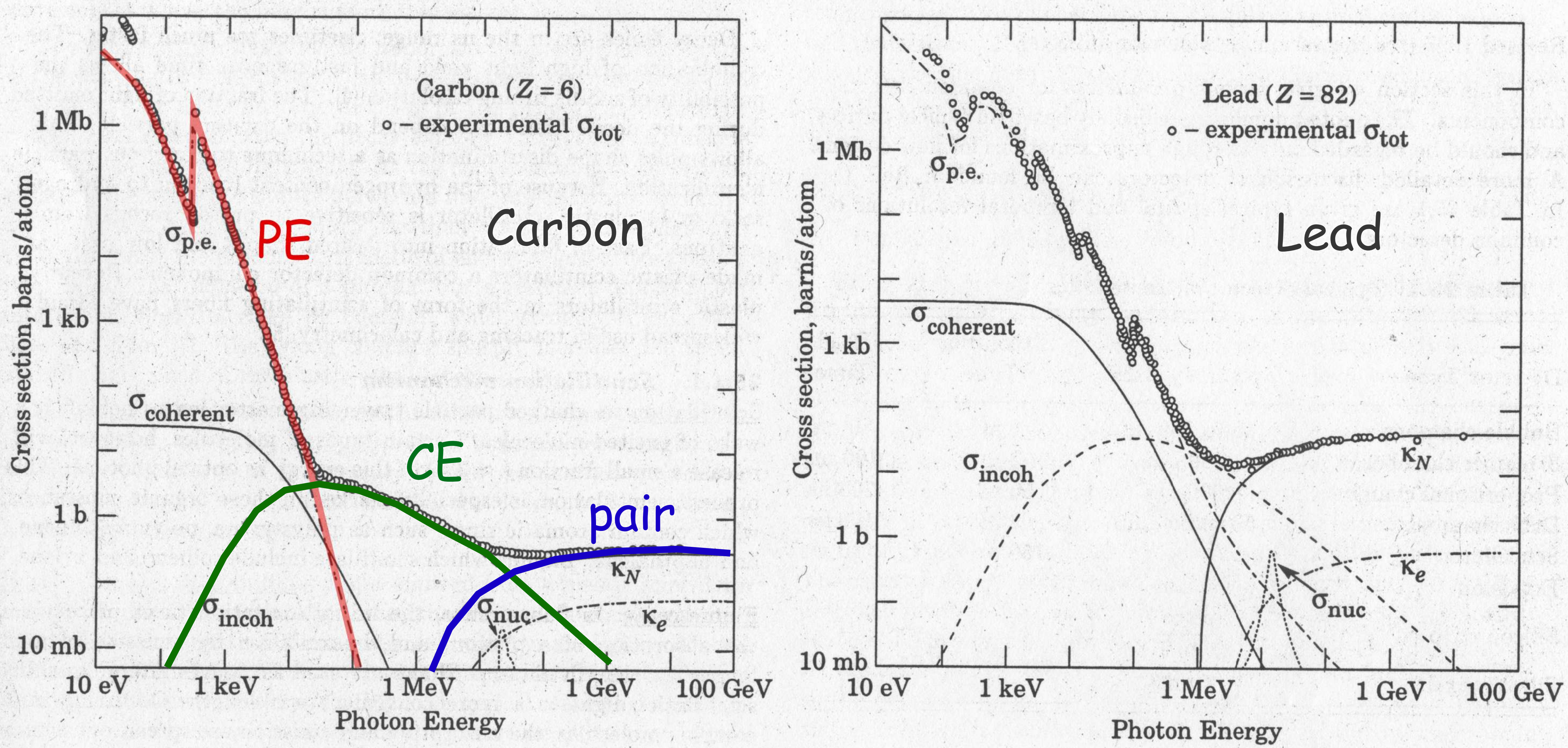

Figure 24.3: Photon total cross sections as a function of energy in carbon and lead, showing the contributions of different processes:

$\sigma_{\mathrm{p.e.}}$ = Atomic photo-effect (electron ejection, photon absorption)

$\sigma_{\mathrm{coherent}}$ = Coherent scattering (Rayleigh scattering—atom neither ionized nor excited)

$\sigma_{\mathrm{incoherent}}$ = Incoherent scattering (Compton scattering off an electron)

κ_n = Pair production, nuclear field

κ_e = Pair production, electron field

σ_{nuc} = Photonuclear absorption (nuclear absorption, usually followed by emission of a neutron or other particle)

From Hubbell, Gimm, and Øverbø, J. Phys. Chem. Ref. Data **9**, 1023 (80). Data for these and other elements, compounds, and mixtures may be obtained from `http://physics.nist.gov/PhysRefData`. The photon total cross section is assumed approximately flat for at least two decades beyond the energy range shown. Figures courtesy J.H. Hubbell (NIST).

Interactions of Neutrons with Matter

Neutrons are neutral ....

i.e. they can penetrate a lot of matter easily

they have to interact to be detected

- collision creating a charged recoil particle that ionises

  highest energy transfer, if $m_{target} \approx m_{neutron}$

  best for H (i.e. protons) as targets

  (or H-rich materials: Methane, Carbo-Hydrates, ...)

- neutron capture: e.g. $n + {}^{10}B \longrightarrow {}^{11}B \longrightarrow \alpha + {}^{7}Li + \gamma$

high n-capture cross section

$t \approx 10^{-12}$ sec

1.47 MeV

0.84 MeV

0.48 MeV

with detection of the reaction products.

Some neutron capture cross sections:

Oxygen	0.00019 barn
Carbon	0.0035
....	
Boron	767
Cadmium	2450
Samarium	5922
Gadolinium	49000

Interactions of Radiation with Matter: Summary

- charged particles:
  - all charged particles ionise ! (most common/important process)
  - charged particles radiate photons: *
    - bremsstrahlung (high energy photons)
    - Cherenkov effect (low energy photons)
- photons: are not directly detectable !
  - always need to produce electrons, which are detectable (see above).
    - photo effect (< 0.1 MeV)
    - Compton effect * (0.1 ... 10 MeV)
    - pair production * (> 10 MeV)

  (* particle multiplication involved)
- electrons + photons: (at high energy, i.e. E > few MeV)
  - bremsstrahlung + pair production: shower development ***
- neutrons:
  - collision and recoil, n-capture and decay

Detection of a particle goes ultimately always over electric charge!

Gamma Rays

point back
easy to detect
some absorption

… by far most productive messenger at high energies.

γ Ray Sources

How to detect a γ ray source in the sky?

Cosmic rays come diffusely from everywhere.

γ rays come straight from their sources
(i.e. point-like)

Search for an excess from a certain point in the sky above the diffuse background.

γ Rays:

pick them out of the CR background
point back at sources

< 100 GeV: direct observations on satellites
γ via direct identification

> 100 GeV: indirect obs. via air showers
γ via shower shape, muon content
or via localised excess of events
from certain sky positions

Altitude Gamma-Ray Detectors

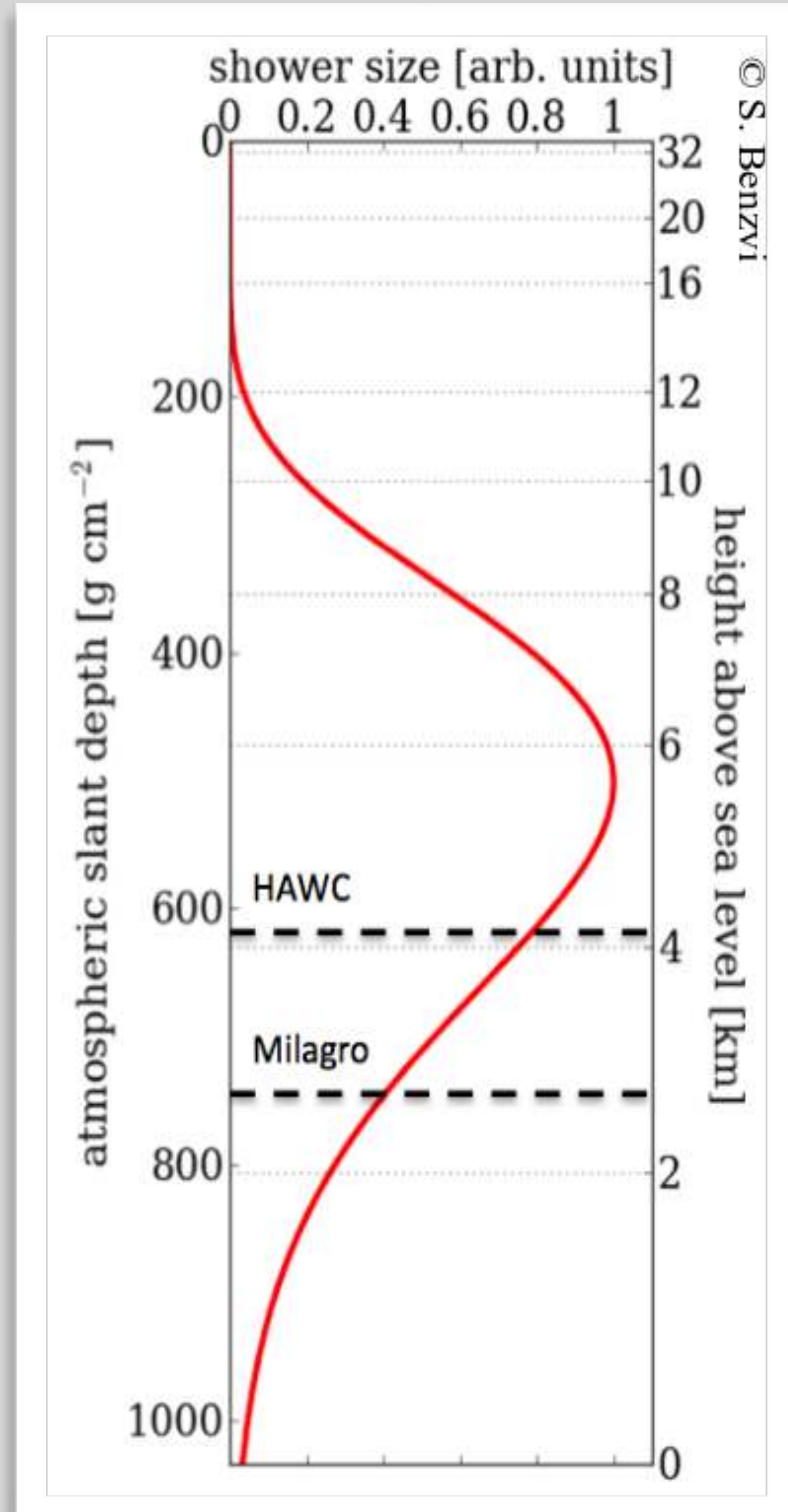

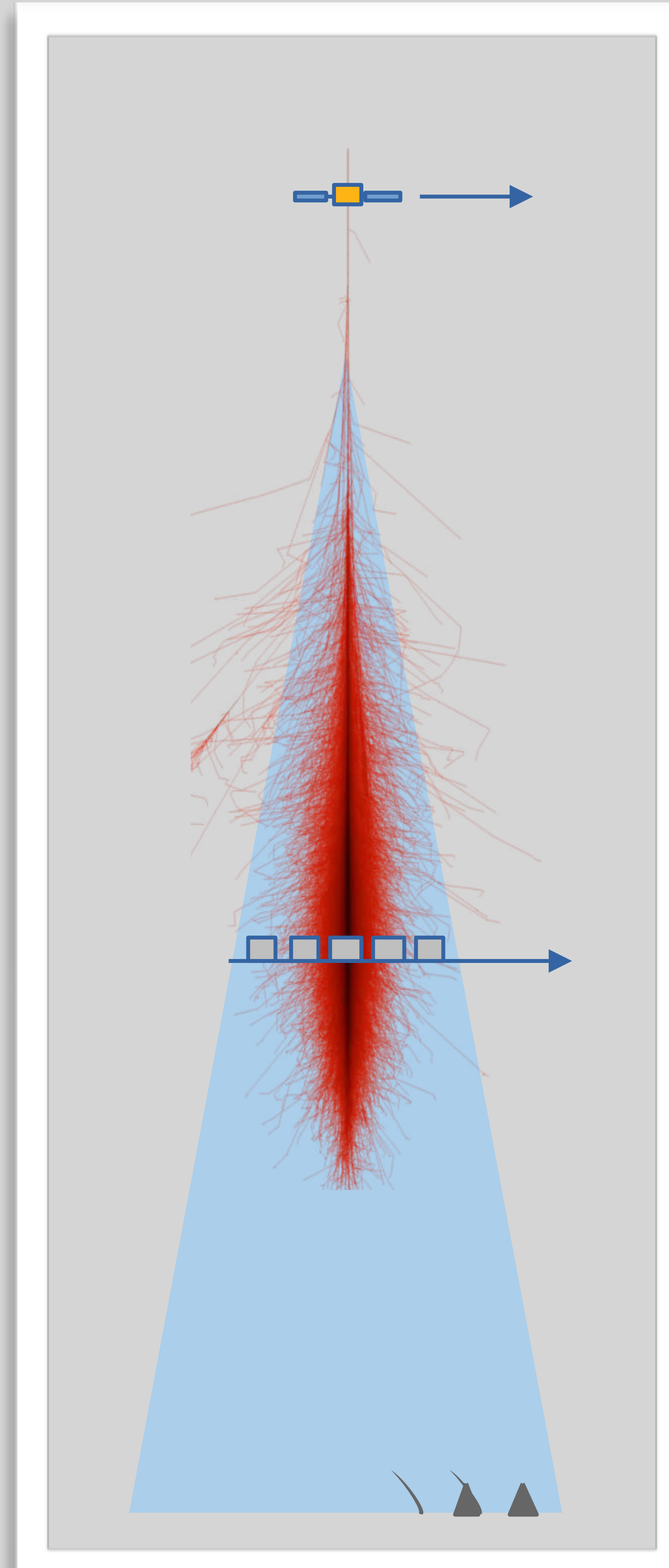

Historic Development

Many slides and historic information from talks by:

R Mirzoyan (HESS Centenary Meeting, Bad Saarow, 2012)

S Sarkar (School for Cosmic Ray Astrophysics, Erice, 2012)

Historic Timeline – Part 1

1910: E Curie observes bluish light in water with Radium salt

1912: V Hess discovers Cosmic Rays

1912: CTR Wilson invents the cloud chamber

1934: P Cherenkov's brilliant experimental work
to explain the bluish light (Cherenkov effect)

1938: P Auger discovers air showers (CR energies up to 10^{15} eV
a total mystery at the time)

many discoveries in particle physics using CRs and
cloud chambers; interactions, particle production, ...

1948: E Fermi publishes acceleration theory of cosmic rays
(... and if protons are accelerated, then there should also be secondary γ rays)

1948: P Blackett recognised that Cherenkov light from relativistic particles
in air showers ($e^{\pm}$, $\mu^{\pm}$) should contribute to the light of night sky (~10^{-4} ?).

... ingredients ready for gamma-ray astronomy
with Cherenkov telescopes.

Air shower arrays were used abundantly for cosmic ray research.
Some were used to look also for point sources (i.e. photons) in the sky.

Initially unsuccessful: sources claimed, but could not be substantiated
too much diffuse cosmic ray showers.

Cherenkov light from showers

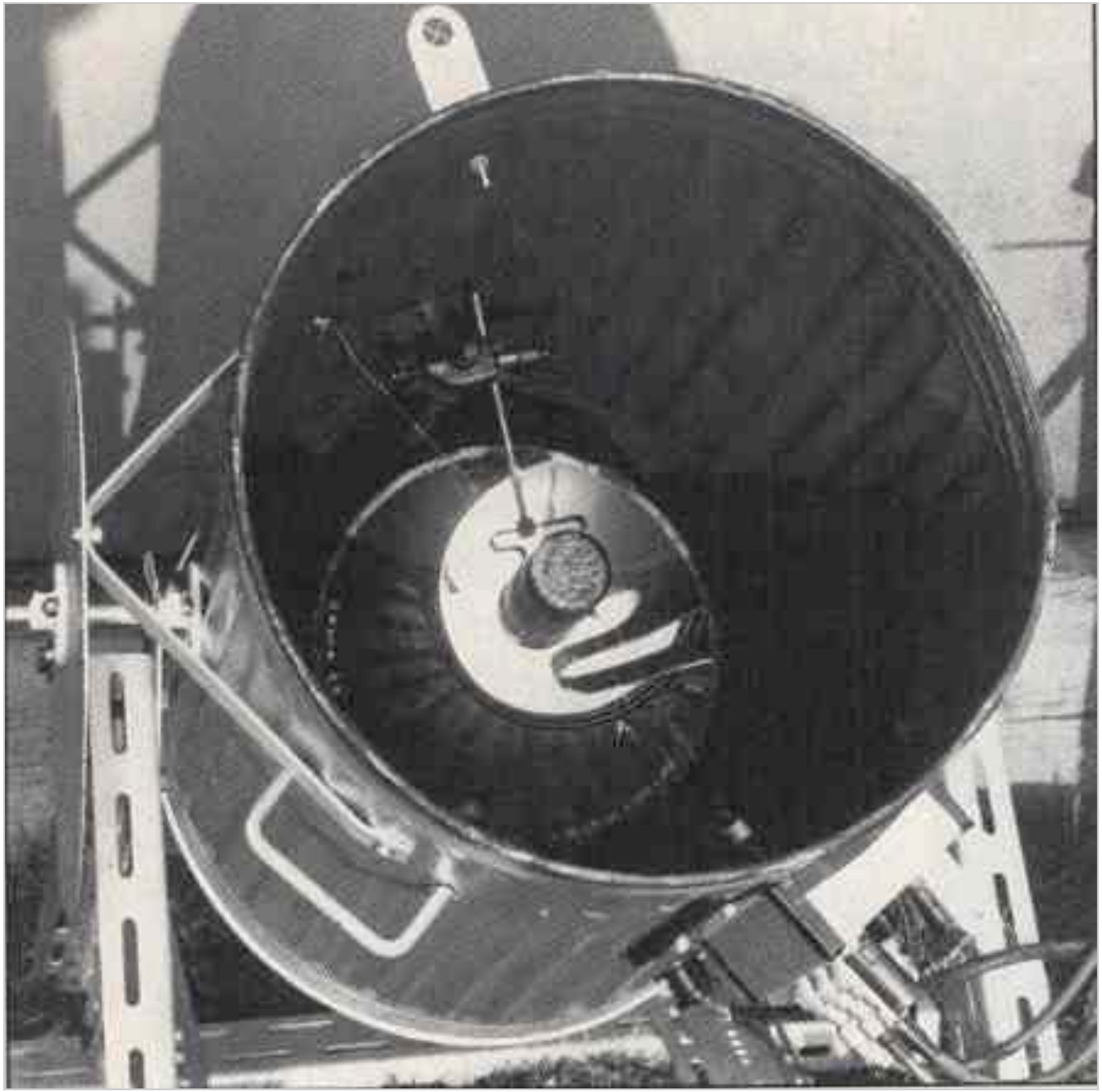

garbage can, 60 cm search light mirror,
1 PMT (fast light flashes)

Galbraith, Jelley (Harwell, UK)
record Cherenkov flashes from air showers

February 21, 1953 NATURE

Light Pulses from the Night Sky associated with Cosmic Rays

In 1948, Blackett[1] suggested that a contribution approximately 10^{-4} of the mean light of the night-sky might be expected from Čerenkov radiation[2] produced in the atmosphere by the cosmic radiation. The purpose of this communication is to report the results of some preliminary experiments we have made using a photomultiplier, which revealed the

....

thank Mr. W. J. Whitehouse and Dr. E. Bretscher for their encouragement, and Dr. T. E. Cranshaw for the use of the extensive shower array.

W. Galbraith
J. V. Jelley

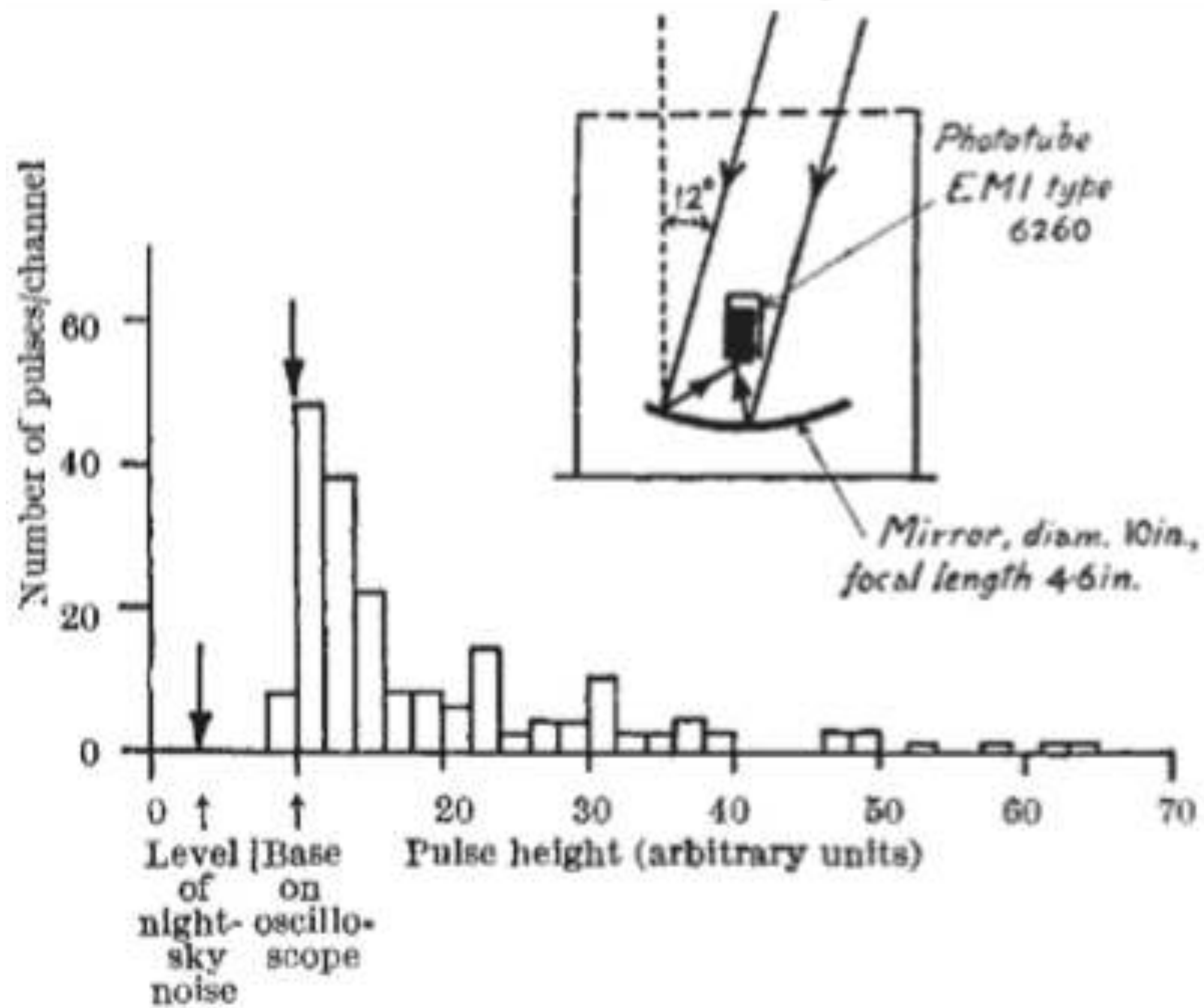

Gamma Ray Astronomy

requires separation of photons from the cosmic ray background

1958: seminal paper by P Morrison

1959: G Cocconi (CERN) suggests to observe the Crab Nebula
(ICRC 1959 Moscow)

AN AIR SHOWER TELESCOPE
AND THE DETECTION OF 10^{12} eV PHOTON SOURCES

Giuseppe Cocconi *
CERN - Geneva.

1) This paper discusses the possibility of detecting high energy photons produced by discrete astronomical objects. Sources of charged particles are not considered as the smearing produced by the magnetized plasmas filling the interstellar spaces probably obliterates the original directions of movement.

Crab Nebula

1 TeV

The Crab Nebula: Visual magnitude of polarized light m = 9.
Magnetic field in the gas shell $H \simeq 10^{-4}$ gauss.
Therefore: $U_\nu = 10^{12} eV$ and $R(10^{12} eV) \approx 10^{-3.2}\ m^{-2} s^{-1}$.
The signal is thus about 10^{6} times larger than the background (2). Probably in the Crab Nebula the electrons are not in equilibrium with the trapped cosmic rays, and our estimate is over-optimistic. However, this source can probably be detected even if its efficiency in producing high energy photons is substantially smaller than postulated above.
487, the Jet Nebula: m = 13.5 $H \simeq 10^{-4}$ gauss.
$R(10^{12} eV) \simeq 10^{-5} m^{-2} s^{-1}$, still well above the background (2). For this object our evaluation is probably not fundamentally wrong.

Military surplus of
- parabolic search-light mirrors 1-2 m in diameter
- gun mounts with drive systems

G.T. Zatsepin (from GZK cutoff) asked Chudakov
to measure the predicted gamma-ray sources.
Crimea: Chudakov got 12 parabolic mirrors of 1.5 m
made measurements for almost 4 years.

Crimea Experiment
1959-1965

only upper limits

Cocconi's estimate
far too optimistic

First mention of the potential of the stereo imaging

SOVIET PHYSICS JETP VOLUME 20, NUMBER 2 FEBRUARY, 1965

THE ANGULAR DISTRIBUTION OF INTENSITY OF CERENKOV RADIATION FROM EXTENSIVE COSMIC-RAY AIR SHOWERS

V. I. ZATSEPIN

P. N. Lebedev Physics Institute, Academy of Sciences, U.S.S.R.

Submitted to JETP editor March 2, 1964

J. Exptl. Theoret. Phys. (U.S.S.R.) 47, 689-696 (August, 1964)

The angular distribution of intensity is calculated for the Cerenkov radiation produced in the terrestrial atmosphere by extensive air showers of cosmic rays. Calculations are made for showers arriving from the zenith and for conditions of observation at sea level and at an altitude of 3860 m above sea level. Photographic observation of the shape of the flash of light against the celestial sphere, as obtained in [2,3] is evidently in satisfactory agreement with the calculations.

1. INTRODUCTION

In the registration of extensive air showers (EAS) by means of Cerenkov counters,[1,2] a knowledge of the angular distribution of the Cerenkov radiation is important primarily from the methodological point of view (choice of the angle subtended by the Cerenkov counters to obtain optimal signal-to-noise ratio, estimates of the accuracy of the angular coordinates of high-energy primary particles, and so on). Besides this, the angular distribution of the light from showers is already itself the object of physical investigation,[3] and therefore it is important to ascertain what kind of information about a shower can be obtained from such data. The present calculation has been made for this purpose, and is based on the following ideas.

Cerenkov radiation is mainly caused by the electronic component, which makes up the bulk of the charged particles in a shower. Owing to multiple Coulomb scattering by the nuclei of atoms in the air, electrons of energy E at a depth p have a Gaussian distribution of distances r from the axis of the shower, and a Gaussian distribution of angles relative to a mean angle ϑ, which depends on r. The dispersions of the transverse and angular distributions depend on E. The energy spectrum of the electrons is an equilibrium one and does not depend on the degree of development of the shower in depth. For the case of primary photons the variation of the electrons with height is taken to be that given by the electromagnetic cascade theory,[4] and for the case of primary protons, that given by the calculations of Nikol'skiĭ and Pomanskiĭ.[5] The light emitted by the electrons is at the angle ϑ_{Cer} with the direction of their motion. Neither the scattering of the light by density inhomogeneities in the air nor absorption of the light is taken into account.

2. STATEMENT OF PROBLEM AND METHOD OF CALCULATION

The purpose of the calculation is to determine the number I of light quanta in the frequency range from λ_1 to λ_2 that fall on unit area of the earth's surface at distance R from the axis of the shower, and in the direction from any given point of the celestial sphere.

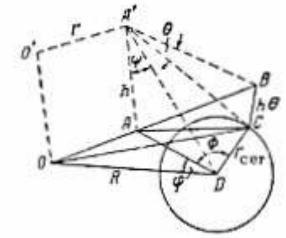

FIG. 1

Let us turn to Fig. 1. Here O is the trace of the axis of the shower on the earth's surface, D is the point of observation, and A' is an arbitrary point which is at height h over the level of observation and is characterized by the angular coordinates ψ (the zenith angle) and φ (the azimuthal angle). We agree to measure the azimuthal angle from the direction from the point of observation D to the trace O of the axis of the shower on the earth's surface. The figure OBCD lies in the plane of the drawing, and OO'A'B in the perpendicular plane. We shall determine for the neighborhood of

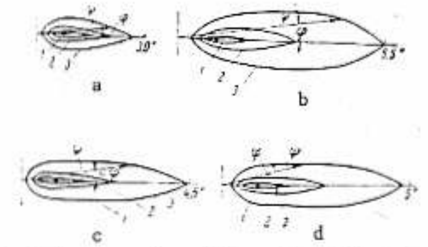

FIG. 6. Contours of equal intensity in light flashes from showers from primary protons and primary photons of various energies, for sea level and R = 100 m from the axis. The curves 1, 2, 3 correspond to intensity values $10^{-1} I_{max}(100)$, $10^{-2} I_{max}(100)$, and $10^{-3} I_{max}(100)$. Diagrams a and b cor-

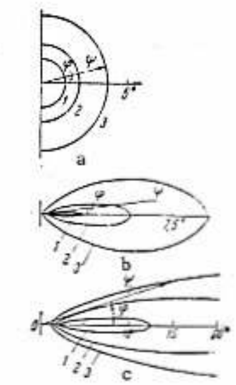

CONCLUSION

The calculations that have been made enable us to draw the following conclusions:

1. Since the maximum intensity of the light from a shower does not coincide with the direction of arrival of the primary particle, in researches in which the determination of the angular coordinates of the primary particle is made by photographing the light flash from the shower one should seek improved accuracy in this determination by photographing the shower simultaneously from several positions.

2. If the distance from the axis of the shower to the detector is determined from independent data, then an analysis of the shape of the light flash from the shower and its total intensity gives information both about the initial energy of the primary particle and about the position in the atmosphere of the maximum of the shower, and can thus be used for the analysis of fluctuations in the development of showers in the atmosphere.

V.I. Zatsepin 1965

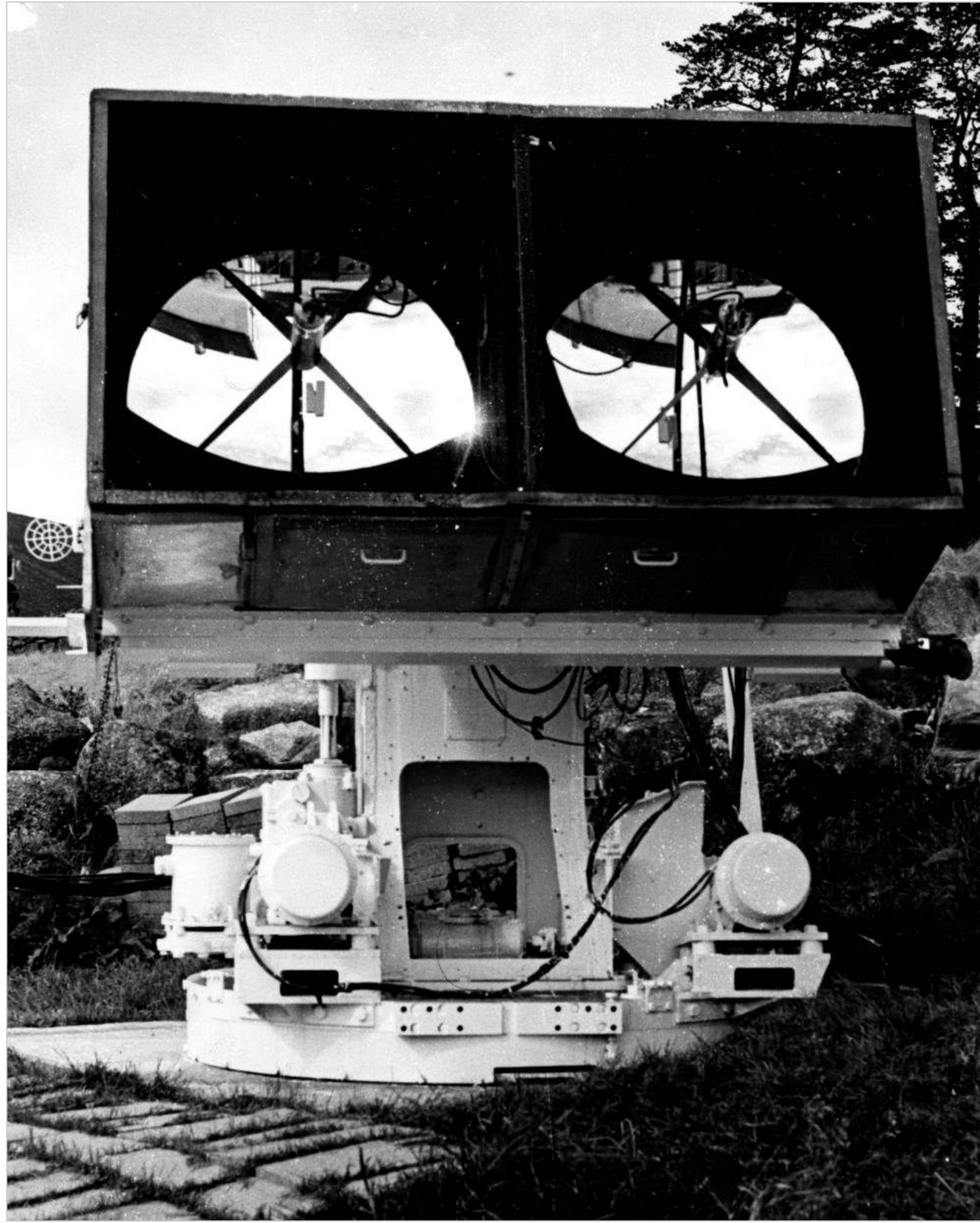

Ireland:
Porter & Jelley
1962-66

First imaging "stereo" telescopes: GT-48 in Crimea 1985-89

A Stepanian

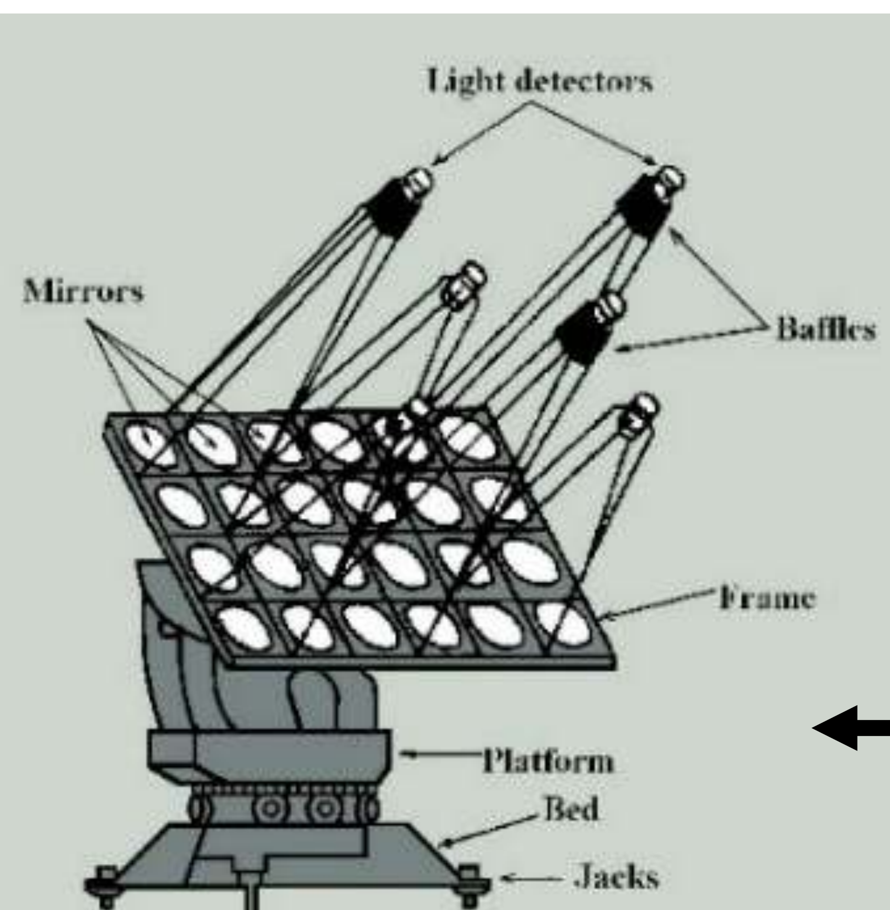

20 m

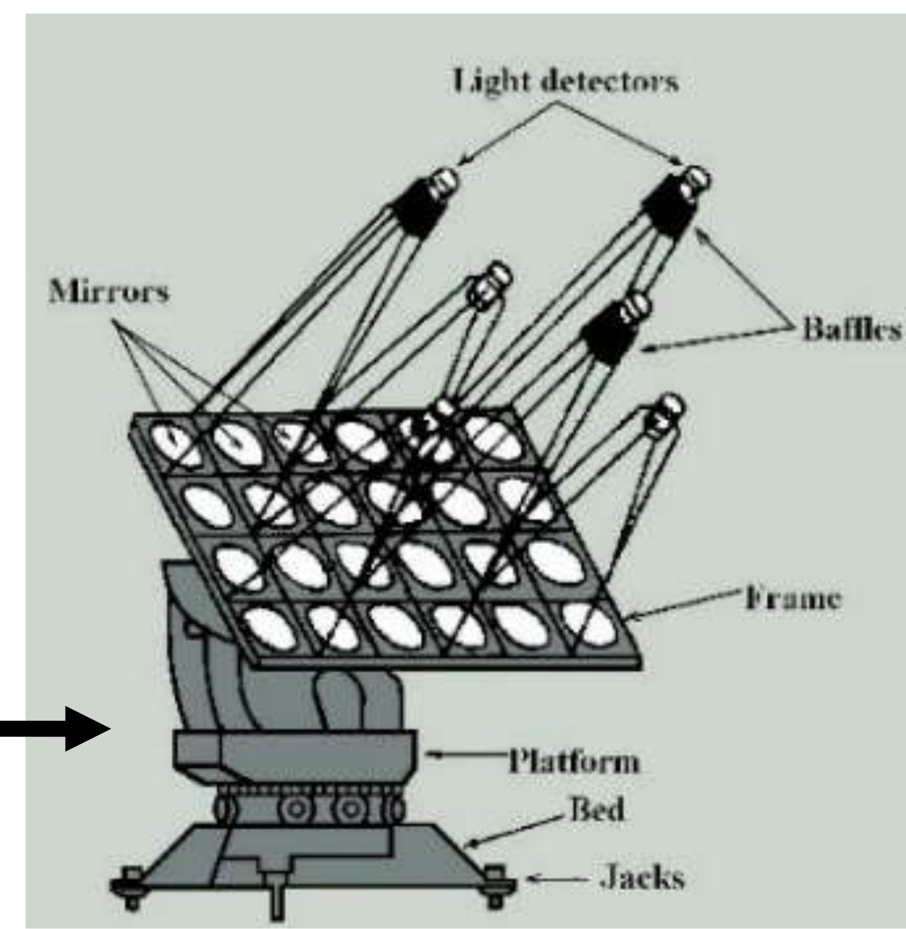

First gamma-ray experiment at Whipple Observatory, 1967-68

Work on the Mt. Hopkins Observatory proceeds at an astonishing pace. The laser and Baker-Nunn systems are now installed and operating and the large optical reflector is scheduled to arrive by the end of next month. In preparation for the LOR installation, Trevor Weekes (above, left) and George Rieke have conducted seeing tests with two movable searchlight reflectors. Look carefully—some outcroppings at the base of Mt. Hopkins are visible upside-down in the reflector.

THE ASTROPHYSICAL JOURNAL, Vol. 154, November 1968

1968

A SEARCH FOR DISCRETE SOURCES OF COSMIC GAMMA RAYS OF ENERGIES NEAR 2×10^{12} eV

G. G. FAZIO AND H. F. HELMKEN
Smithsonian Astrophysical Observatory and Harvard College Observatory, Cambridge, Massachusetts

G. H. RIEKE
Mount Hopkins Observatory, Smithsonian Astrophysical Observatory, Tubac, Arizona, and Harvard University, Cambridge, Massachusetts

AND

T. C. WEEKES*
Mount Hopkins Observatory, Smithsonian Astrophysical Observatory, Tubac, Arizona
Received September 3, 1968

ABSTRACT

By use of the atmospheric Čerenkov nightsky technique, a study has been made of the cosmic-ray air-shower distribution from the direction of thirteen astronomical objects. These include the Crab Nebula, M87, M82, quasi-stellar objects, X-ray sources, and recently exploded supernovae. An anisotropy in the direction of a source would indicate the emission of gamma rays of energy 2×10^{12} eV. No statistically significant effects were recorded. Upper limits of $3\text{–}30 \times 10^{-11}$ gamma ray cm^{-2} sec^{-1} were deduced for the individual sources.

10 m Whipple Telescope

built in 1968

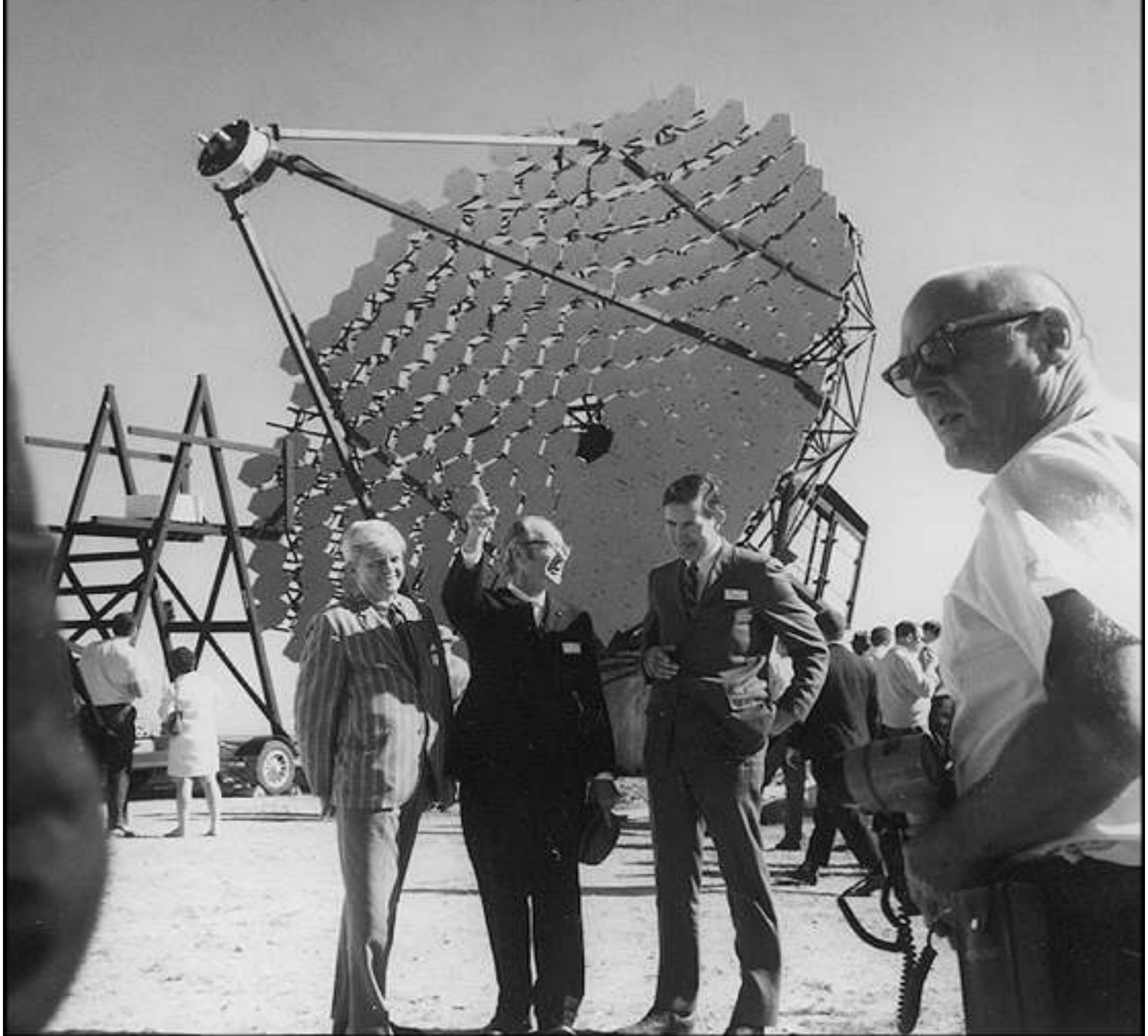

1970-80's: plenty of "discoveries" on 3-4 σ level

A.M. Hillas, University of Leeds:

"A physicist's apparatus gradually learns what is expected of it. It has a dog-like desire to please."

"Concentration" is a good parameter

(>75% of light is concentrated in 2 pixels)

Plyasheshnikov, Bignami (1985) showed that α is a useful parameter

La Jolla, 1985: Hillas suggests to use the "Hillas image parameters"

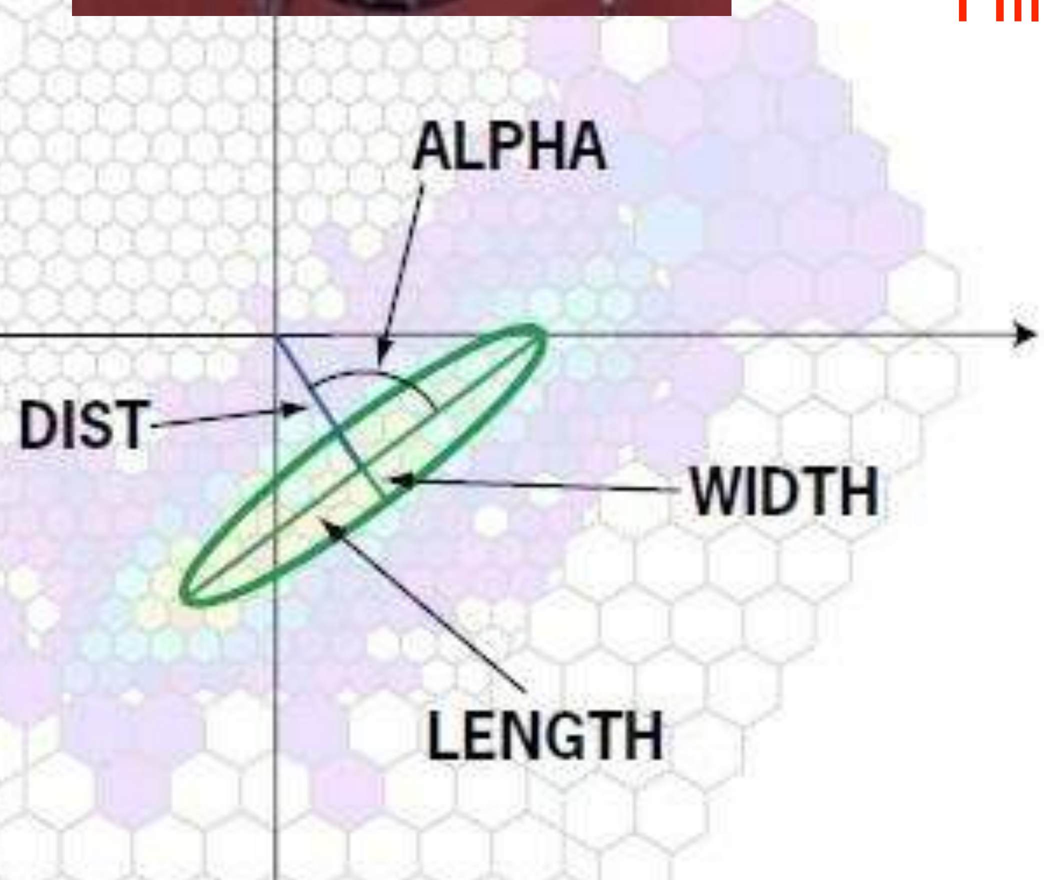

gamma showers are:

- slimmer,
- more concentrated
- oriented towards source

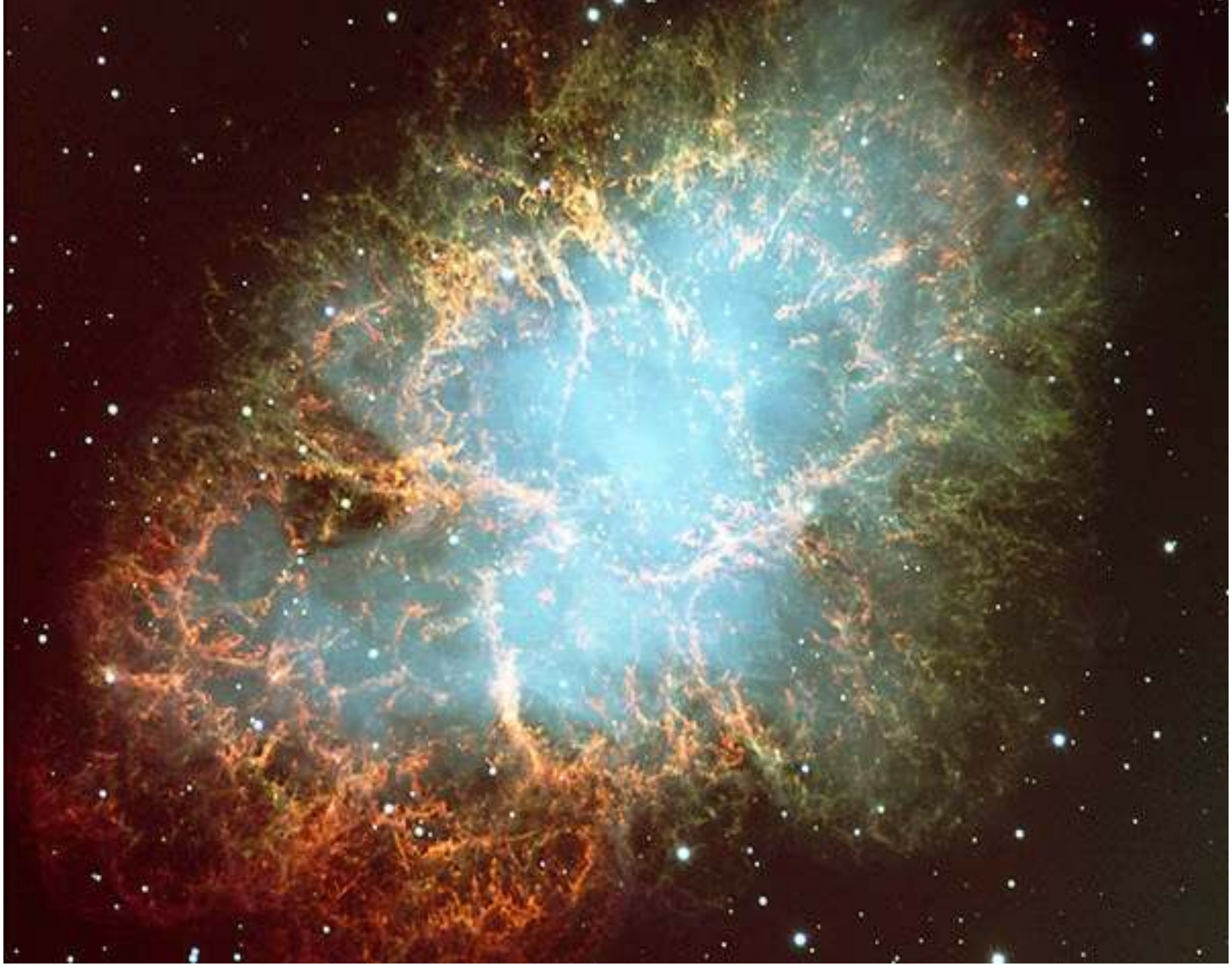

1989:
Detection of the Crab Nebula

9σ significance

5σ signal in 50 h,
with 159 pixel camera
and Hillas image analysis.

1990's: sources were seen everywhere, up to 10^{15} eV

e.g.

CONCLUSIONS

It was shown that Vela X-1 emits steady, pulsed TeV emission over five years of observations, at a period corresponding with the expected X-ray period. No orbital modulation could be established. For Cen X-3 pulsed emission was found only in a part of the orbit, corresponding with the known accretion wake. It also seems that the emission in the wake is steady over time scales of years. In both cases weak evidence for a period shift was found. With the detection of AE Aqr as a possible source of TeV gamma-rays, a new area of candidate sources has been opened up for TeV astronomy. In all cases it will be imperative to observe sources over a number of years, and if possible, make use of multiwavelength observations to investigate the behaviour of these objects.

... which could not be confirmed.

Reliable source detection needs $>5\sigma$ significance and independent confirmation.

Hegra, La Palma

37.

Proposal
for
Imaging Air Cherenkov Telescopes in the HEGRA Particle Array

F.A. Aharonian, A.G.Akhperjanian, A.S. Kankanian,
R.G. Mirzoyan, A.A. Stepanian*

Yerevan Physics Institute

* Crimean Astrophysical Observatory

M. Samorski, W. Stamm

Institut für Kernphysik, University of Kiel

M. Bott-Bodenhausen, E. Lorenz, P. Sawallisch

Max-Planck-Institute for Physics and Astrophysics
Munich

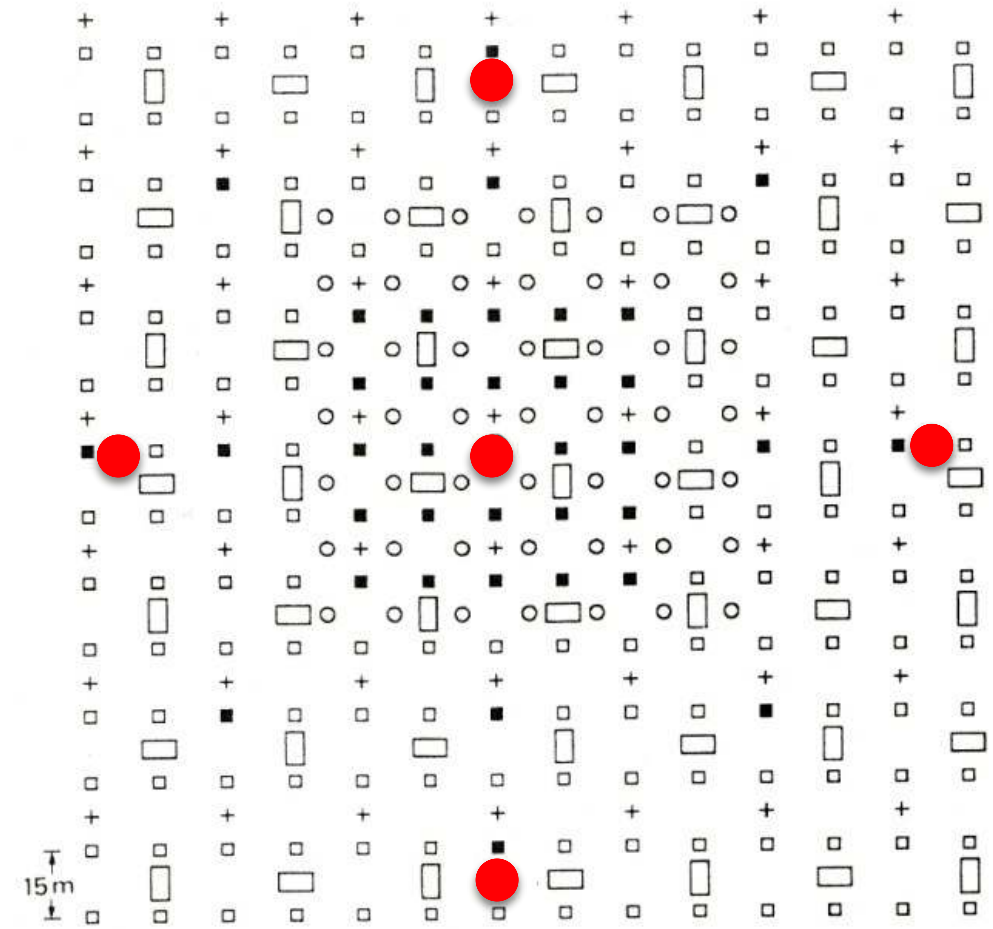

ELECTRON DETECTORS: 1 m^2 scintillation counters for particle density and fast-timing measurements (2 PM's each), with 5 mm of lead for photon conversion.

- ■ 37 detectors in operation since July 1988 (University of Kiel)
- □ 159 additional detectors, 90 of them in operation since July 1989, the rest since December 1990 (MPI Munich together with University of Madrid)
- ○ 49 further detectors to increase the detector density in the centre of the array, planned for 1991 (University of Hamburg)

▭ 49 MUON DETECTORS: 15 m^2 each, consisting of sandwiches of Geiger tube and absorber layers, planned for 1991/92 (University of Wuppertal together with University of Kiel)

\+ 49 CHERENKOV-LIGHT DETECTORS: each consisting of a 20 cm diameter PM and a light-collecting cone, planned for 1991 (MPI Munich together wit h University of Madrid)

● 5 CHERENKOV TELESCOPES: 3 m in diameter with 19 mirrors and 37 PM's each, imaging technique, planned for 1991/92 (Yerevan Institute of Physics together with MPI Munich and University of Kiel)

Fig. 1: Status and planned extensions of the HEGRA detector array.

CT1 (3 m diam.)
1992 first signal from
Crab Nebula

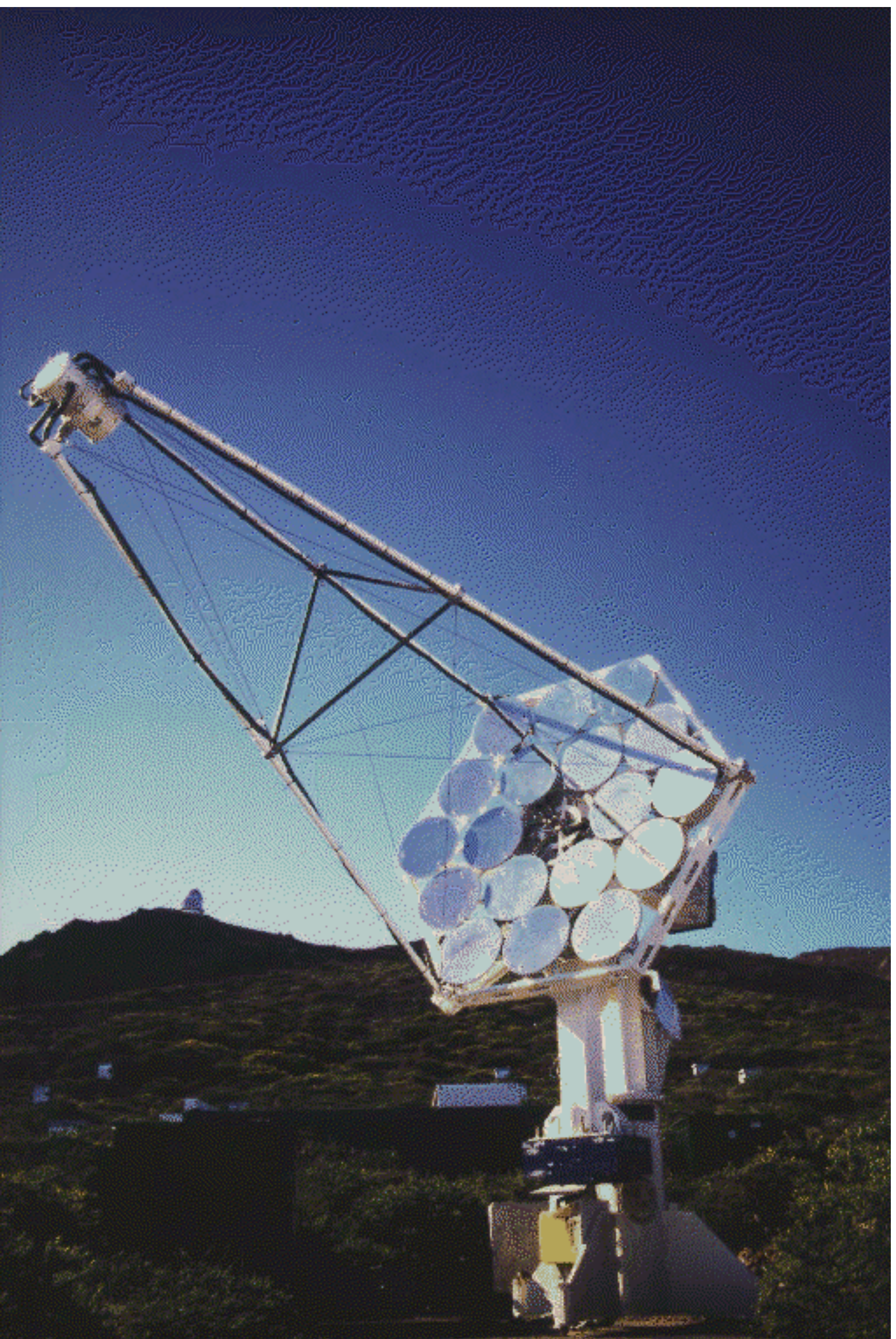

CT2 – CT6: (4 m diam.)
5 more telescopes until 1997.

first successful
stereo detection of γ-ray sources

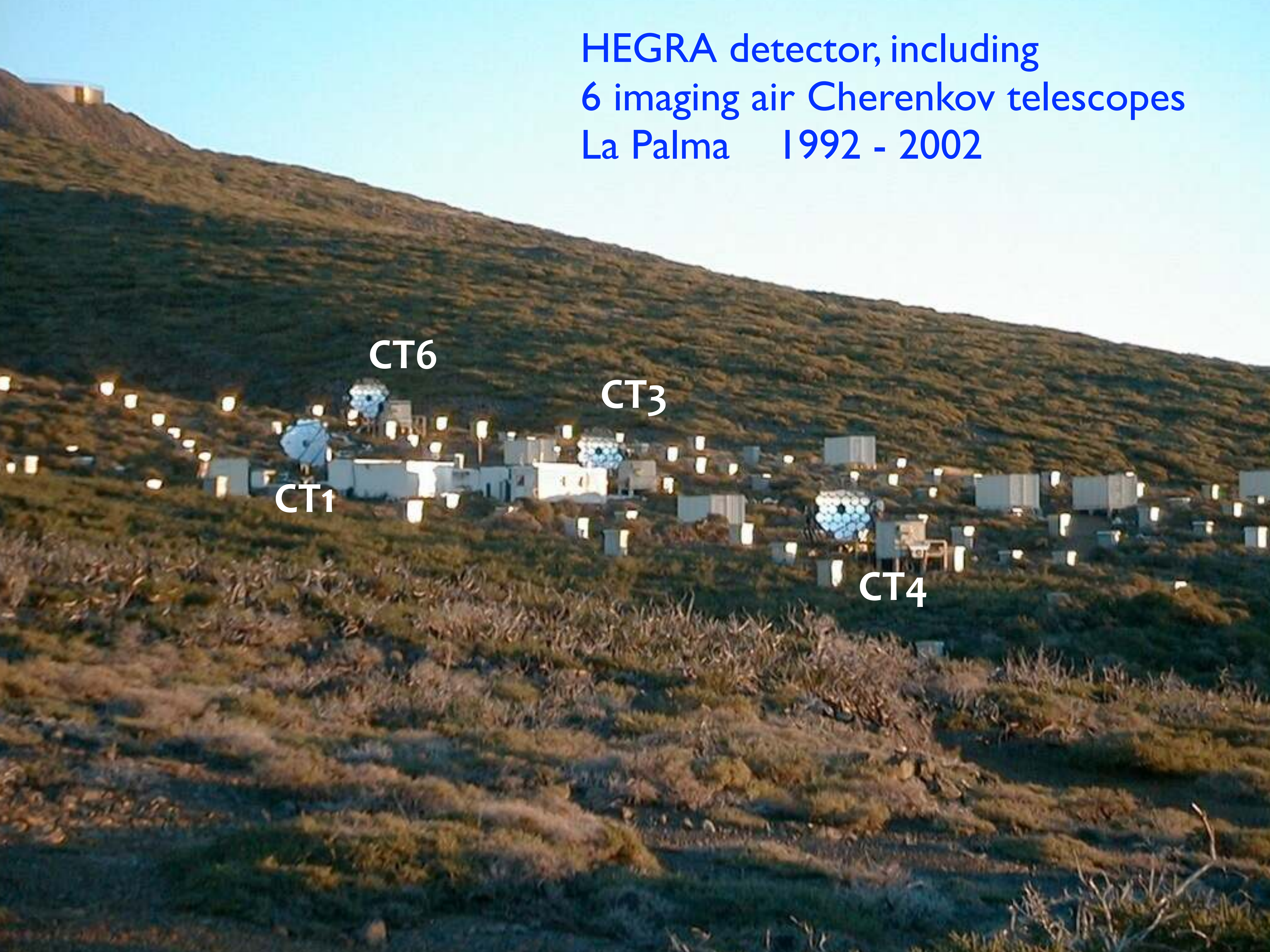

HEGRA detector, including
6 imaging air Cherenkov telescopes
La Palma 1992 - 2002

HESS: High Energy Stereoscopic System
Namibia: Khomas Highlands

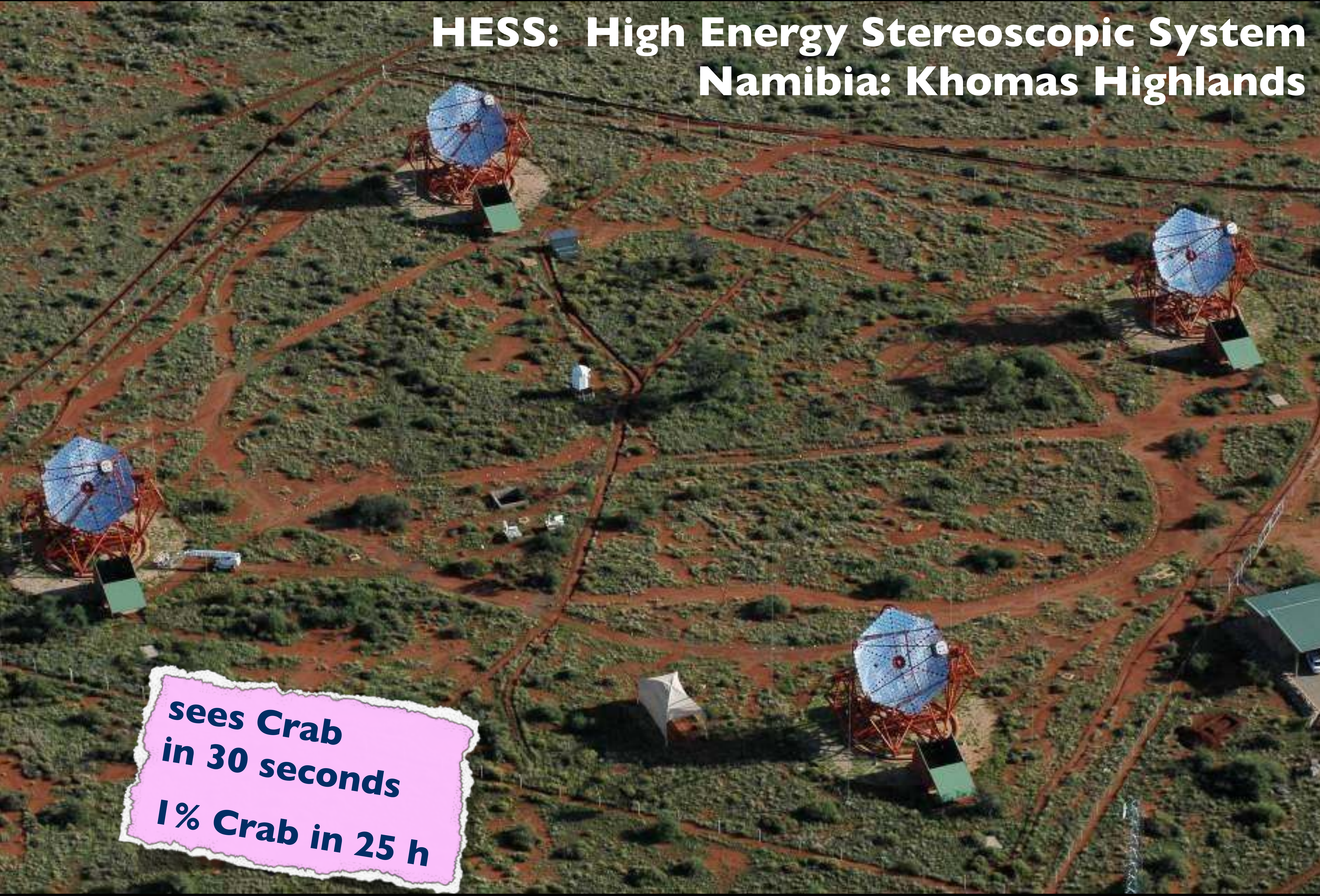

Four 12-m telescopes, 5° field of view
960 pixels / camera, Data taking since 2004

… a major step forward

Historic Timeline – Part 2

Ingredients ready		1948	
Whipple 10-m telescope built		1968	

~40 years

first detection

Crab Nebula	PWN	1989	Whipple
Markarian 421	HBL	1992	Whipple
Markarian 501	HBL	1996	Whipple
3C66A	IBL	1998	Crimea
1ES 2344+514	HBL	1998	Whipple
PKS 2155-304	HBL	1999	Durham Mark 6
1ES 1959+650	HBL	1999	Telescope Array
RX J1713.7-3946	Shell	2000	Cangaroo
Cas A	Shell	2001	HEGRA
BI Lac	IBL	2001	Crimea
H 1426+428	HBL	2002	Whipple
TeV J2032+4130	UNID	2002	HEGRA
M87	FR I	2003	HEGRA
Galactic Centre	UNID	2004	Cangaroo

~10 years

~5 years

HESS started observations

... 16 new sources	2005
... 17 new sources	2006

Cosmic rays, gamma rays and neutrinos come likely from the same sources

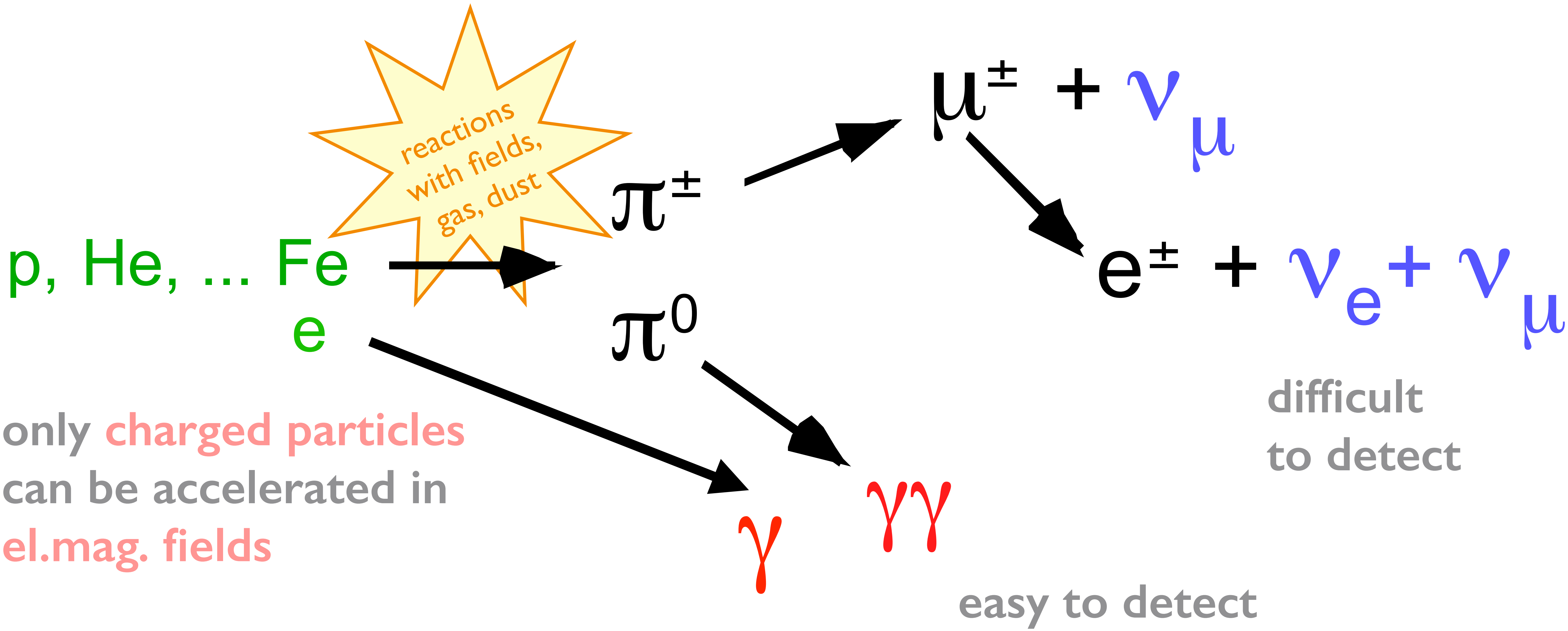

“multi-messenger astrophysics”

but gamma rays are currently the most “productive” messengers.

γ, ν

point back to sources
(good for astronomy)
but serious backgrounds

Gamma Ray Production

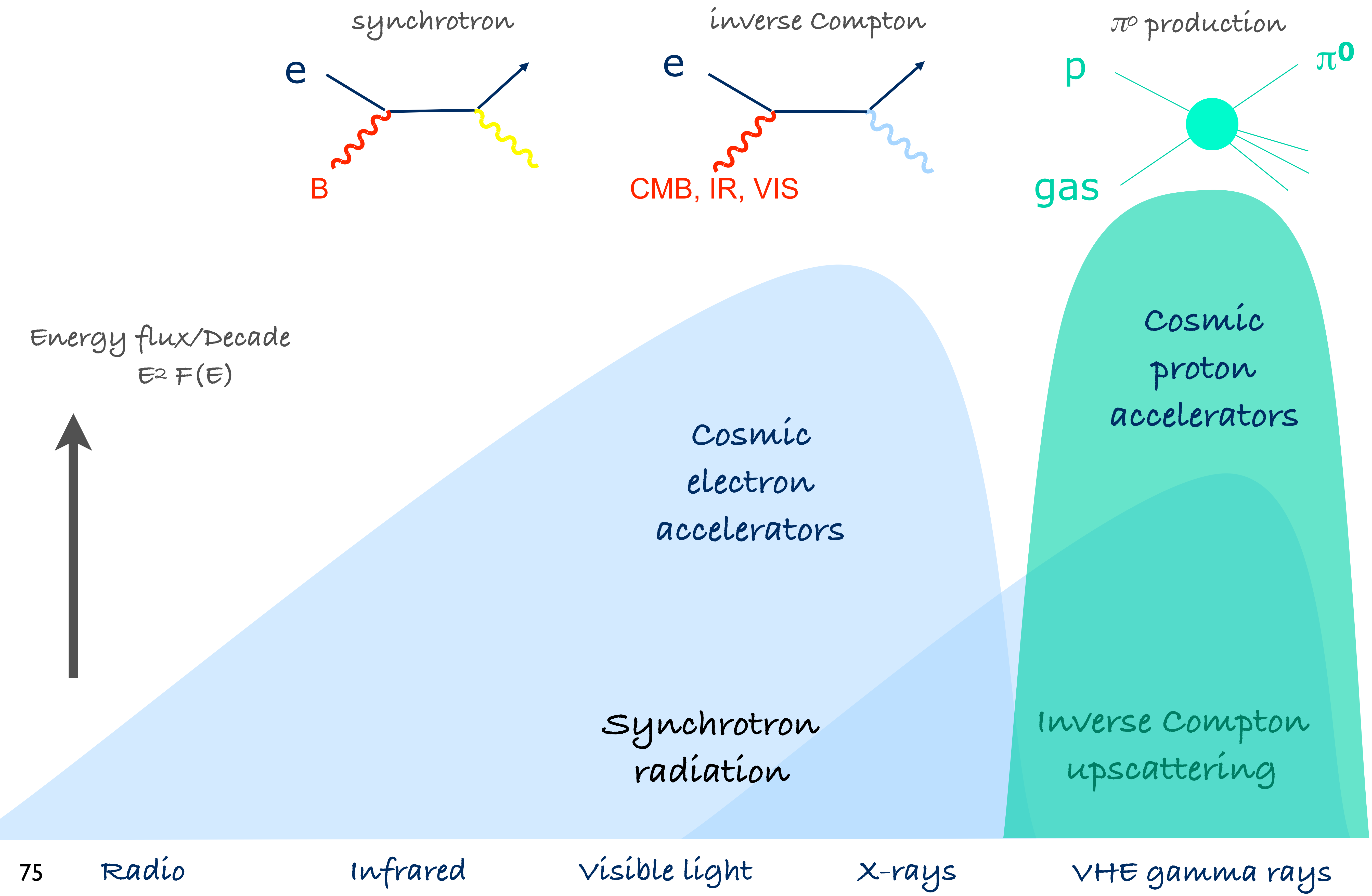

Experiment Types

Air shower arrays
Imaging Cherenkov telescopes

Altitude Gamma-Ray Detectors

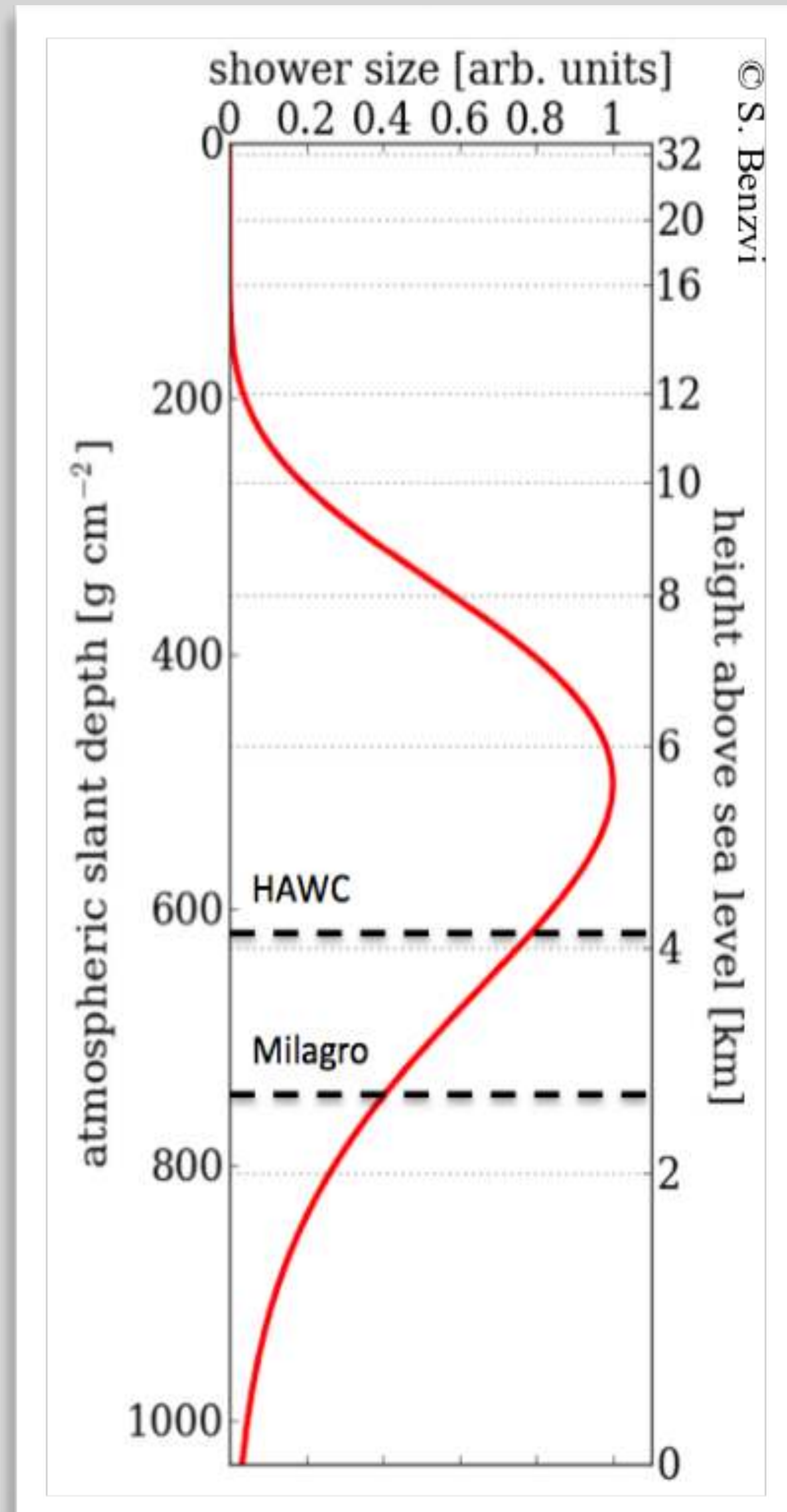

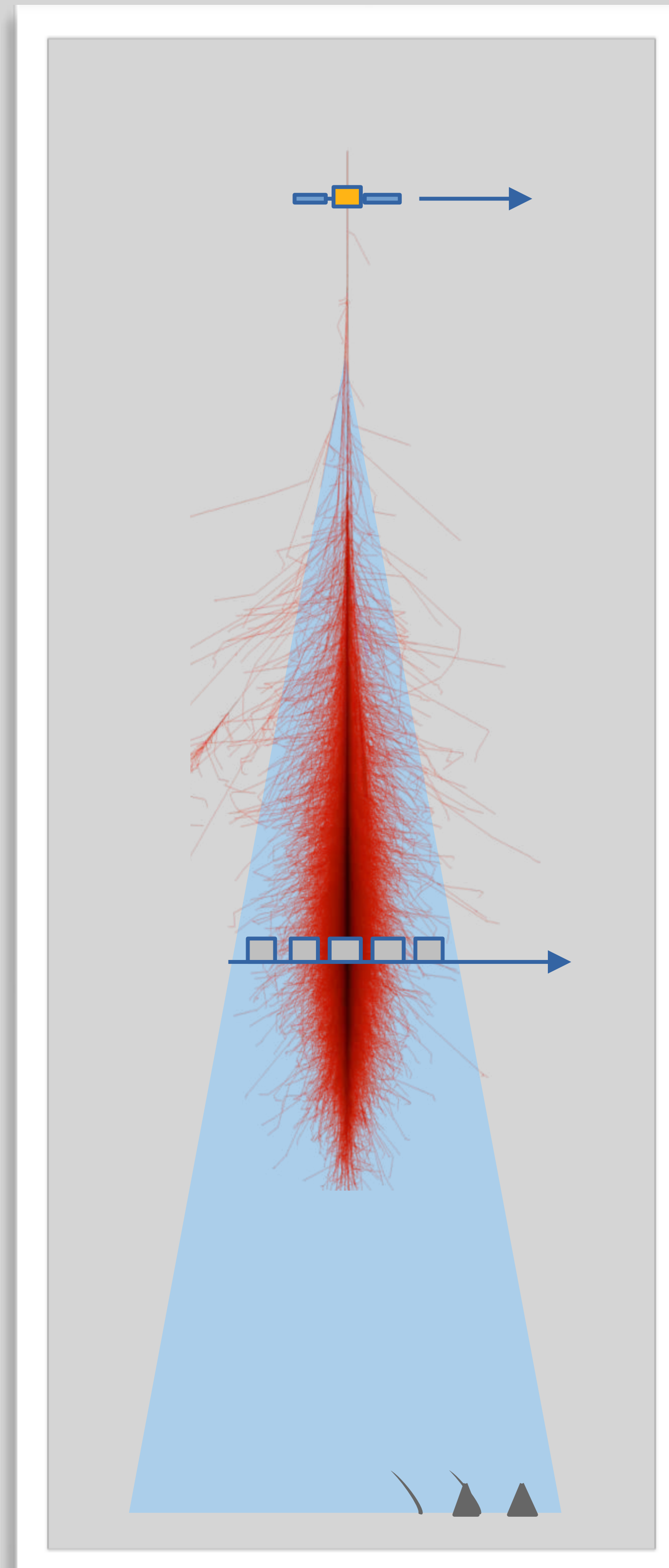

4200 m.a.s.l.

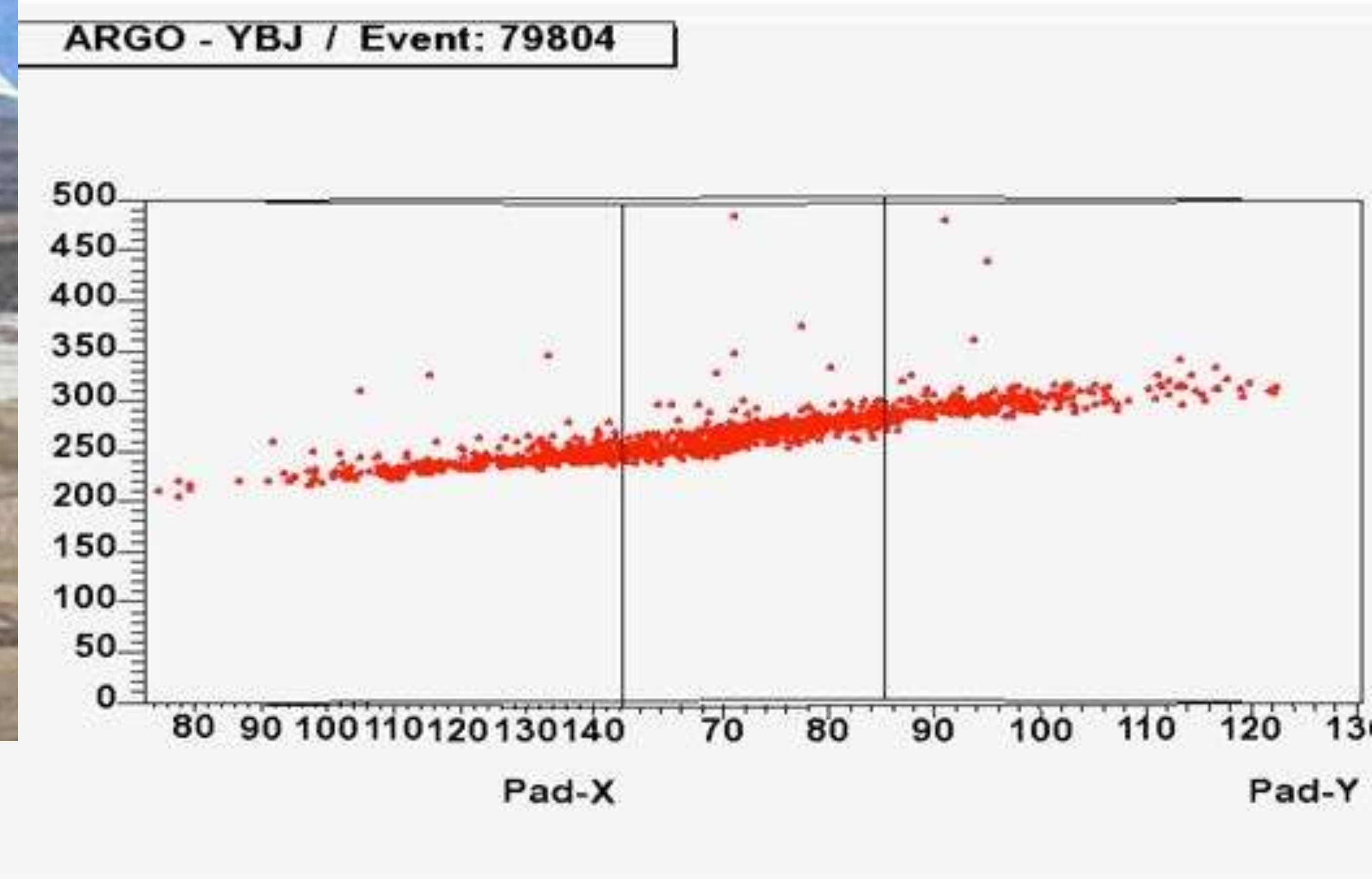

Argo

gamma sources

RPCs full coverage

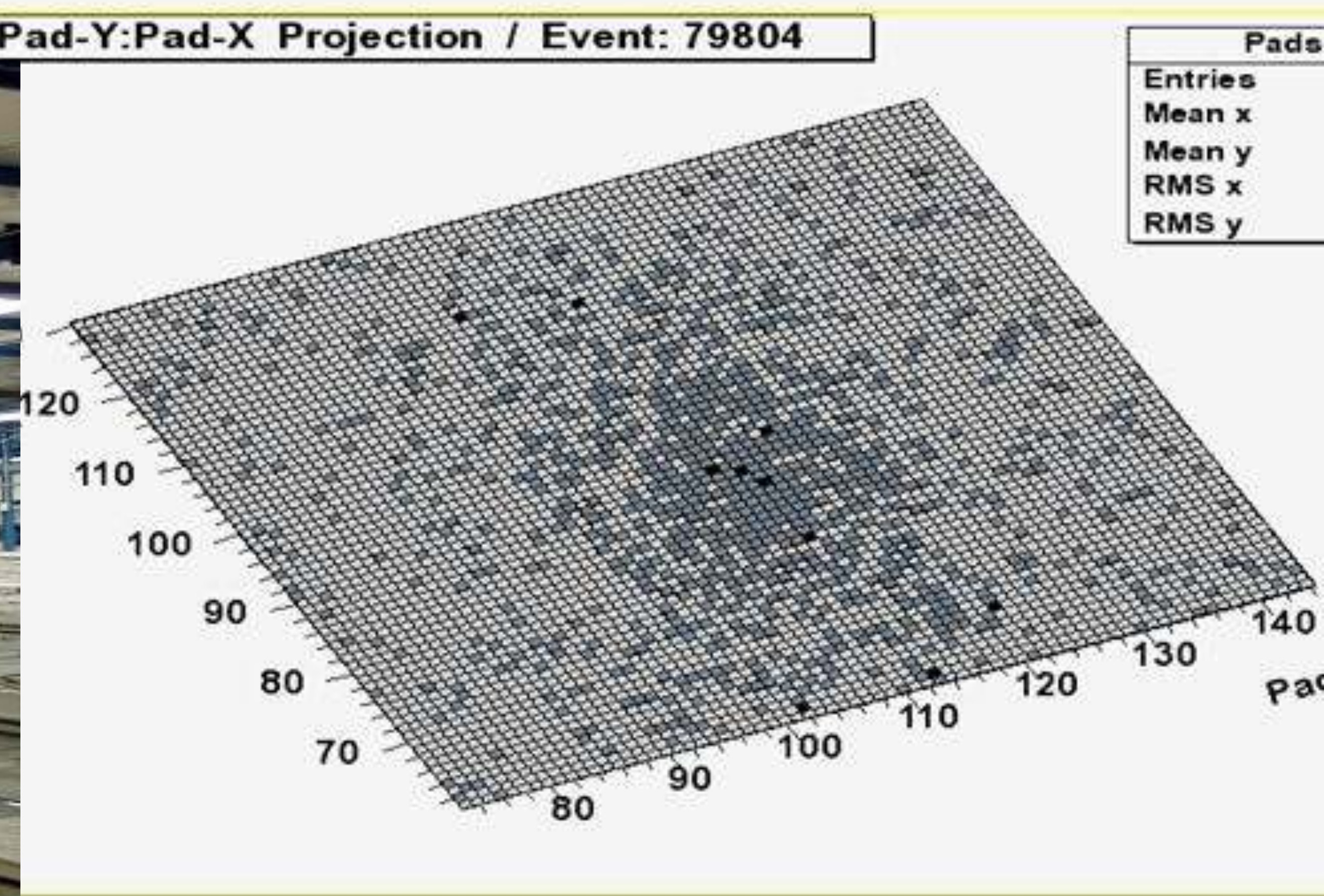

Tibet AS Gamma

4200 m.a.s.l.

Milagro

2650 m.a.s.l.
New Mexico

80 m x 60 m water pond
8 m deep.

Detect shower particles via Cherenkov light in water

PMTs in 2 layers for el.mag. and muons.

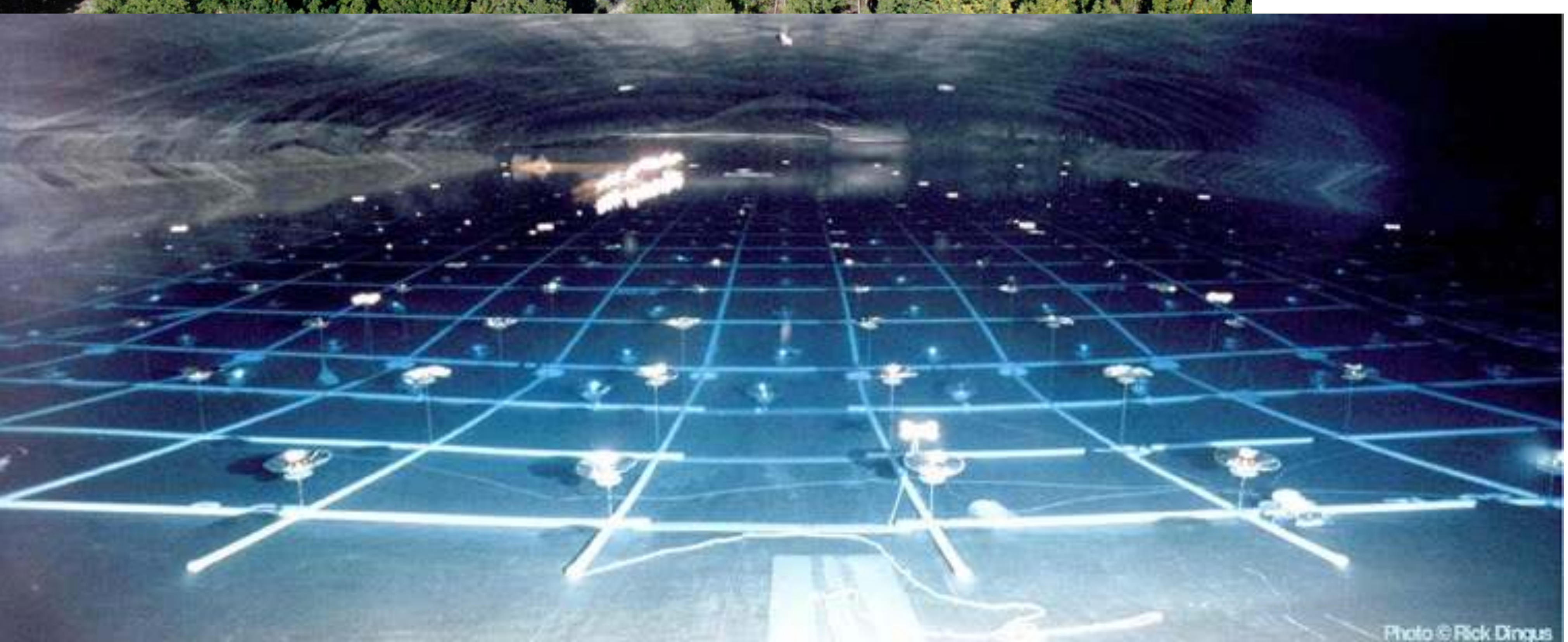

look for excess:
gamma sources

2π sky view

poor γ- hadron separation

via muon content or particle pattern at ground

γ sources detected by excess counts
from certain directions

sources: Moon, Sun shadow

Crab nebula

few strong γ sources

Moon Shadow ... calibration of direction reconstruction

$E \approx TeV$

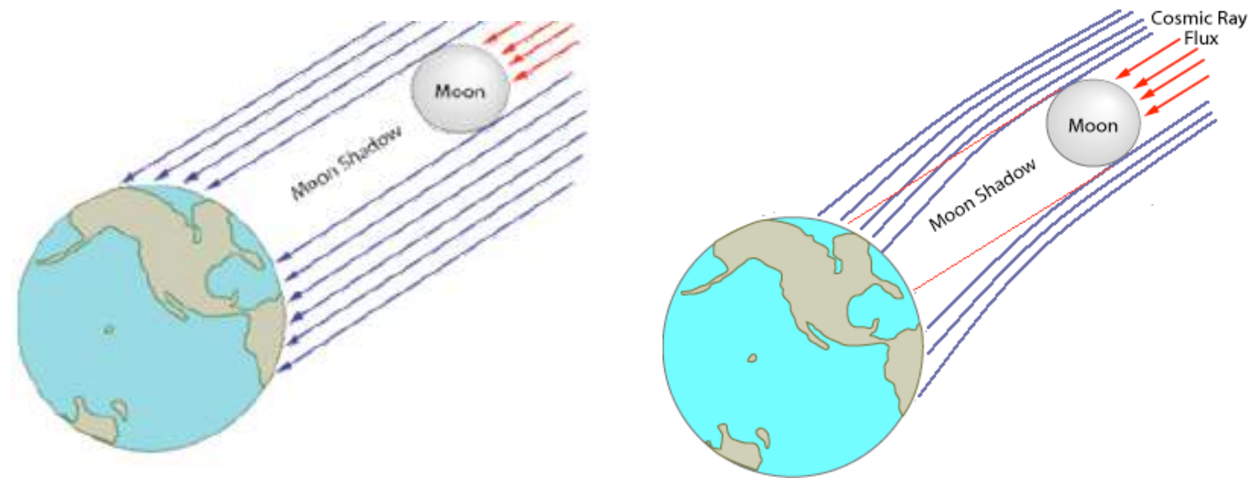

Tibet ASγ

Argo

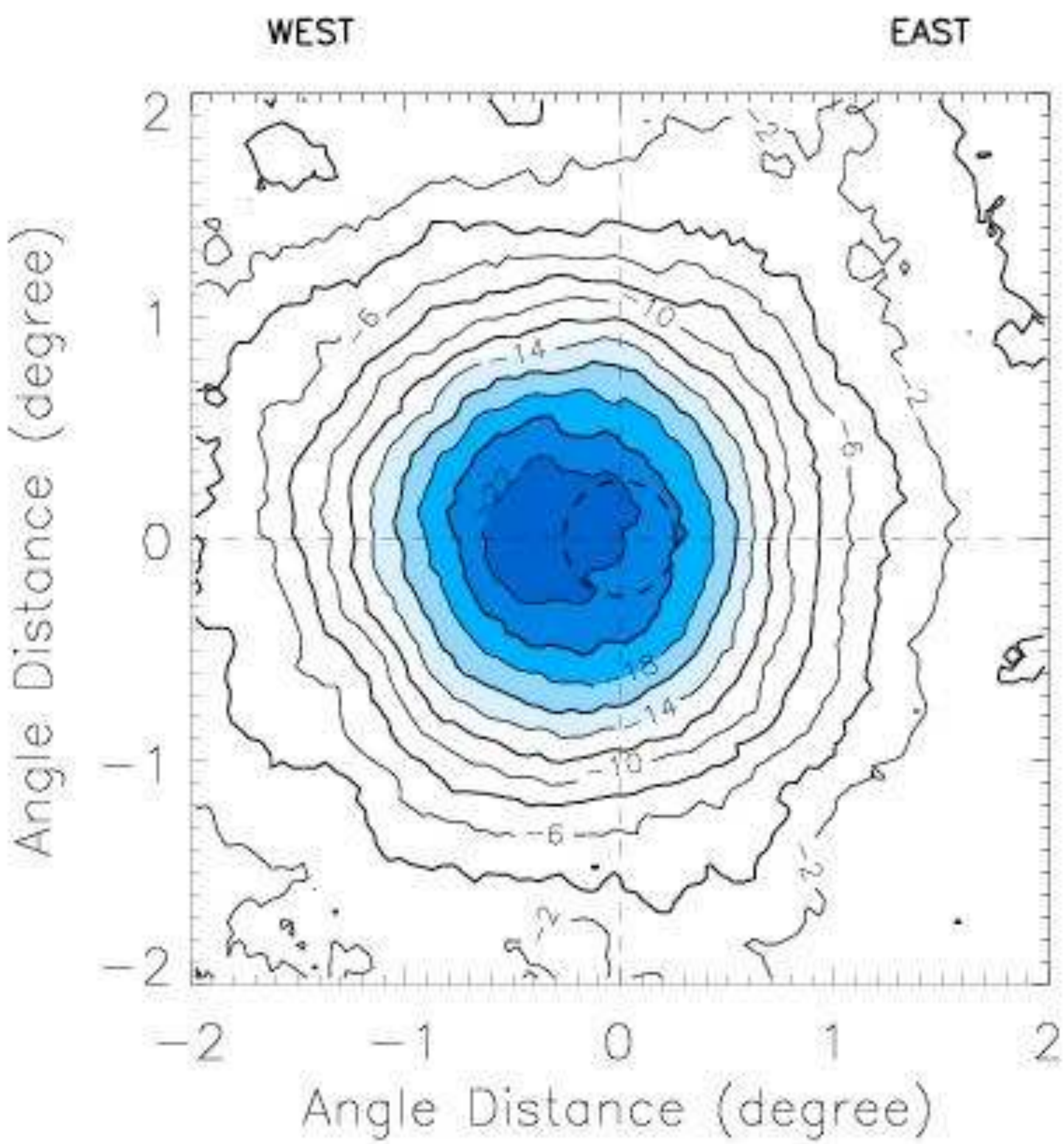

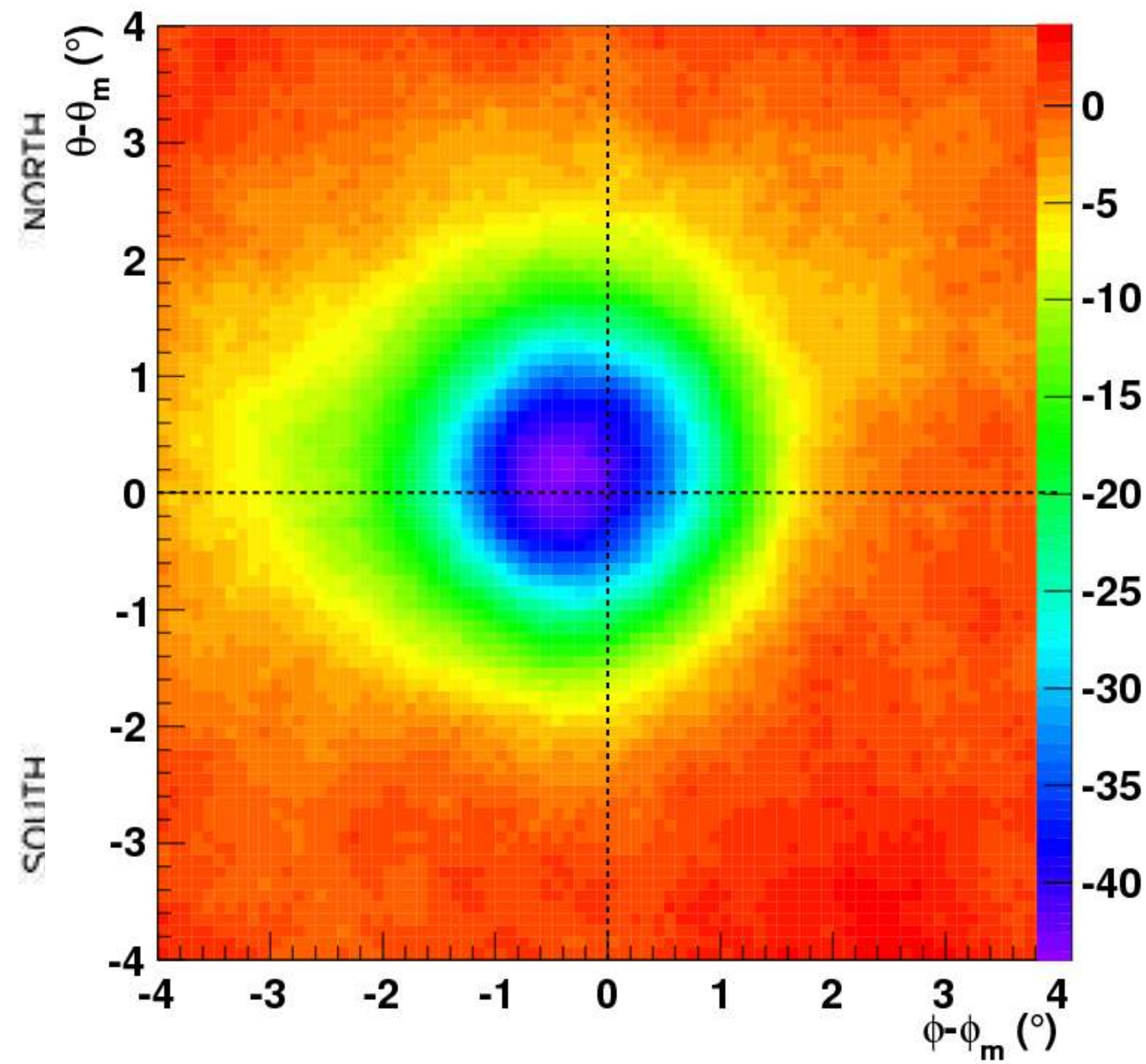

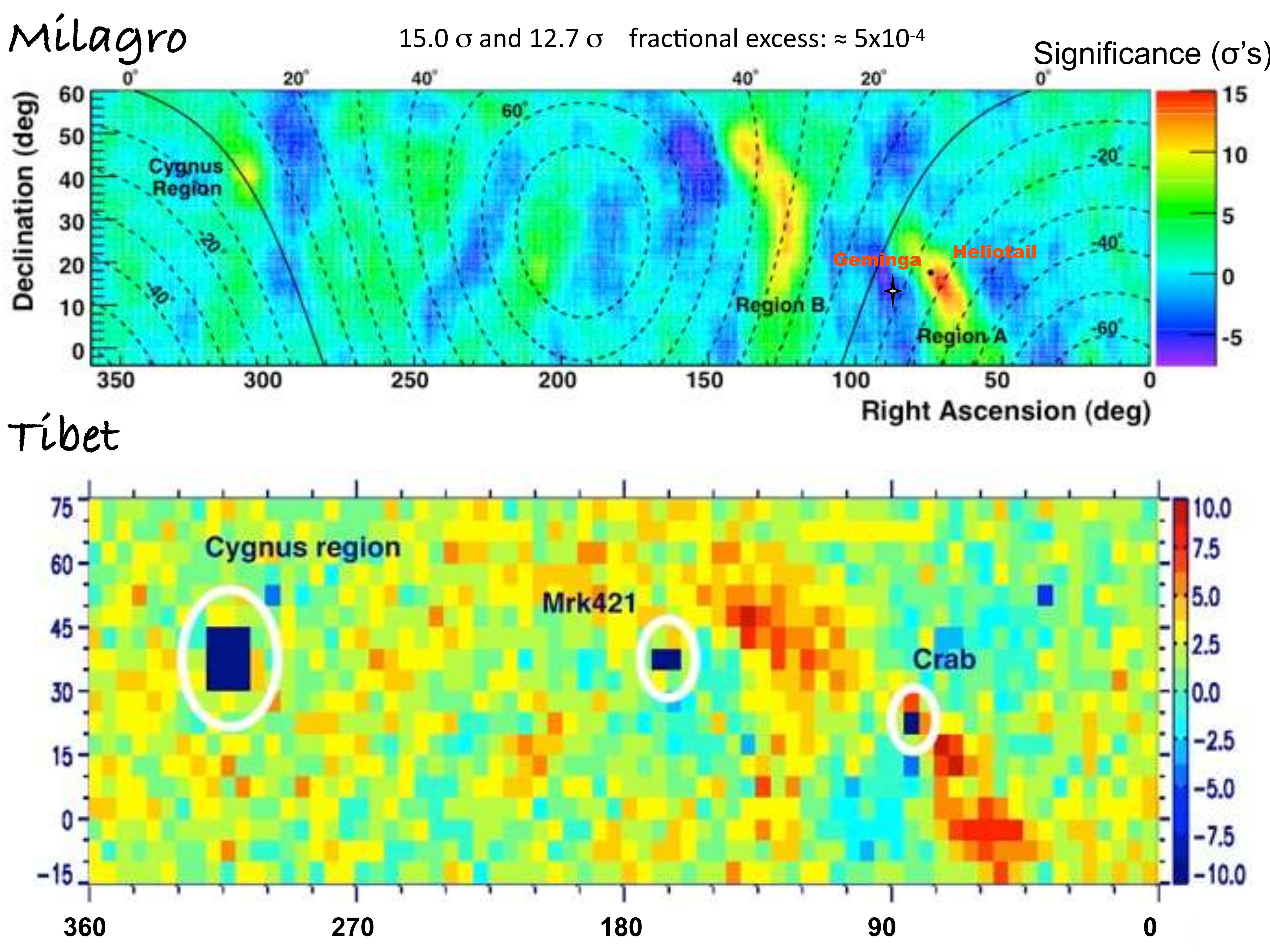
Milagro
15.0 σ and 12.7 σ fractional excess: ≈ 5x10-4
Significance (σ's)
Declination (deg)
Right Ascension (deg)
Cygnus Region
Region B
Region A
Geminga
Heliotail
Tibet
Cygnus region
Mrk421
Crab

MILAGRO
gal. plane

□ EGRET sources

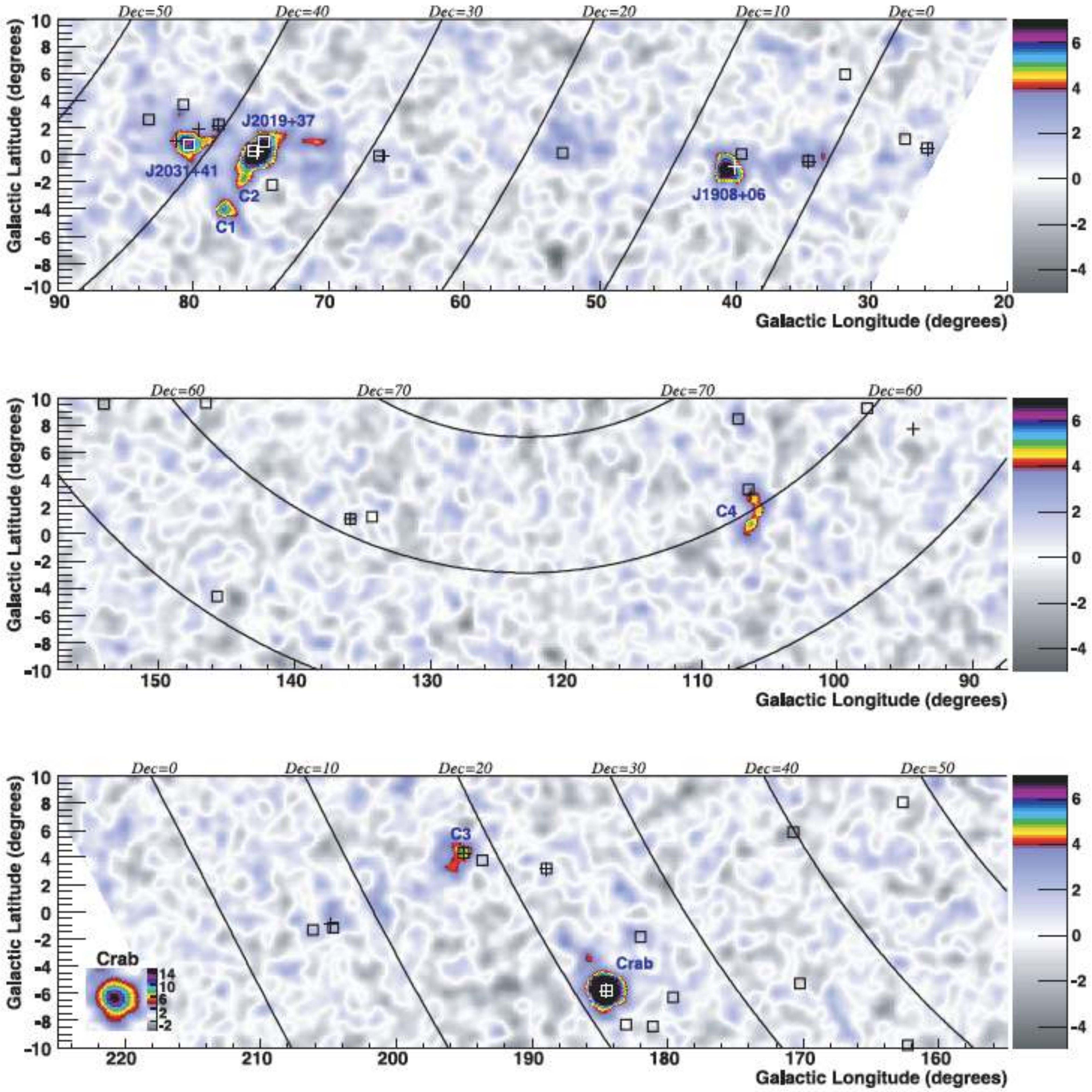

MILAGRO
(3 σ)

strong Fermi sources

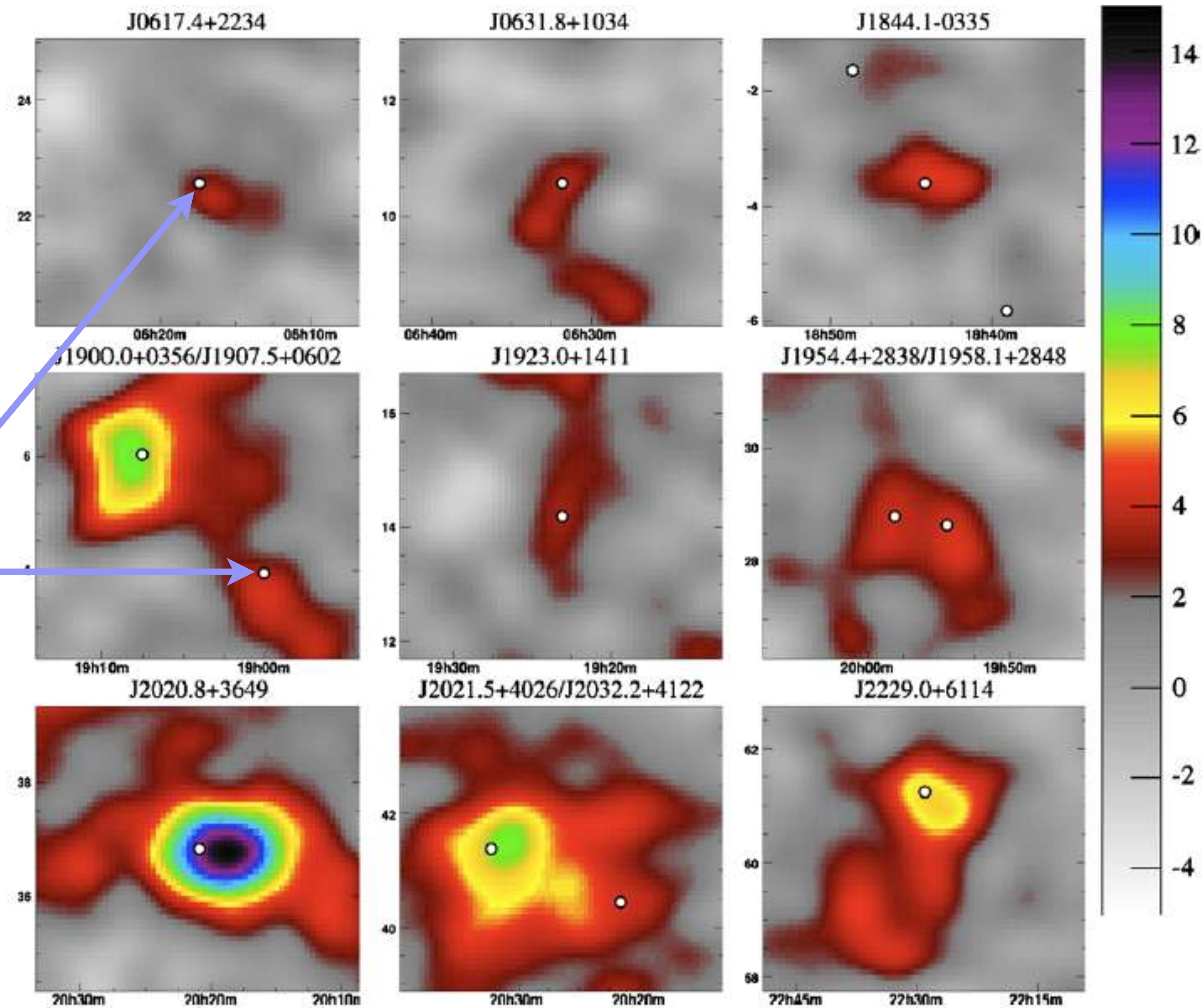

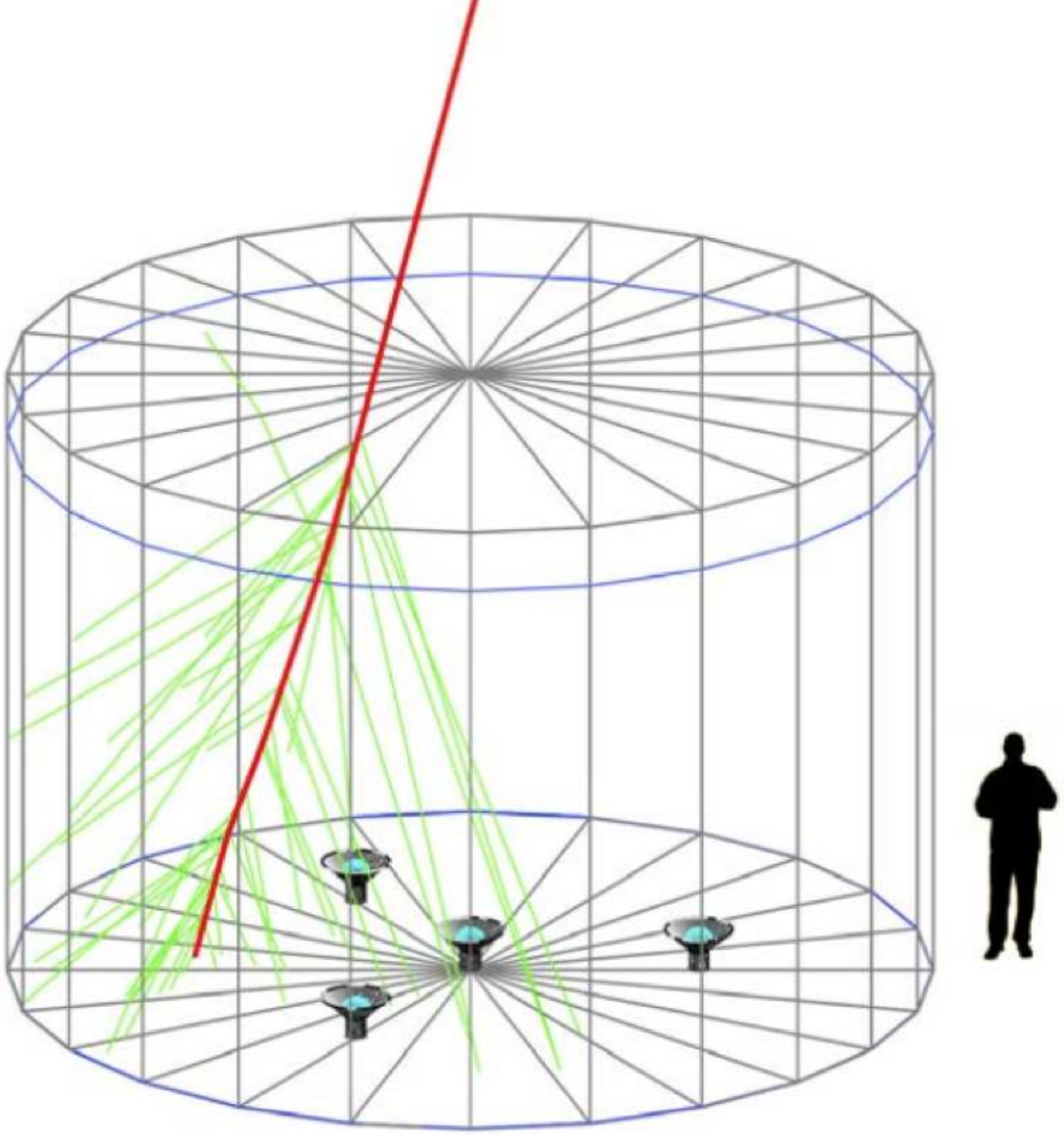

HAWC Mexico

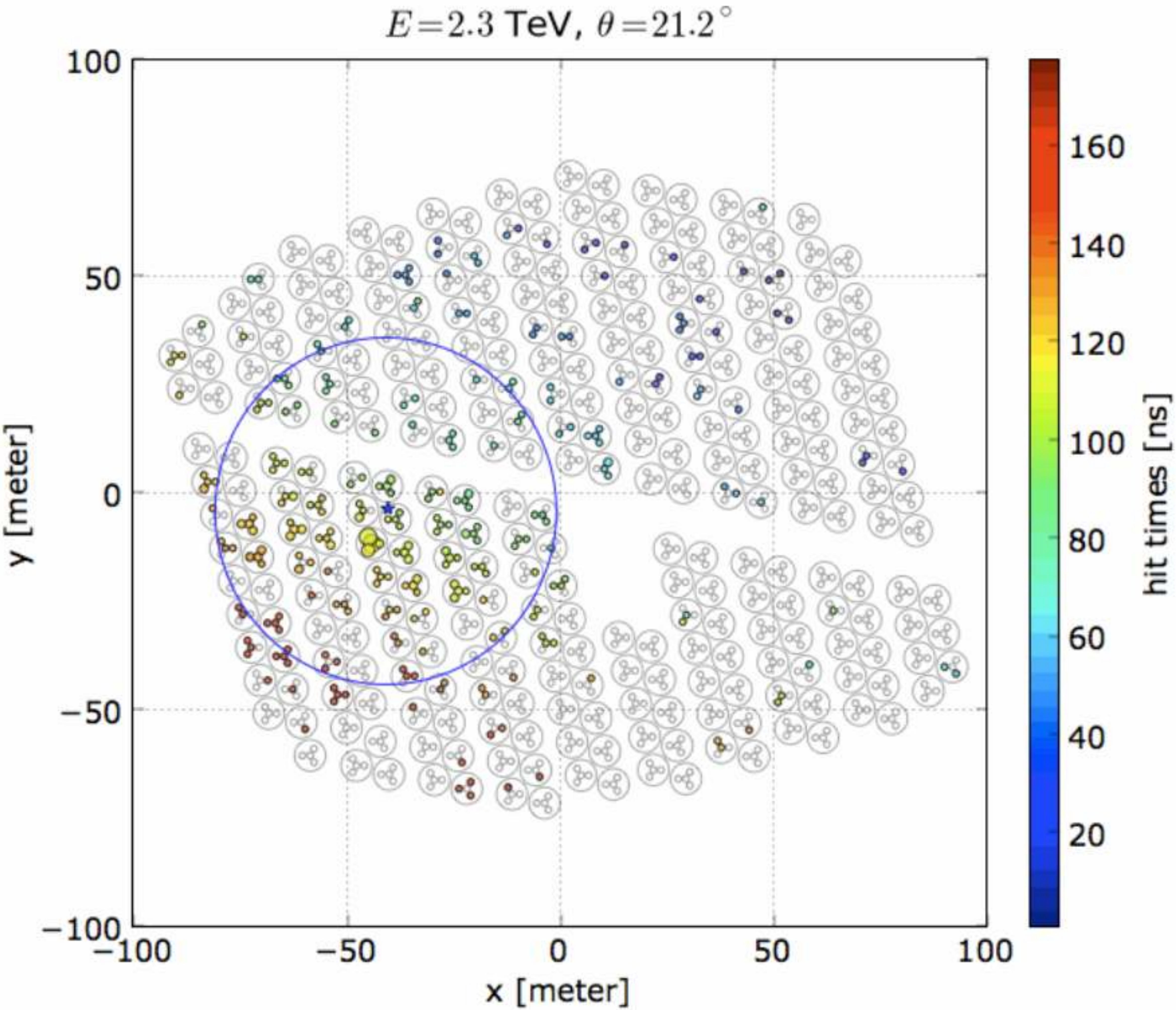

$E = 2.3$ TeV, $\theta = 21.2^\circ$
100
50
0
−50
−100
y [meter]
−100
−50
0
50
100
x [meter]
hit times [ns]
160
140
120
100
80
60
40
20

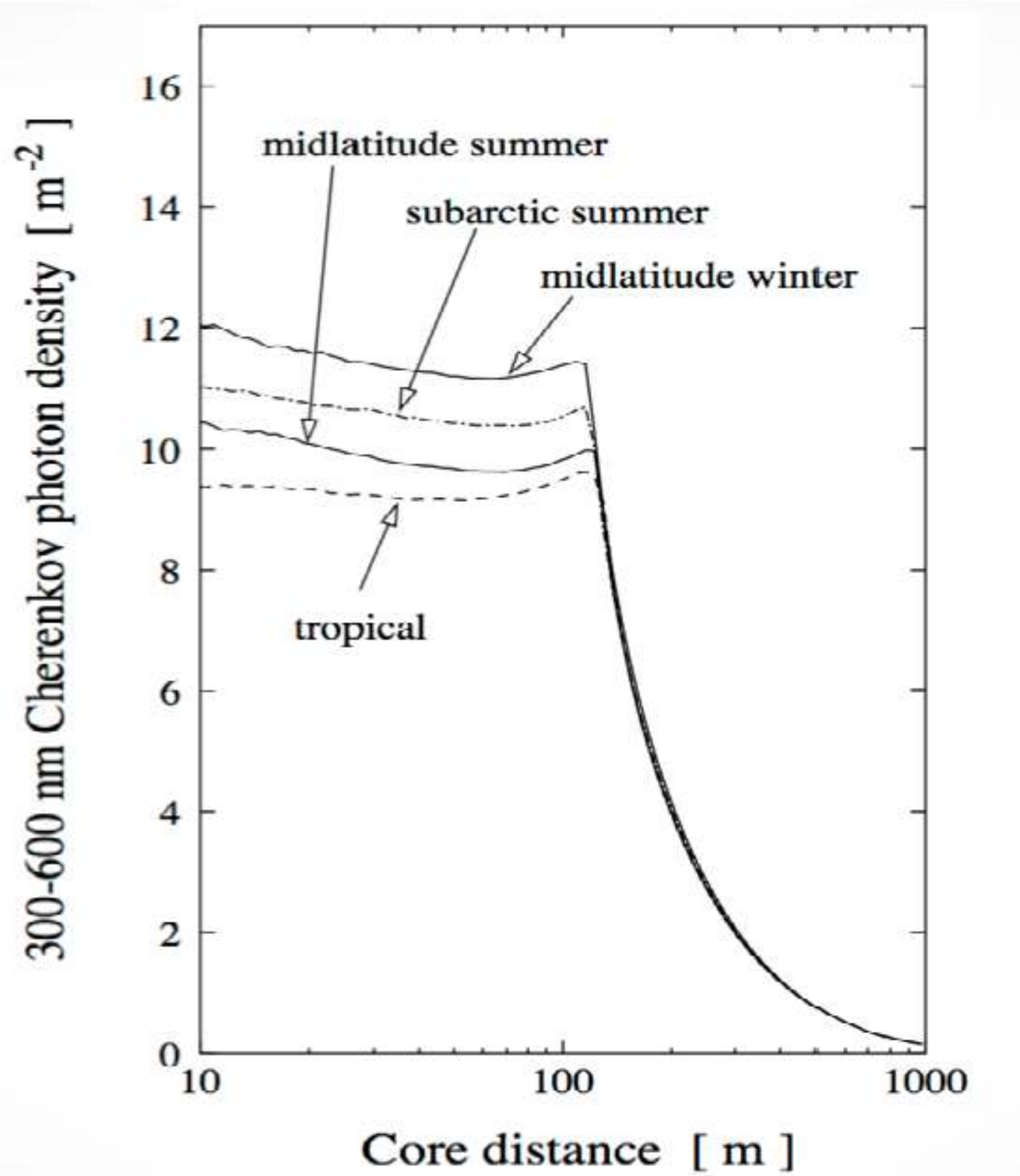

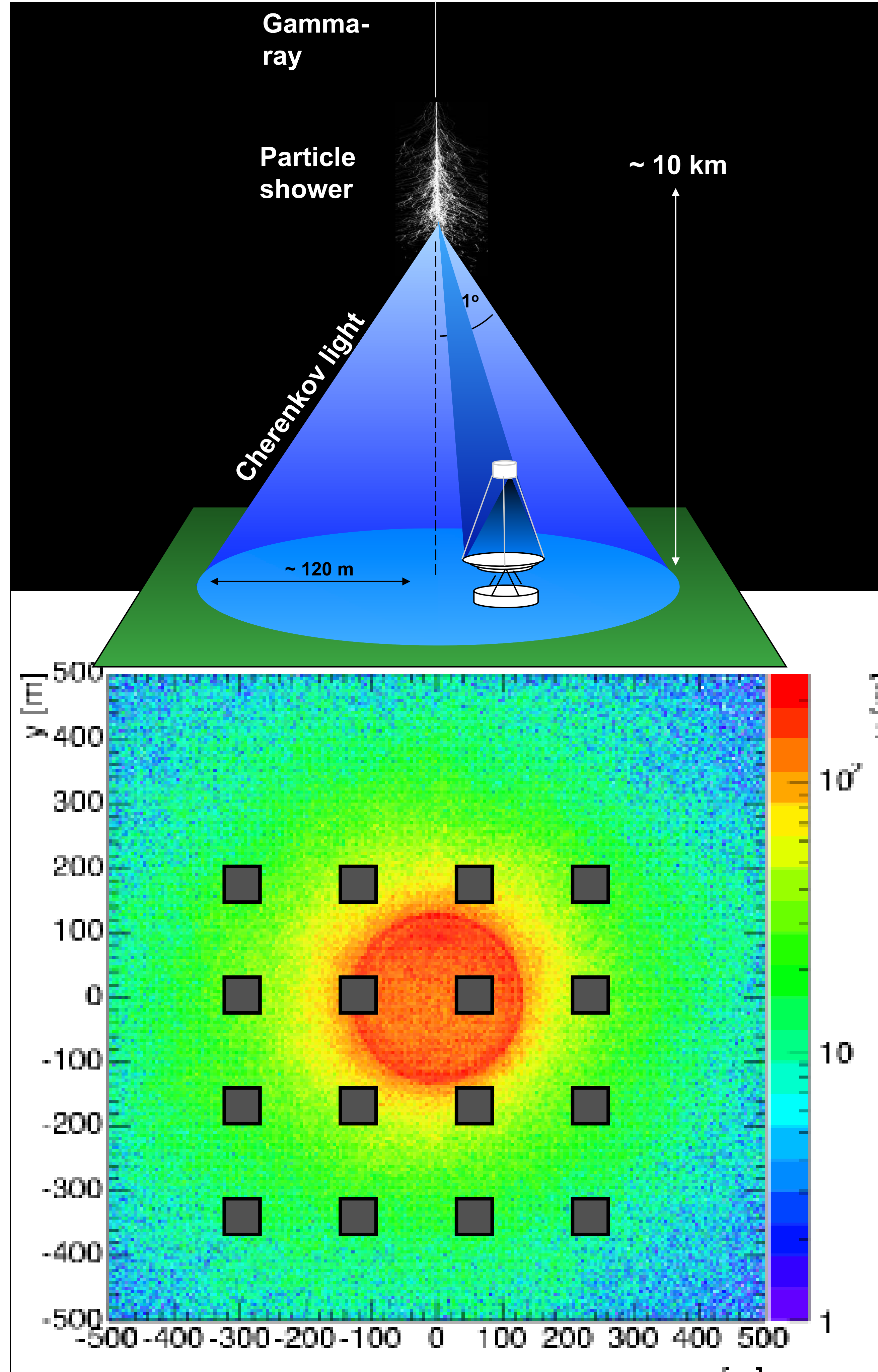

... or sample the light pool
and measure the lateral distribution

good, calorimetric
energy measurement

scintillation counter

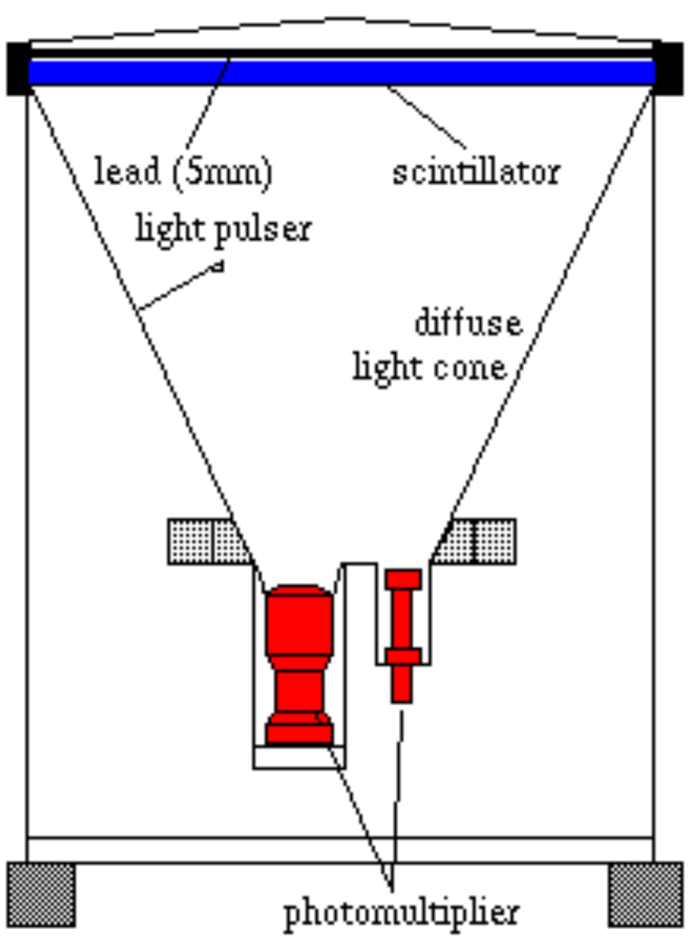

AIROBICC counter

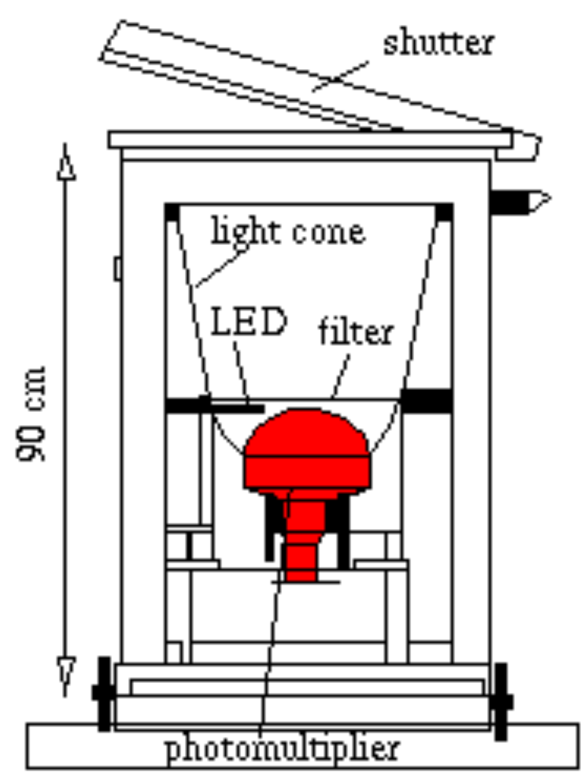

Hegra, Airobicc
La Palma

scintillator array
Muon detectors
Cherenkov counter

HAWC: high-altitude water Cherenkov detector

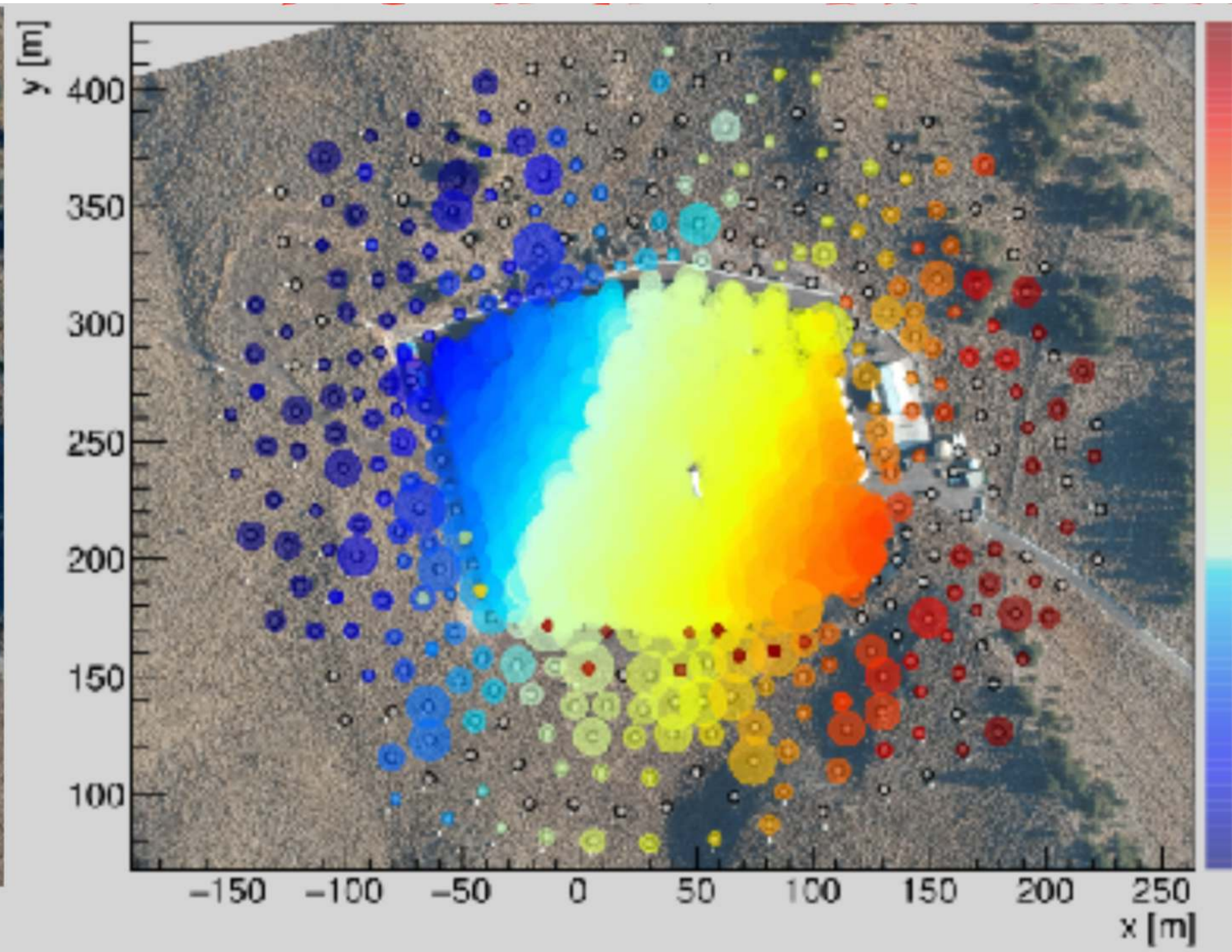

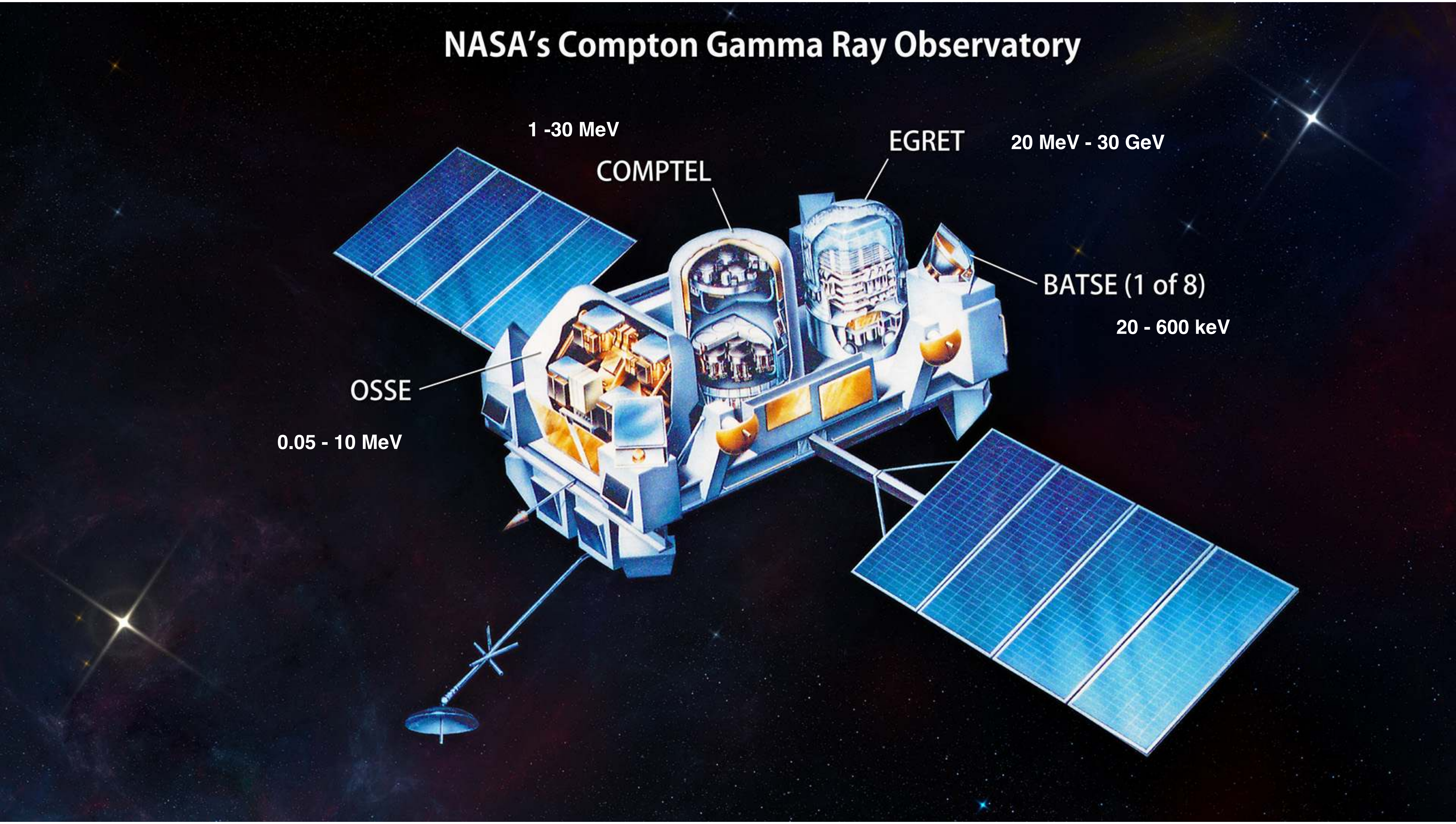

1991 - 2000

271 gamma sources (>100 MeV)
^{26}Al sky map
2000 GRBs

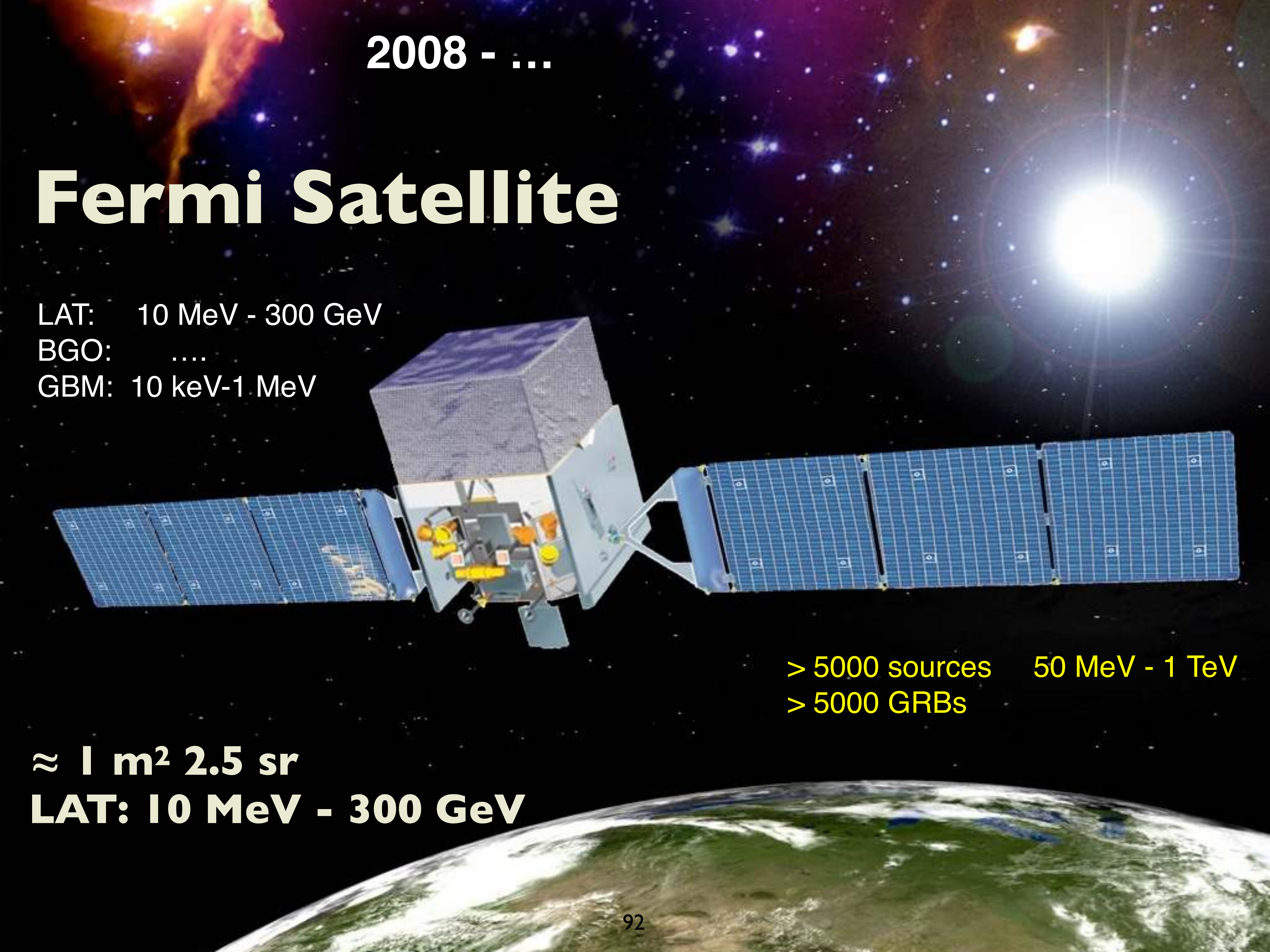
2008 - …
Fermi Satellite
LAT: 10 MeV - 300 GeV
BGO: ….
GBM: 10 keV-1 MeV
> 5000 sources
50 MeV - 1 TeV
> 5000 GRBs
≈ 1 m² 2.5 sr
LAT: 10 MeV - 300 GeV

Fermi - LAT

large angle
telescope

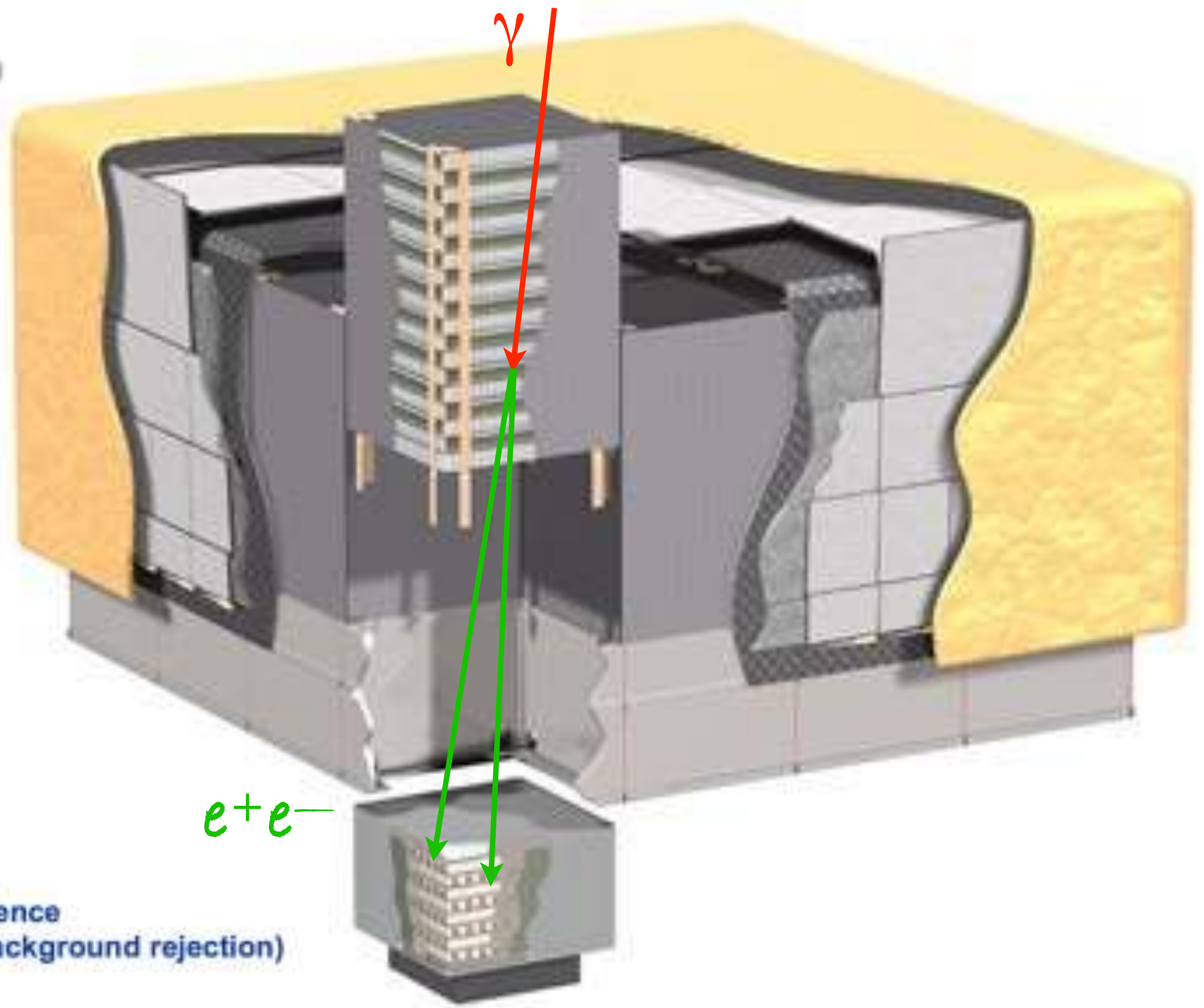

pair-conversion telescope with:

precision trackers
18 layers tungsten converters
and x, y silicon strip detectors.

calorimeter
96 CsI(Tl) crystals in an
8 layer hodoscope (depth: 8.6 X_0)

4x4 modules covered by
anti-coincidence shield

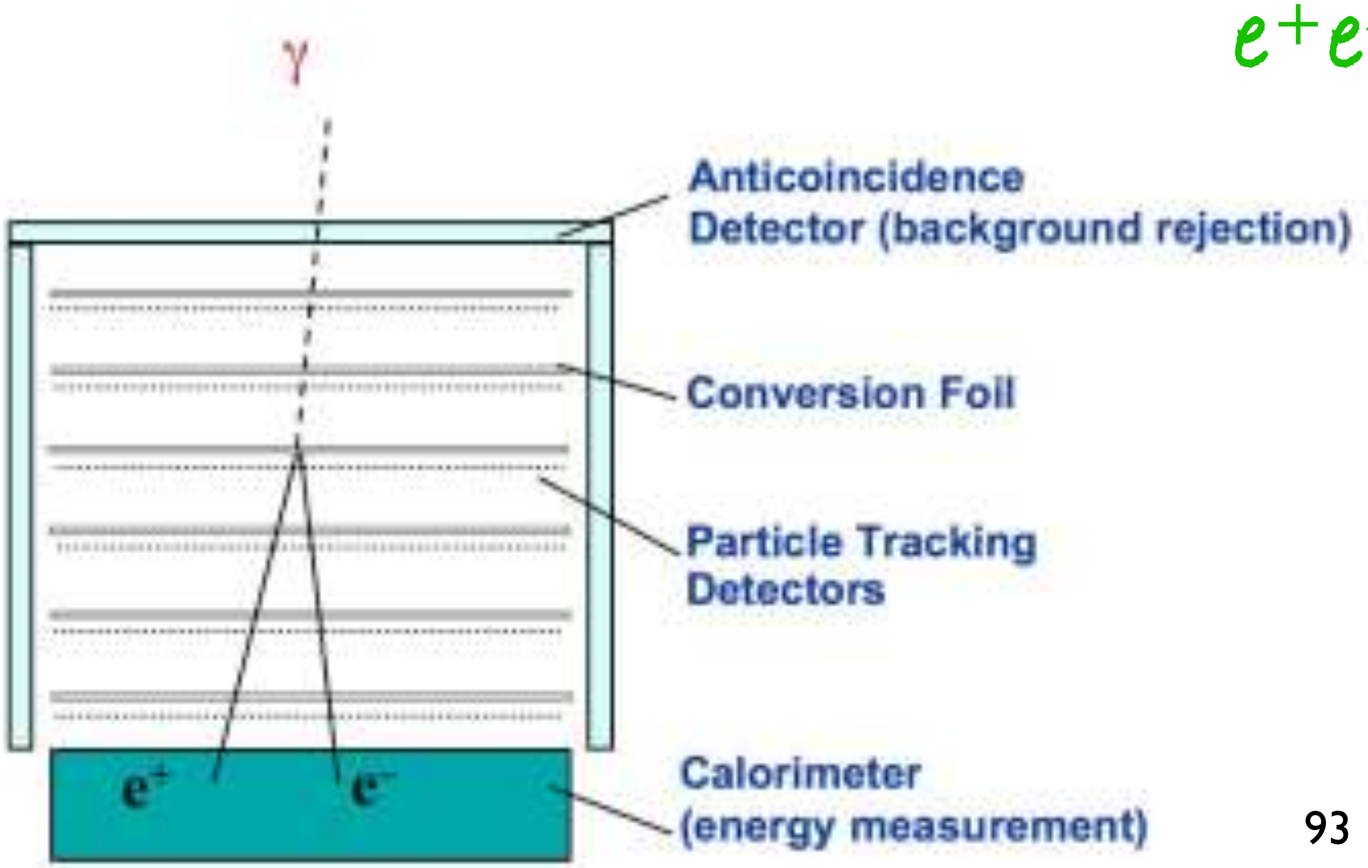

≈ 1 m² 2.5 sr

near-perfect rejection of charged primaries

Exploring the Extreme Universe

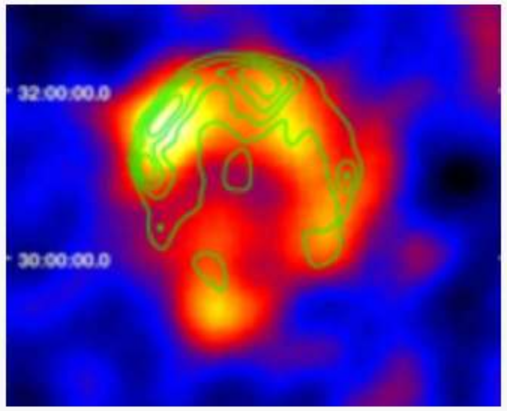

Supernova Remnants

Gamma-ray Bursts

Pulsar Wind Nebulae

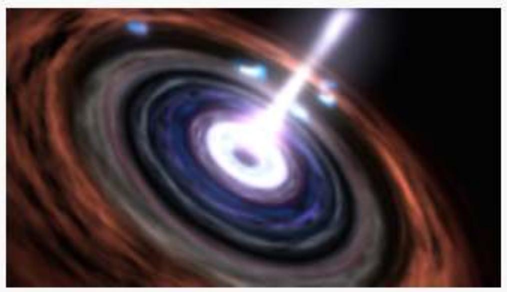

Active Galactic Nuclei

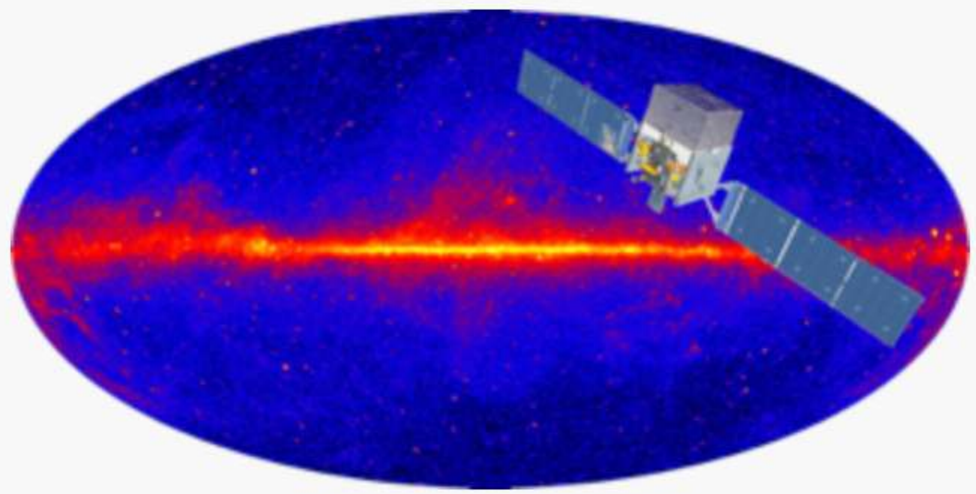

About Fermi

Click on the images or topic name for information about these science topics.

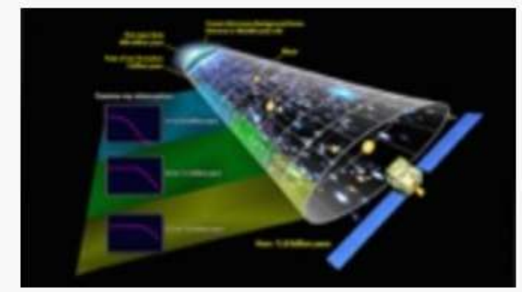

Extragalactic Background

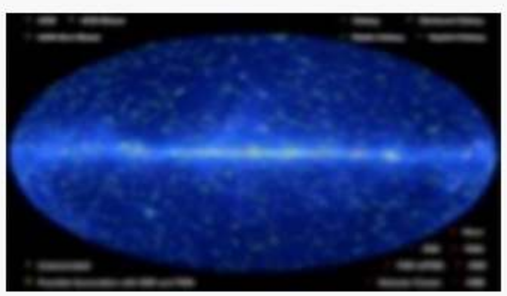

Catalogs

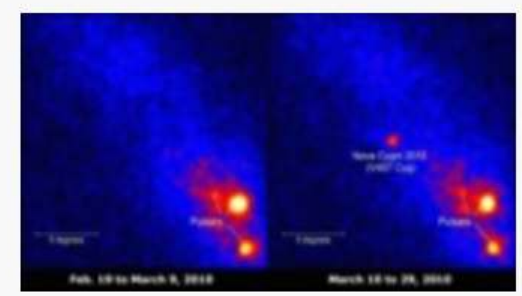

Binary Sources

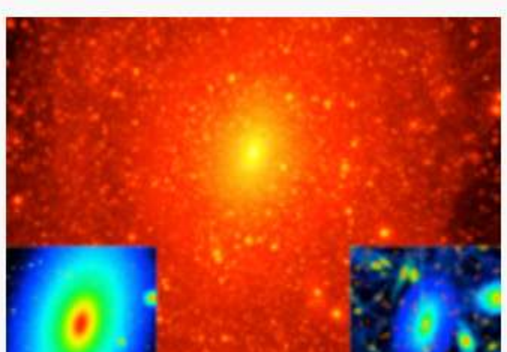

Dark Matter

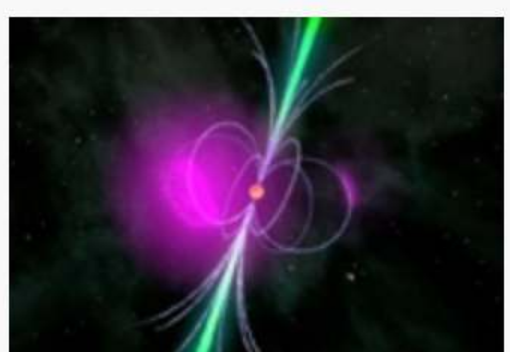

Pulsars

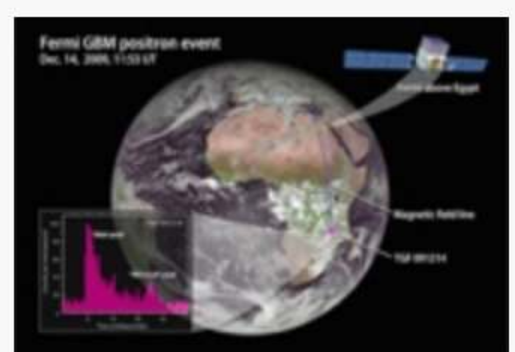

Terrestrial Gamma-ray Flashes

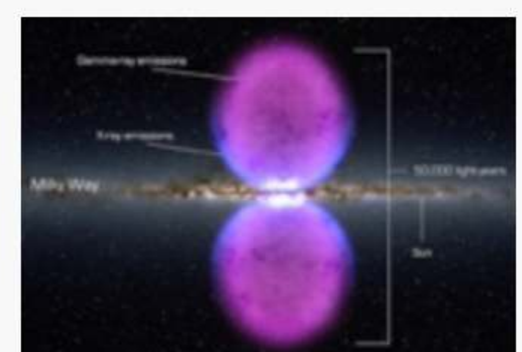

Diffuse Gamma Radiation

Cherenkov Telescopes

most sensitive instruments
for gamma ray astronomy.

<100 GeV .... >300 TeV

only in dark nights
(10% duty cycle)
need good knowledge
of atmosphere

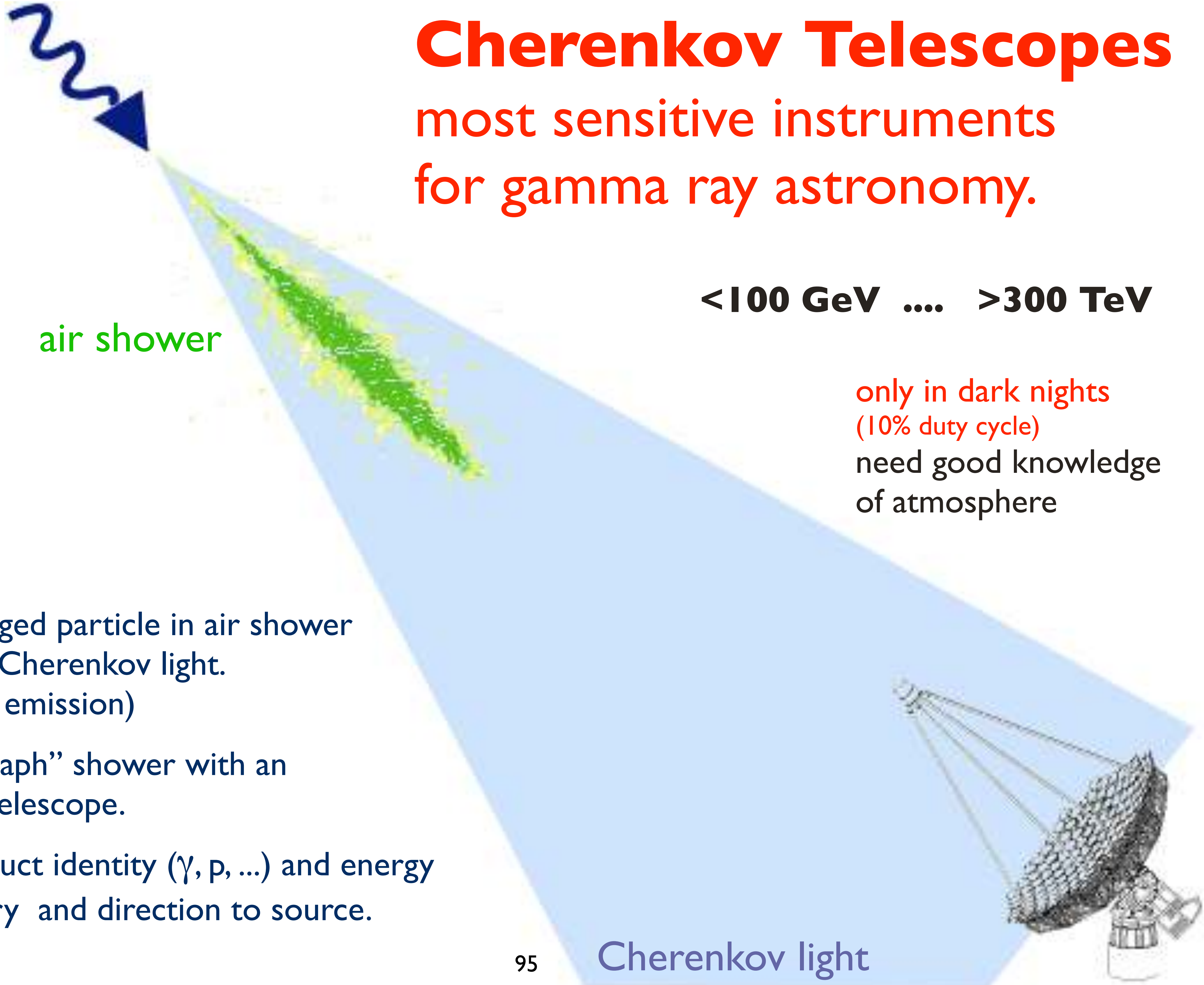

Fast charged particle in air shower
produce Cherenkov light.
(forward emission)

"Photograph" shower with an
imaging telescope.

Reconstruct identity (γ, p, ...) and energy
of primary and direction to source.

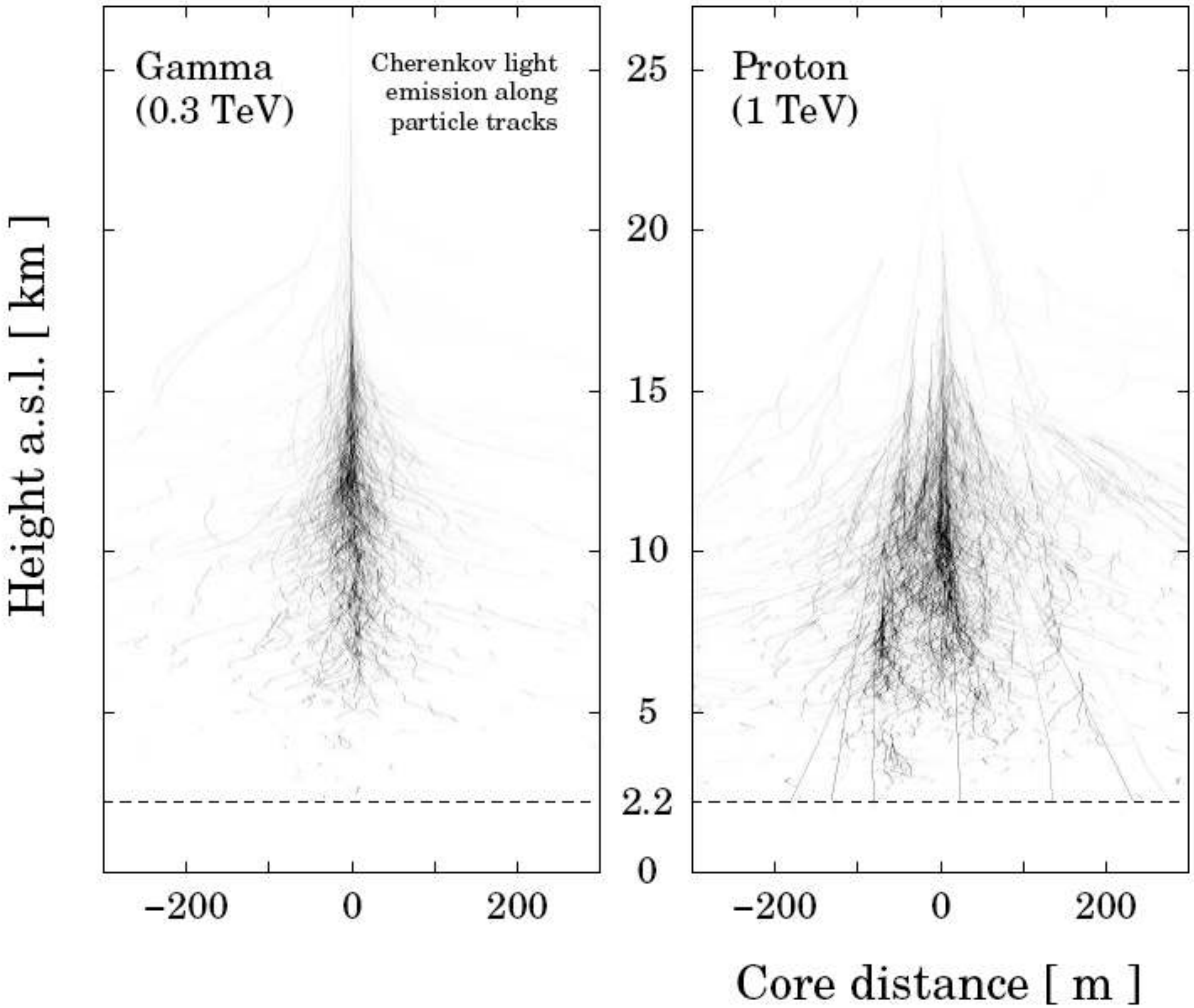

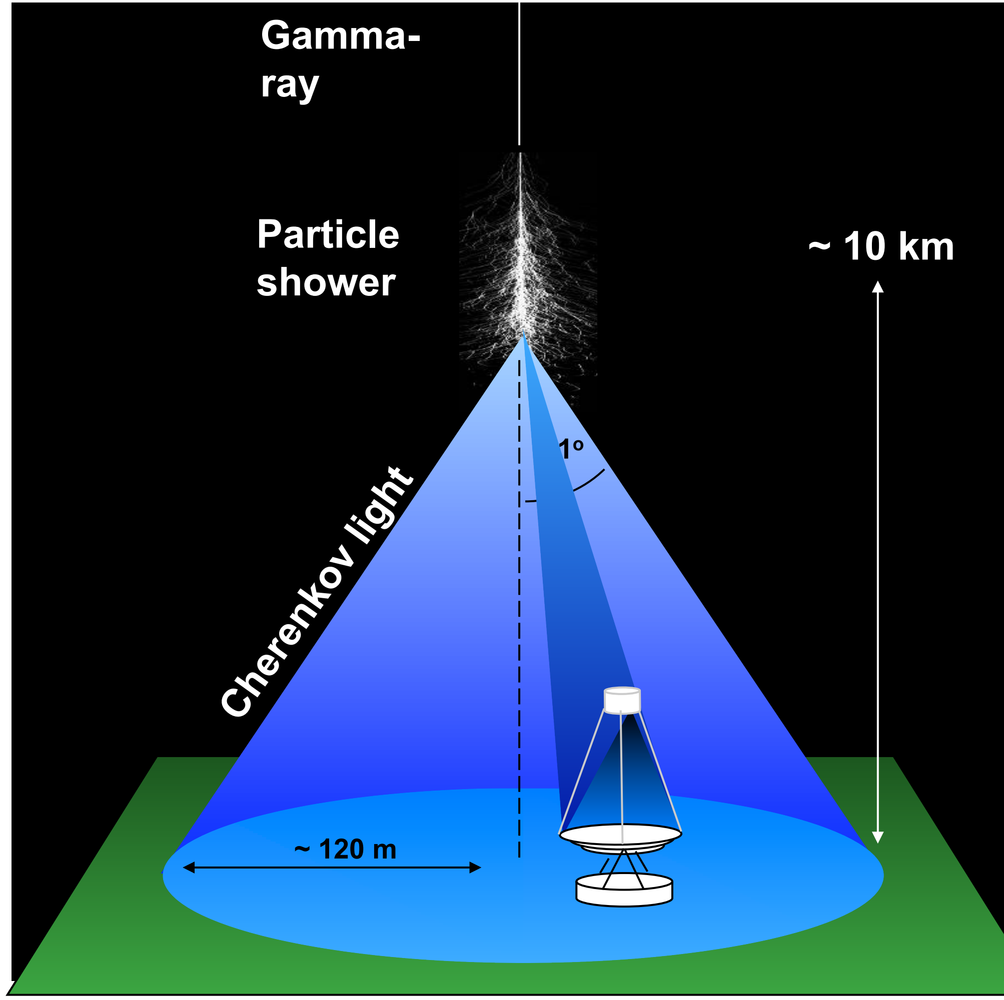

Image the shower,
distinguish protons and photons from the shape of the images.
.... very successful technique

"shower shape"
"excess of events"

also possible to identify e^- and Fe

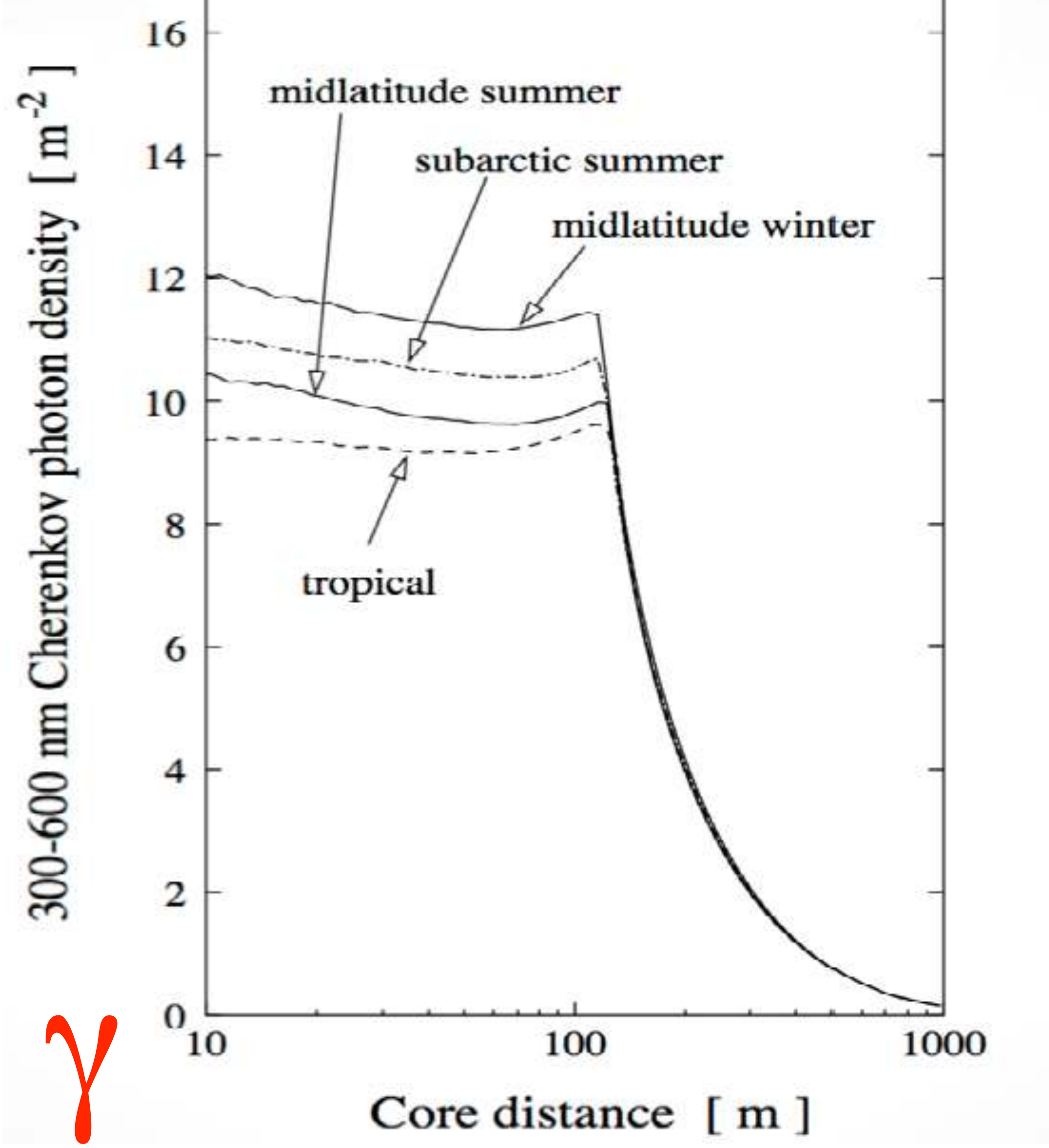

γ

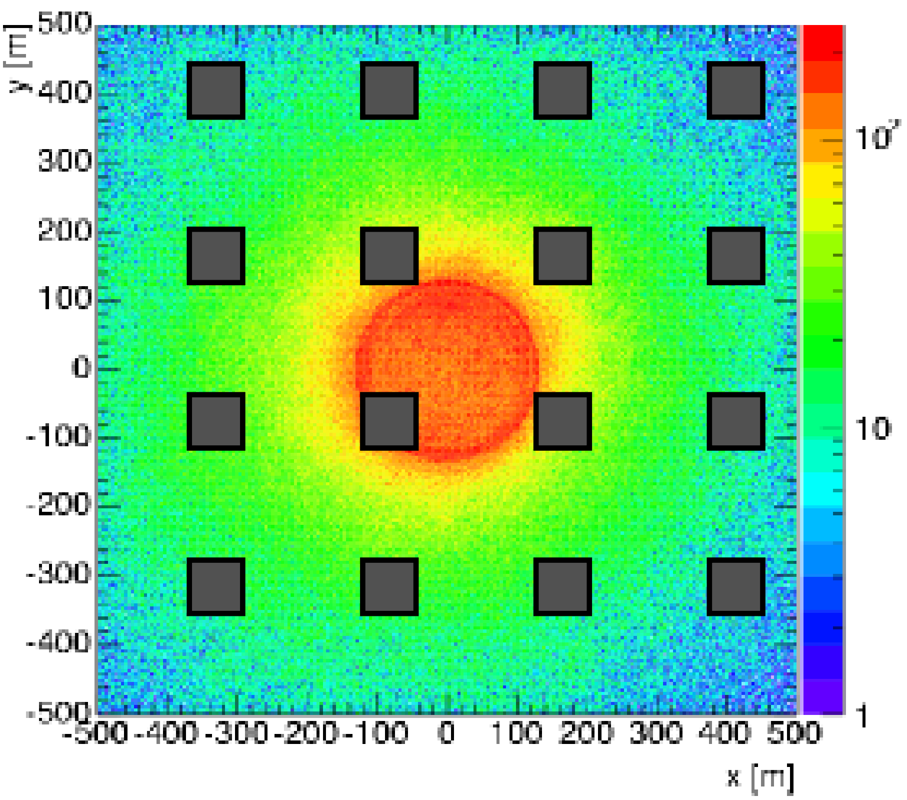

Proton

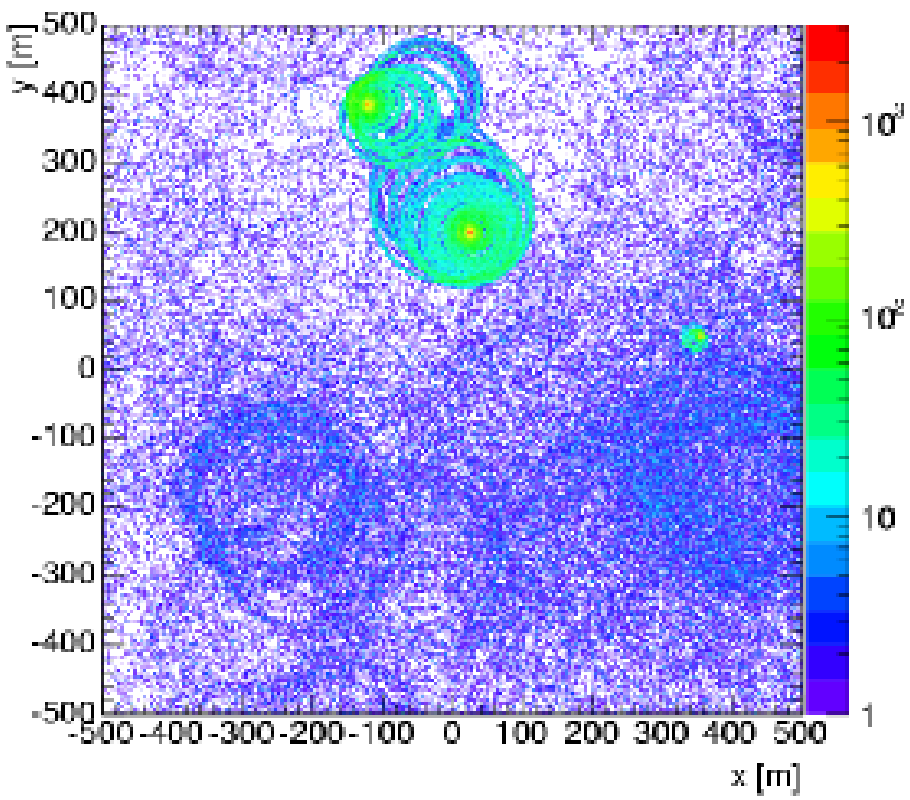

Iron

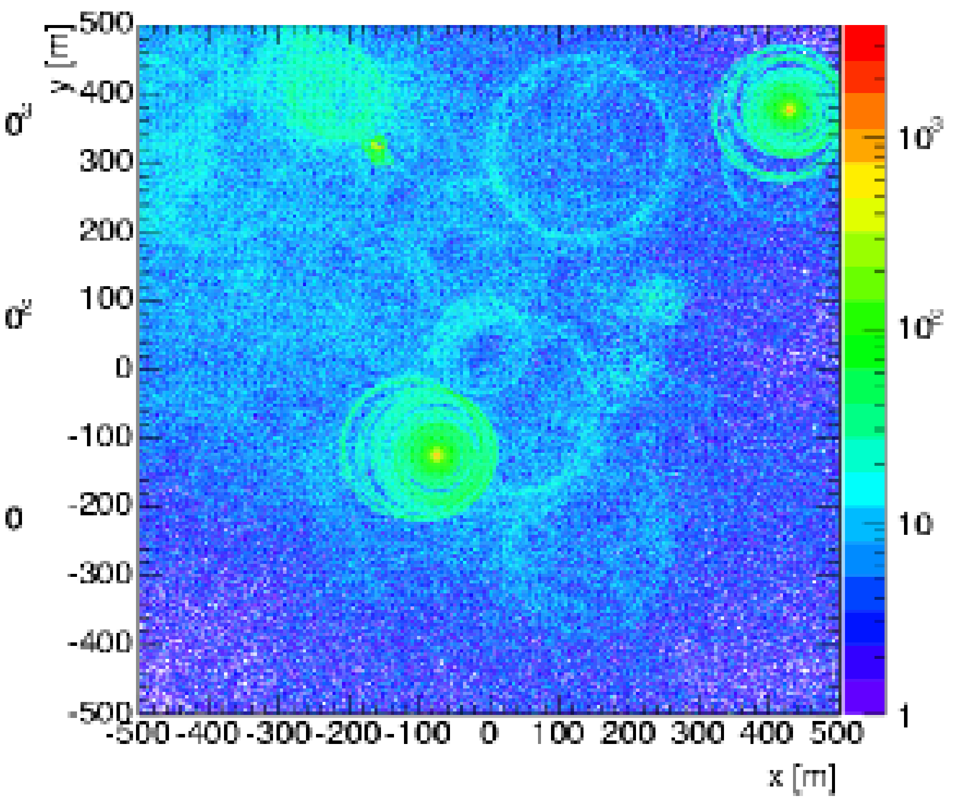

Detection principle

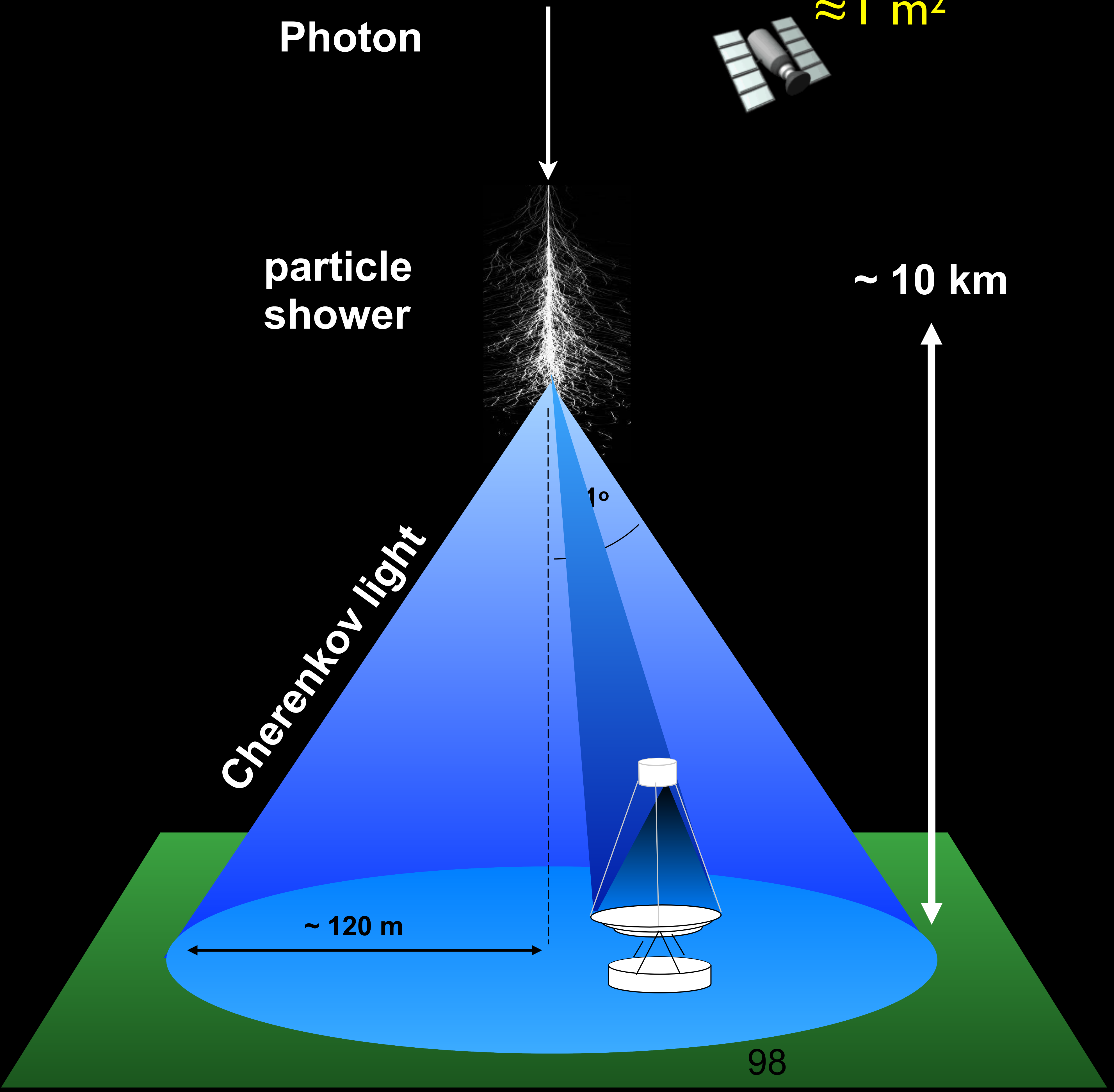

large effective detector area $\approx 10^5$ m²

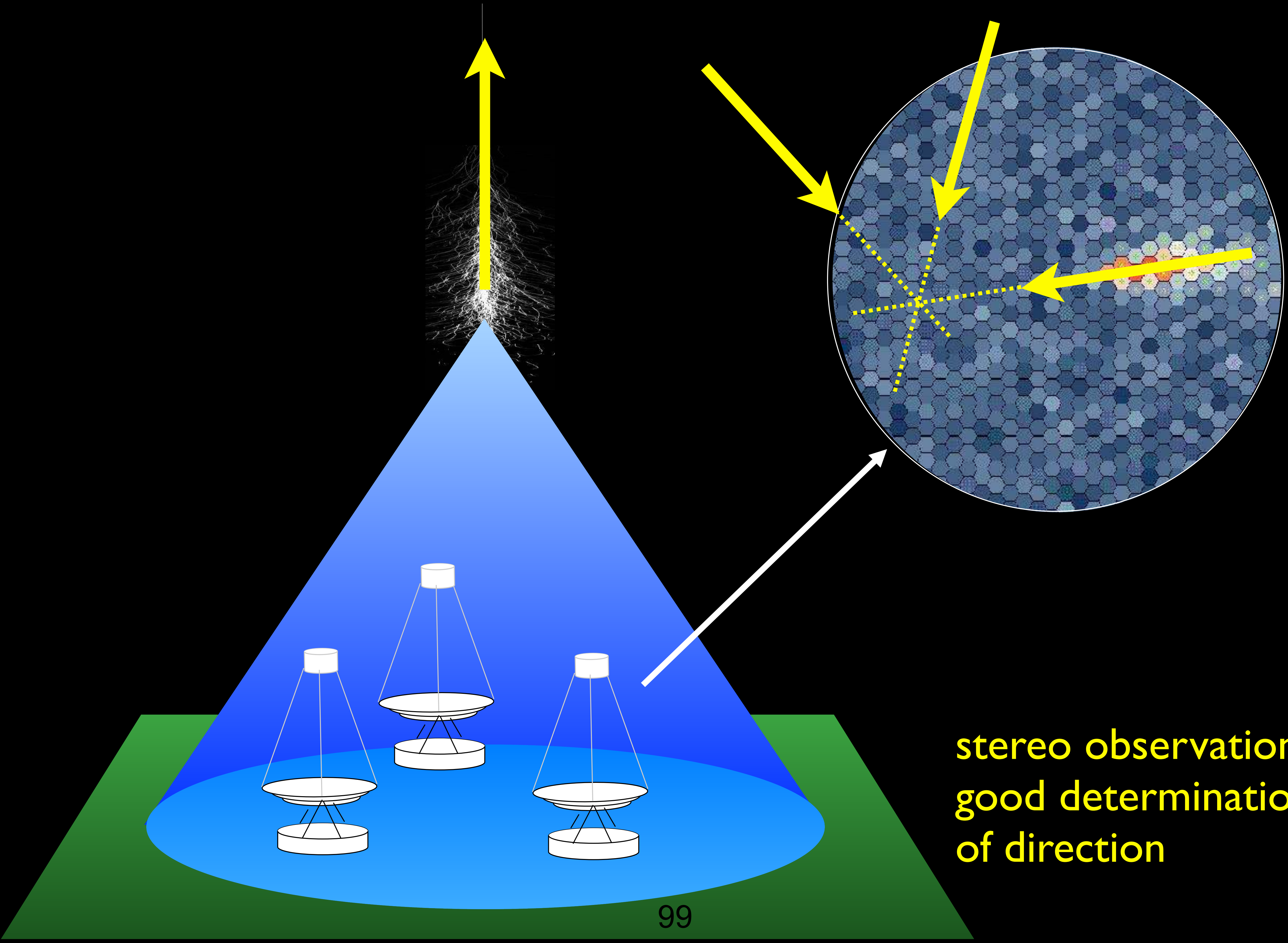

stereo observation:
good determination
of direction

MAGIC camera

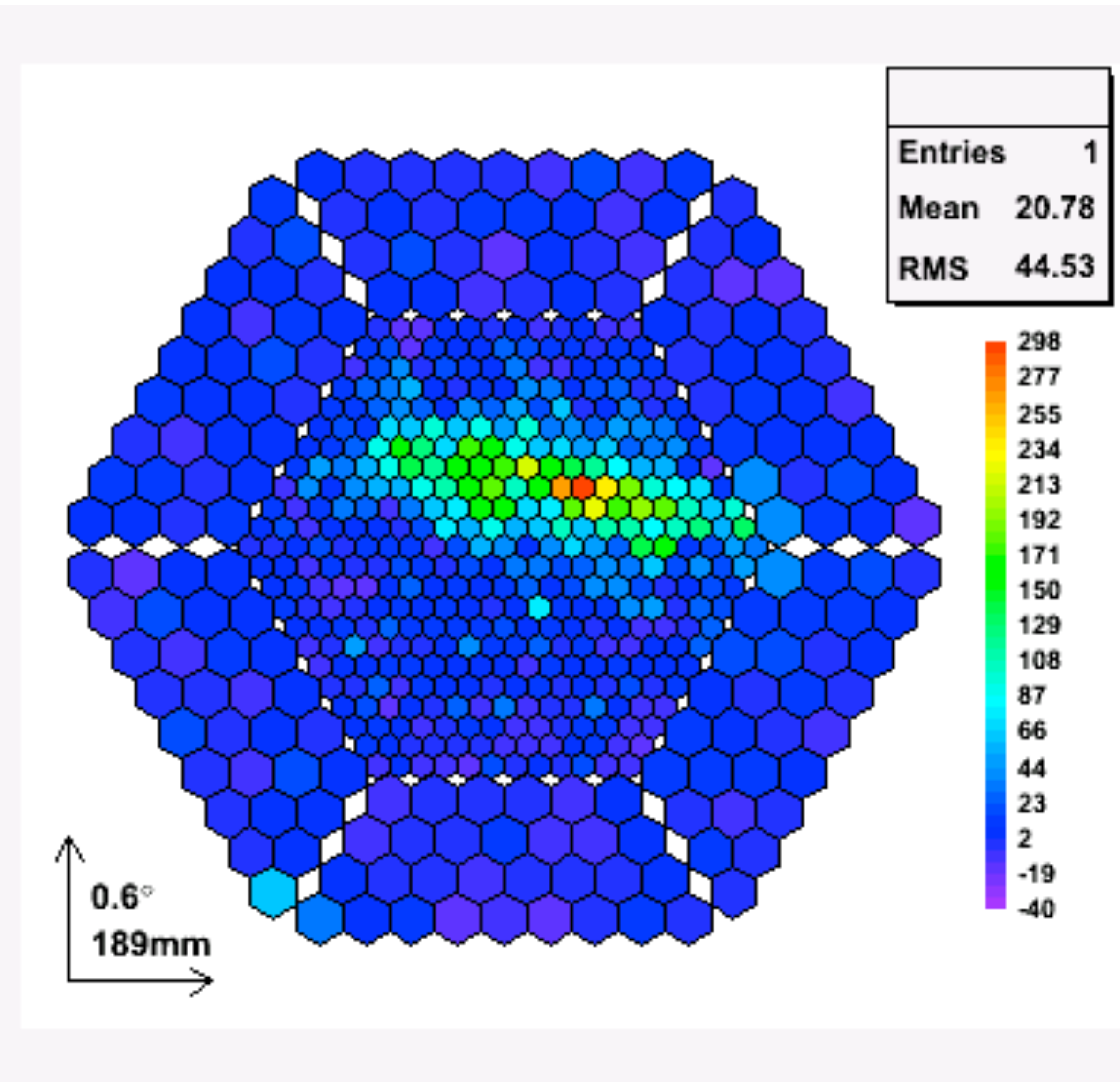

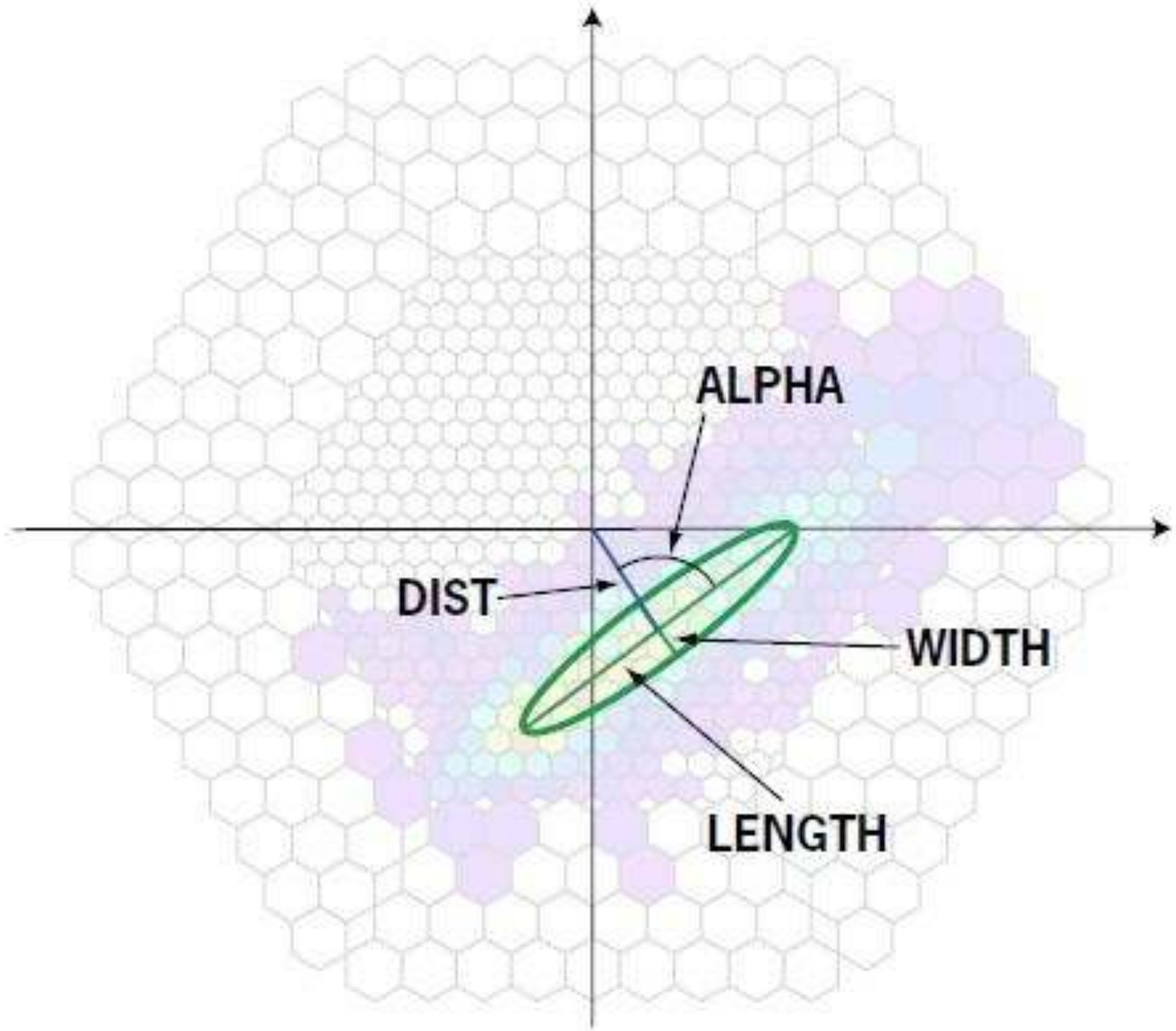

image analysis:
form and orientation

e.g. HESS Observatory (28-m Telescope added in 2012)

Namibia: 0.5 km^2

5 imaging Cherenkov telescopes

TeV-Gamma rays

($E \approx 10^{11}$–10^{14} eV)

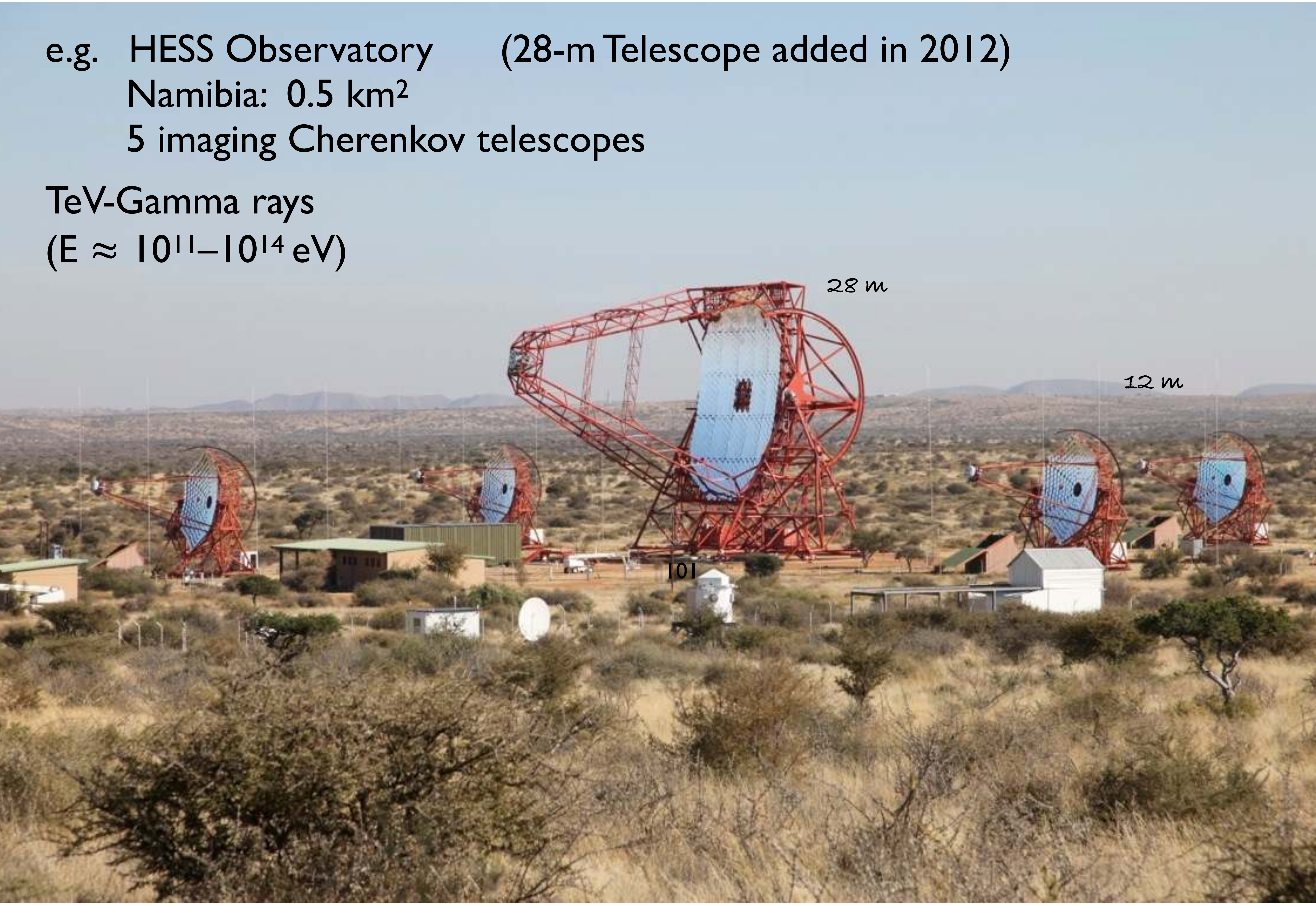

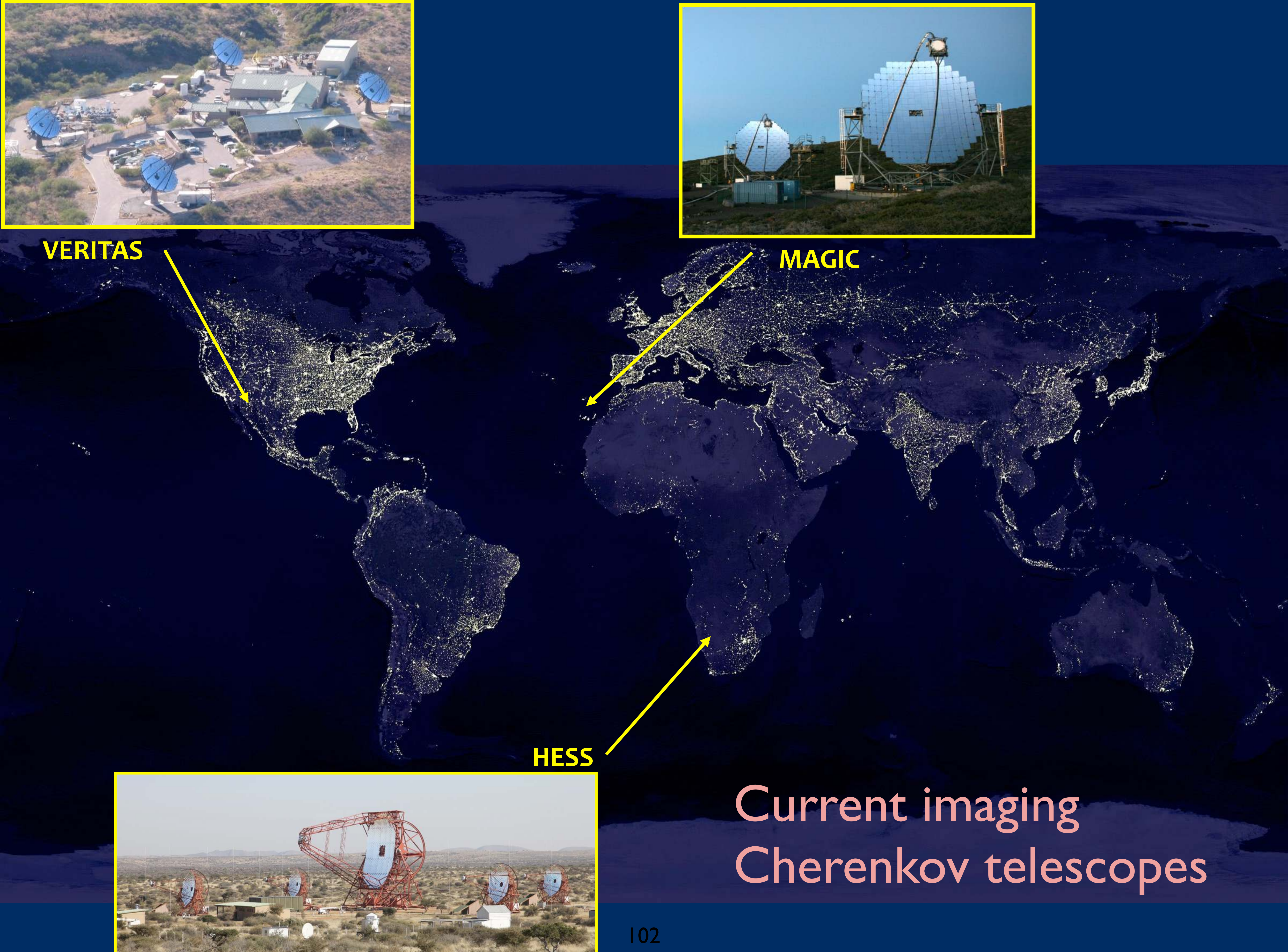

Current imaging Cherenkov telescopes